

ARMY RESEARCH LABORATORY



Transient Electromagnetic Signals from Internal Combustion Engines

Marc Litz, Neal Tesny, Lillian Dilks, and Leland M. Cheskis

ARL-TR-1658

April 2002

Approved for public release; distribution unlimited.

The findings in this report are not to be construed as an official Department of the Army position unless so designated by other authorized documents.

Citation of manufacturer's or trade names does not constitute an official endorsement or approval of the use thereof.

Destroy this report when it is no longer needed. Do not return it to the originator.

Army Research Laboratory

Adelphi, MD 20783-1197

ARL-TR-1658

April 2002

Transient Electromagnetic Signals from Internal Combustion Engines

Marc Litz, Neal Tesny, Lillian Dilks, and Leland M. Cheskis
Sensors and Electron Devices Directorate

Abstract

A series of tests focusing on the frequency content and transient characteristics of the electromagnetic emissions from three different boat engines was performed at the Patuxent Naval Air Station. The transient emissions were compared with respect to engine rpm, amplification, orientation, shielding and against emissions from an engine of the same model. It was found that engine models can be identified according to their frequency content.

Contents

Introduction	1
Experimental Setup	2
Results	7
Conclusions	13
Distribution	55
Report Documentation Page	57

Appendices

A. Sample Waveforms	15
B. Method of Analysis	31
C. Time-Frequency Analysis	39
D. Matlab Program	53

Figures

1. Three test boats: Yamaha 200, NESEA, and dual 150 OMC	2
2. The Experimental Setup: schematic diagram and out at field site ...	3
3. Frequency-domain amplitude calibration of EMCO double-ridge waveguide horn	3
4. Environmental Background Noise at 245°, 6 mV; 65°, 6 mV; 335°, 4 mv; and 155°, 12 mv	4
5. Two boat courses close to dock: sweep circle, and sweep	6
6. Dual 150 hp OMC outboards	6
7. Comparison of amplitude and frequency for starboard and port engine for OMCs	7
8. Comparison of starboard and port sides for Yamaha	7
9. Comparison of shot signal without amplification and with amplification	8
10. Comparison of an engine at idle and with high revolution	9

Figures (cont'd)

11. NESEA plots showing the energy spectrum and voltage for two independent shots 9

12. Yamaha 200 plots showing the energy spectrum and voltage for two independent shots 9

13. Comparison of two shots of the dual 150 OMC engine 10

14. The EM emissions of the OMC engine without foil and with foil ... 10

15. Frequency peak data for Yamaha and OMC 11

Table

1. Data sets collected during field tests 5

Introduction

This report describes an experimental effort to utilize electromagnetic (EM) emissions from boat engines for identification purposes. A series of tests were conducted at Patuxent River Naval Air Station with three different boat engines. The results were evaluated for frequency content and transient characteristics. The goals of this effort were (1) to characterize a signal source by performing near-field measurements with insignificant background noise; (2) to take absolute measurements (as a function of range and orientation) under varying operating conditions; (3) to identify spectral fingerprints; (4) to measure three specific signals of interest for government furnished equipment; and (5) to identify methods that could be used to reduce the signal strength.

Experimental Setup

To study EM emissions from boat engines, field tests were conducted at the St. Igno's campus of the Patuxent River Naval Air Station on the St. Mary's River. We collected engine data from three different boats (figure 1):

- NESEA with dual 502 hp chevy inboards,
- Yamaha 200 hp outboard, and
- Dual 150 OMC.

The experimental setup consisted of the following components (figure 2(a)):

- Tektronix SCD 1000 (>1 GHz bandwidth) transient digitizer,
- RG-223 delay line,
- EMCO model 3106 double-ridge waveguide horn with factory calibrated frequency range of 200 MHz to 2 GHz, a Picosecond Pulse Laboratory 3528 wideband amplifier, and
- Laptop computer.

The delay line was included so that the SCD 1000 could be triggered into a state of readiness before the arrival of the signal to be digitized and recorded. In other words, the incoming signal, after passing through the amplifier, was split. One half traveled down the trigger line directly to the SCD 1000 and triggered it. The other half traveled down the signal line and was delayed by 47 ns. When it arrived at the digitizer, the digitizer was ready to process it.

A photo of the actual experimental setup at the field site appears in figure 2(b). The horn was calibrated for amplitude and phase as a function of frequency separately in the Army Research Laboratory (ARL) anechoic chamber for wider-band usage than the factory intended. The resulting gain curve is shown in figure 3. The horn is visible in the background of figure 2(b).

Figure 1. Three test boats: (a) Yamaha 200, (b) NESEA, and (c) dual 150 OMC.

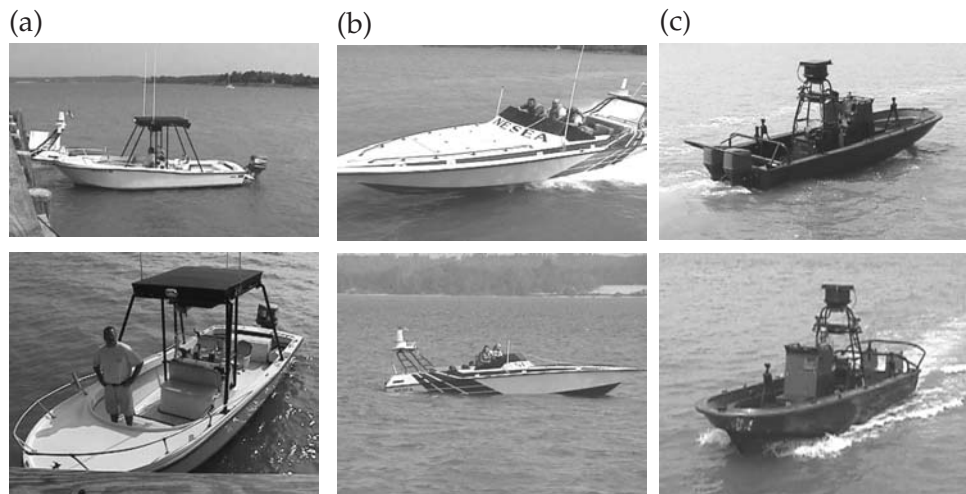


Figure 2. The Experimental Setup:
(a) schematic diagram
(b) out at field site.

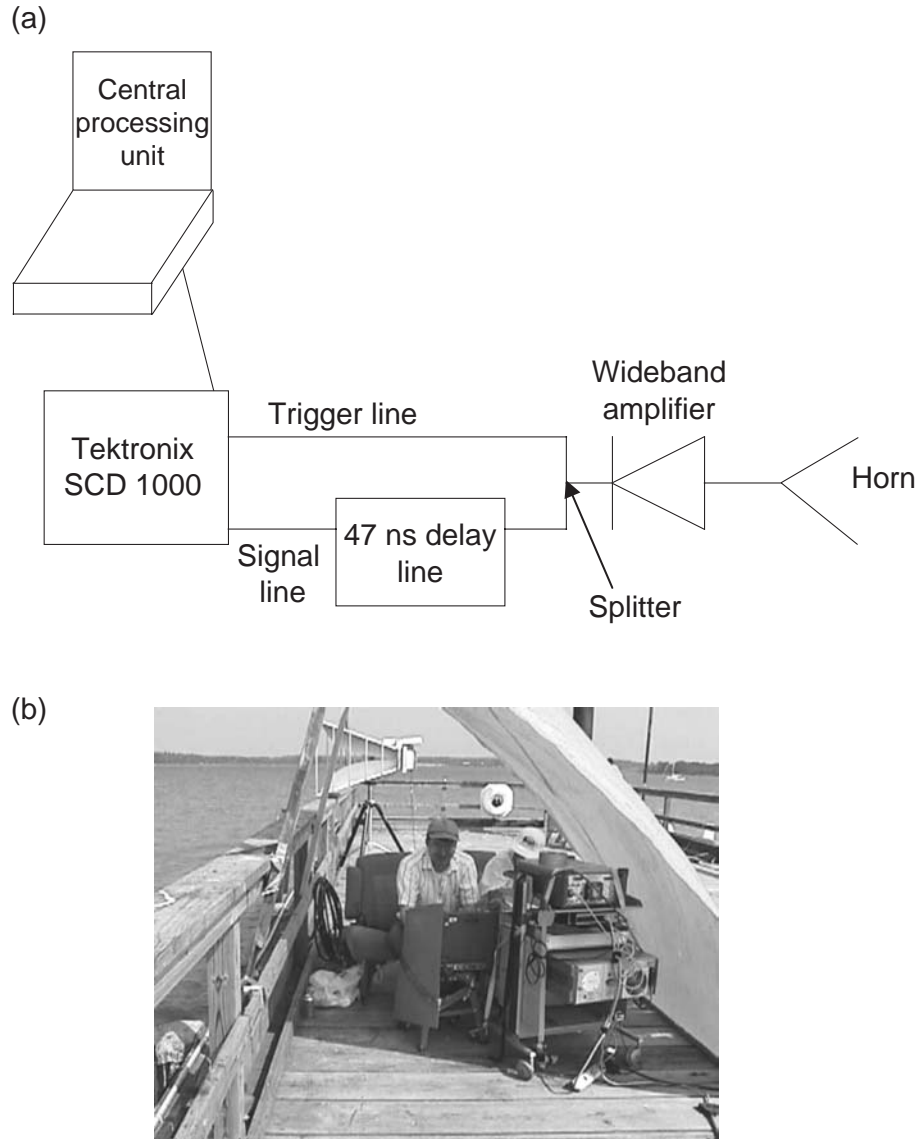
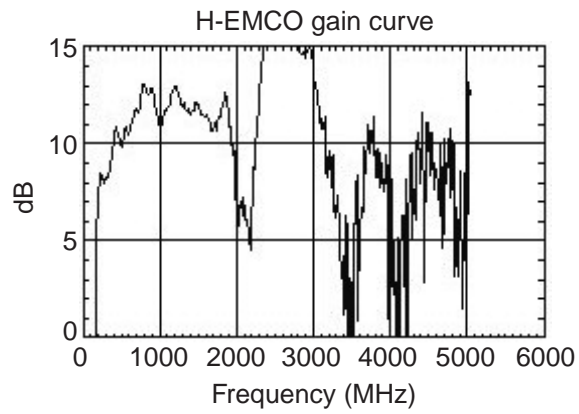


Figure 3. Frequency-domain amplitude calibration of EMCO double-ridge waveguide horn.



Before any meaningful data could be acquired on the targets, we had to determine the environmental background noise. Data was collected in all four quadrant directions—at 65°, 155°, 245°, and 335° with respect to true north. Each direction lagged the previous one by 90°. Plots of the background noise appear in figure 4. Data was collected for 2 min in each direction.

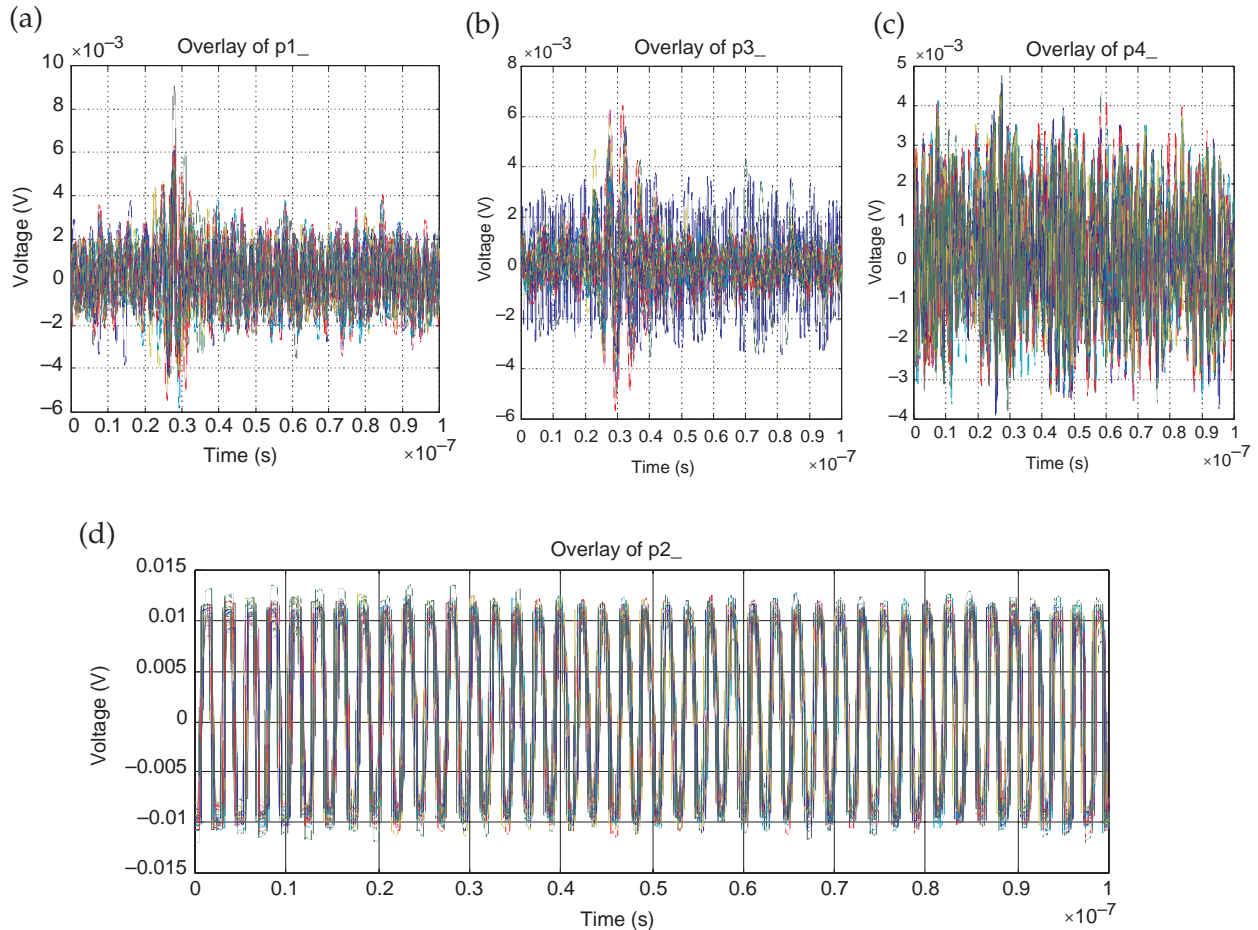


Figure 4. Environmental Background Noise at (a) 245°, 6 mV; (b) 65°, 6 mV; (c) 335°, 4 mV; and (d) 155°, 12 mV.

Table 1 displays all the data sets collected during the field test. The first four data sets (p1–4) contain background noise in the four different directions just described. The next group of data sets (pb1–5a) was collected from the Yamaha engine. The data set pne1 was collected from the NESEA. The final group of data sets (pbl 1–12) was collected from the dual 150 OMC.

The information in table 1 is organized into the following eleven columns:

1. Lists the data set series names.
2. States the trigger level the SCD 1000 was set to.
3. Lists the time delay in the delay line for each run.
4. Lists the internal delay.

5. Lists the boat position.
6. Indicates whether the wideband amplifier was in operation during the run.
7. Provides commentary about what is stated in the “boat position” column.
8. Provides an informal name for a particular boat.
9. Lists how many shots or waveforms are recorded in each data set.
10. States the day in June 2000 on which the test was run.
11. Lists the frequency component in the engine EM transient that had the highest amplitude.

Table 1. Data sets collected during field tests.

series name	mV trig lev	(ns) del line	int del	boat position	amplifier	comment	boat	# shots	Jun-00	freq pk	
p1	1	10	0	245		direction of walkaways	pleasure	30	27	433	
p2	1	10	0	155		towards radar tower	pleasure	30	27	433	
p3	1	10	0	65		towards coast guard station	pleasure	30	27	221	
p4	2.5	10	0	335		end of pier	pleasure	30	27	948	
pb1	10	10	0	dockside			pleasure	50	27		
pb2		10	0	dockside			pleasure	50	27	242	
pb2a		10	0	dockside			pleasure	50	27	369	
pb3	50	10	0	pull away (2)		.21 mi range	pleasure	100	27	383	
pb4		10	0	high speed circle (19)			pleasure	100	27	403	
pb5	3	30	0	sweep (6)		1 sweep is back and forth	pleasure	36	27	262	
pb5a	3.5	10	10	sweep (6)	amp		pleasure	114	27	938	
pne1	5	10	10	high speed circle (15)		.4 mi range, reduced speed after 66	nesea	107	27	393	
pbl1	5	10	10	high speed circle (17)		.22 mi range	whaler	105	27	292	948
pbl2	3.5	30	20	sweeps (6)	amp		whaler	116	28	786	
pbl2a	1	30	20	sweeps (10)			whaler	108	28	363	
pbl3	25	30	20	starboard dockside			whaler	50	28	292	
pbl4		30	20	portside			whaler	50	28	302	
pbl5		30	20	portside		port engine only	whaler	50	28		
pbl6	17 to 25	30	20	portside		idle/4k rpm alternate	whaler	50	28	635	
pbl7	20	30	20	portside		starboard only	whaler	50	28	302	
pbl8	25 to 30	30	20	portside		alternate	whaler	50	28	272	
pbl9	20 to 50	30	20	portside		pretrigger definition	whaler	40	28	282	
pbl10	20 to 5	30	20	portside		A1 line	whaler	50	28	312	
pbl11		30	20	portside		hi rev	whaler	50	28	322	221
pbl12		30	20	portside		lower trig lev	whaler	50	28	322	
						total shots		1546			

Note: The first four entries in column 5 are the number of degrees off of true north for the environmental noise measurements. For the three boats, there are various entries. "Dockside" indicates the boat remained stationary at dockside. "Pull away" indicates the boat traveled in a perpendicular direction away from the dock. "Speed circle" denotes traveling in a circle (figure 5(a)). The diameter of a circle for a given run is listed in the comment column. Its point of closest approach is 10 ft from the dock. For instance, the pbl1 run has ".22 mi range" for its comment; therefore it traveled in a circle with a diameter of 0.22 mi. "Sweep" refers to traveling back and forth along a line (figure 5(b)). The number in parenthesis to the right of a maneuver indicates the number of times it was executed. "Starboard" or "portside" for the dual 150 OMC indicates which of the two engines was running (figure 6).

Figure 5. Two boat courses close to dock: (a) sweep circle, and (b) sweep.

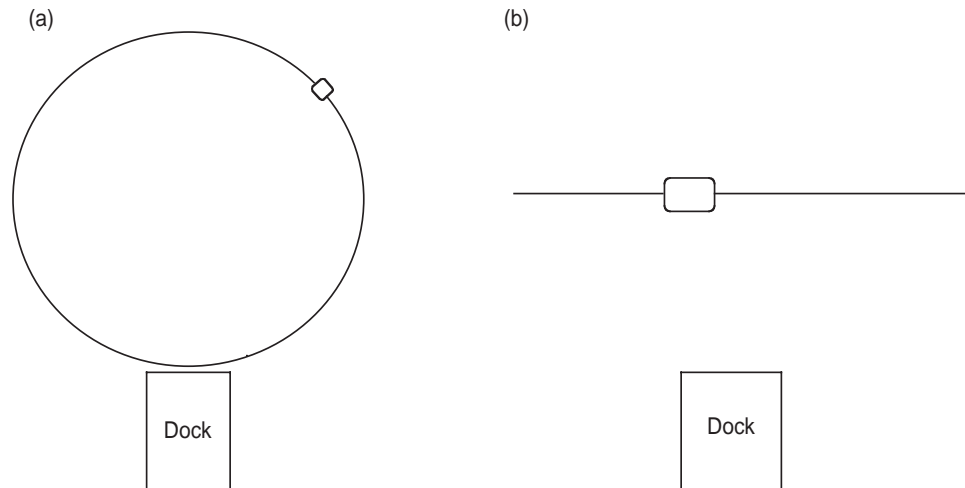
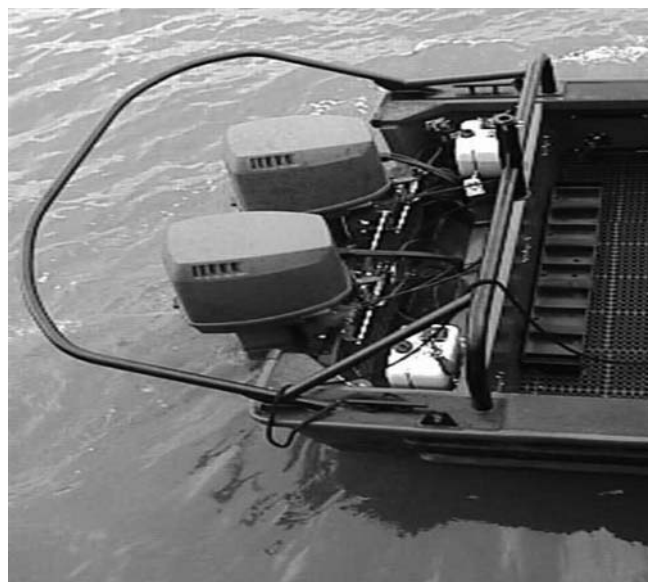


Figure 6. Dual 150 hp OMC outboards.



Results

This section compares the differences in transient emissions due to several parameters. These comparisons include finite range of transient, variations due to engine rpm differences, two-of-a-kind of the same engine model, amplification of received transient, and shielding effectiveness.

Figure 7 compares the starboard and port-side engines for the OMC. Note that the starboard-side voltage plot has a vertical scale of 100 mV/div, and the port-side voltage plot has a vertical scale of 50 mV/div. The port engine amplitude is about one-half that of the starboard engine. The frequency amplitudes of the two engines are similar.

In comparing the starboard and port sides of the Yamaha, we see that they both have a frequency peak at 250 MHz, but otherwise we need to collect more data to do a good comparison. Note that the voltage plots in figure 8 (a) and (b) have a vertical scale of 50 mV/div.

The plots in figure 9 provide the results of two sweep runs that were identical, except that the run represented in (a) employed no amplification whereas that in (b) did. The amplification introduced some noise, as can be

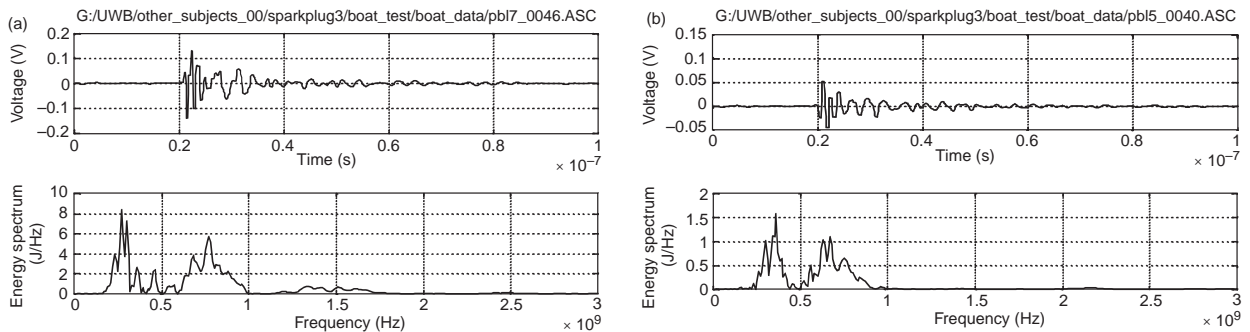


Figure 7. Comparison of amplitude and frequency for (a) starboard and (b) port Engine for OMCs.

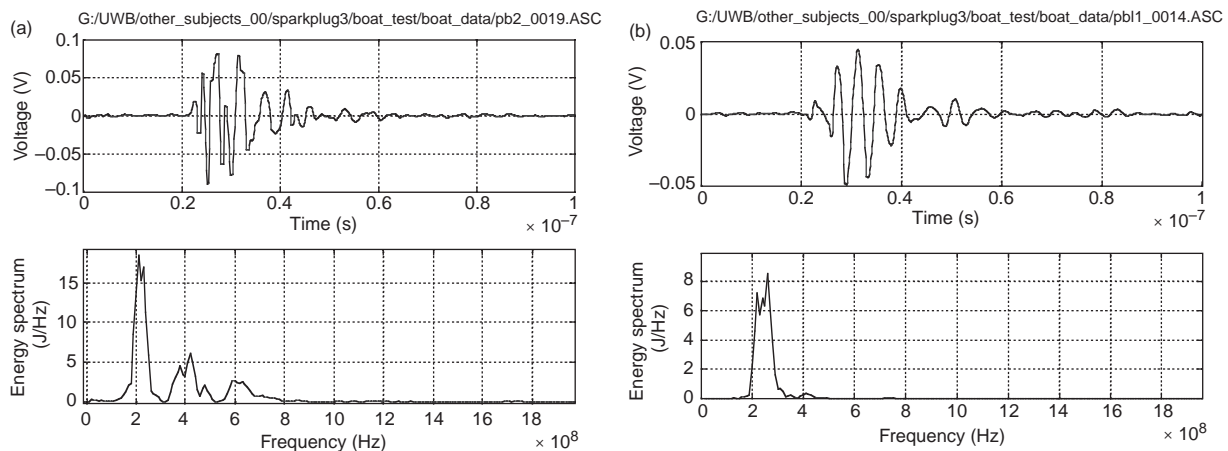


Figure 8. Comparison of (a) starboard and (b) port sides for Yamaha.

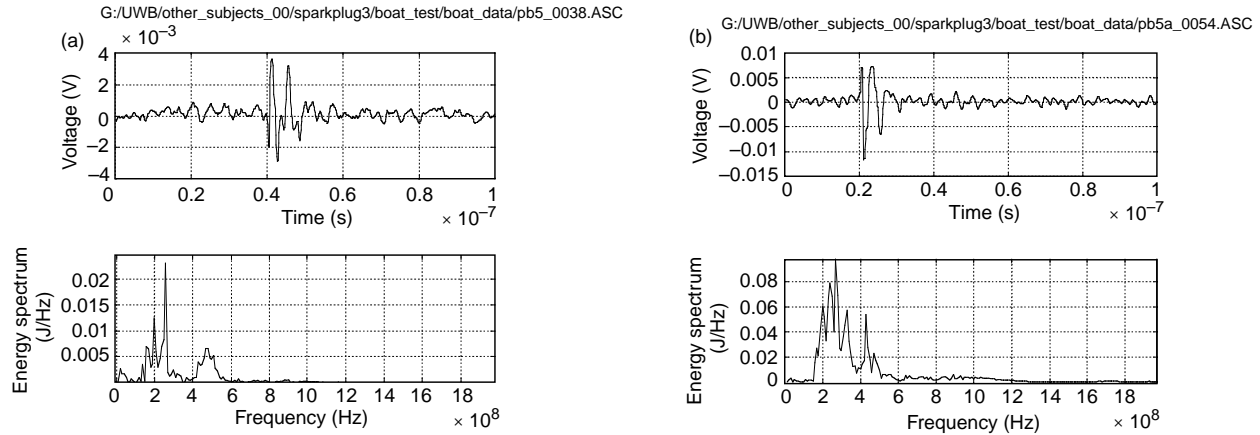


Figure 9. Comparison of shot signal (a) without amplification and (b) with amplification.

observed by comparing the voltage plots. This was to be expected. The amplifiers also invert the signal. Another result is that amplification made some of the higher frequency components more visible on the linear scale. Without amplification the frequency curve extended out to about 900 MHz, whereas with amplification it extended out as far as approximately 1.3 GHz.

We next compare the OMC engine at idle with that engine at high revolution (figure 10). The idling engine has a voltage amplitude an order of magnitude larger than that of the high revolution engine in the first 20 ns and then settles down to a lower amplitude, in the subsequent 20 ns, that is close to that of the high revolution engine. The idling engine has a frequency spectrum extending out to 2.5 GHz, but the frequency spectrum of the high revolution engine has a much narrower frequency spectrum. Its spectrum has no components above 450 MHz.

Next, let us confirm that voltage and frequency plots from different boat engines are easy to distinguish from each other. By the same token plots of the same boat engine but from different shots should look very much alike. A comparison of figures 11, 12, and 13 shows that this is, in fact, the case.

If a means of spotting a boat by the EM radiation from its engine is developed, those traveling on such boats may try to conceal the engine by utilizing shielding. The OMC engine was lined with aluminum foil to provide it with electrostatic shielding. The effect of shielding appears in figure 14. The foil attenuated the emissions by 14 dB. The frequency components in the energy spectrum above 500 MHz were attenuated even more.

Appendix B contains slides with plots displaying the results of all except two runs. Each slide with plots represents the results of one run. One plot is a “waterfall” plot, which is a composite of all the shots comprising the run. Each waveform in the waterfall is a plot of voltage vs. time.

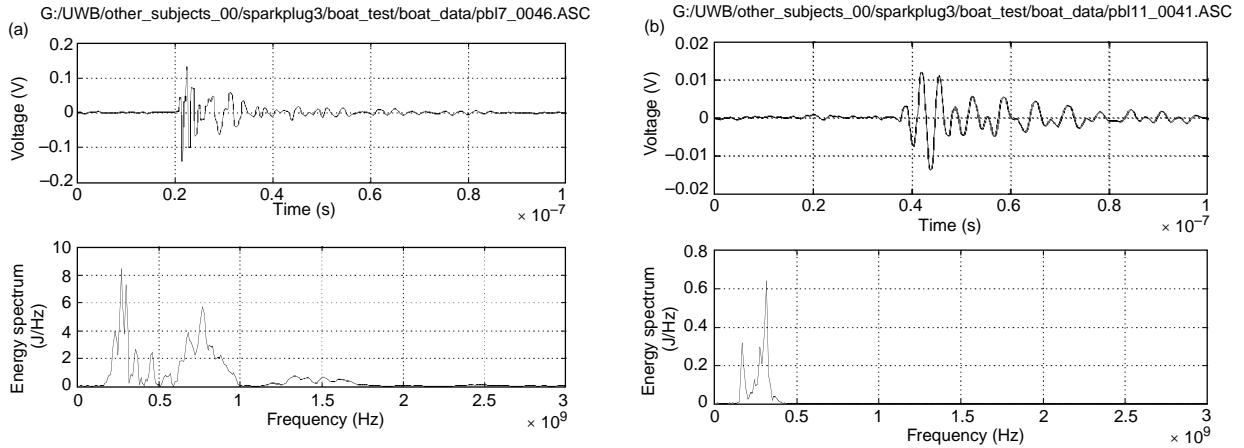


Figure 10. Comparison of an engine (a) at idle (b) with high revolution.

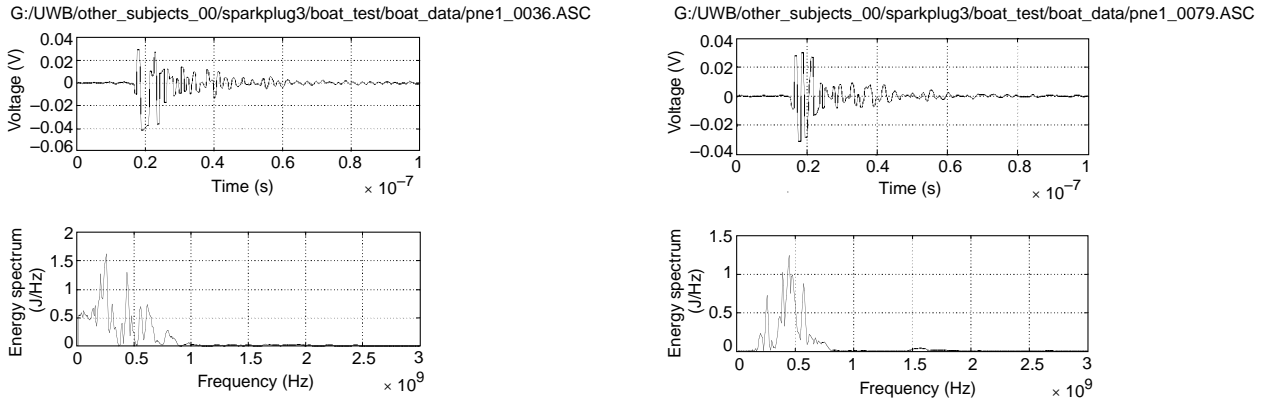


Figure 11. NESEA plots showing the energy spectrum and voltage for two independent shots.

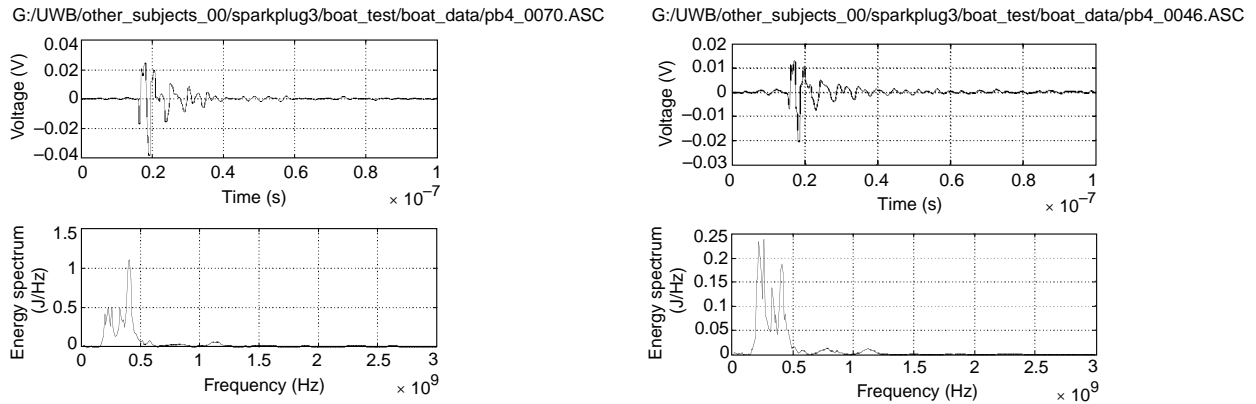


Figure 12. Yamaha 200 plots showing the energy spectrum and voltage for two independent shots.

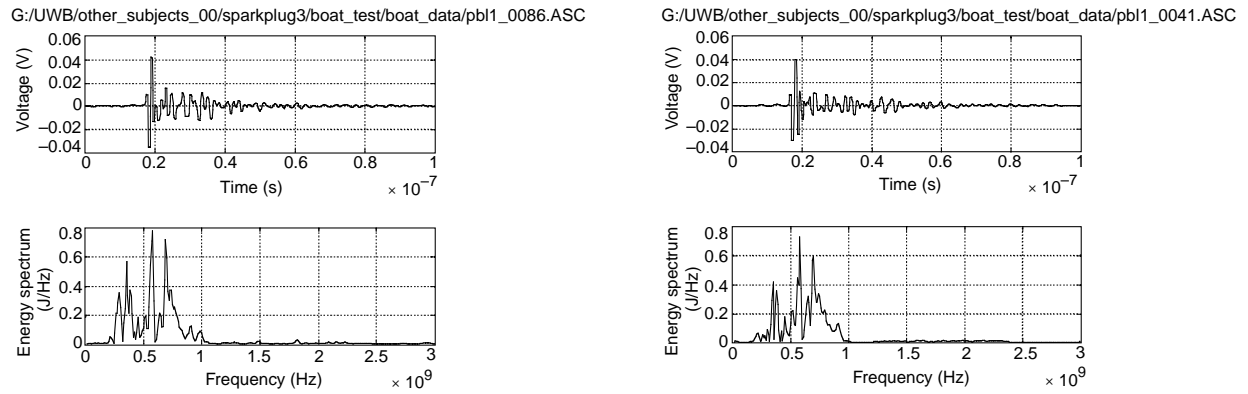


Figure 13. Comparison of two shots of the dual 150 OMC engine.

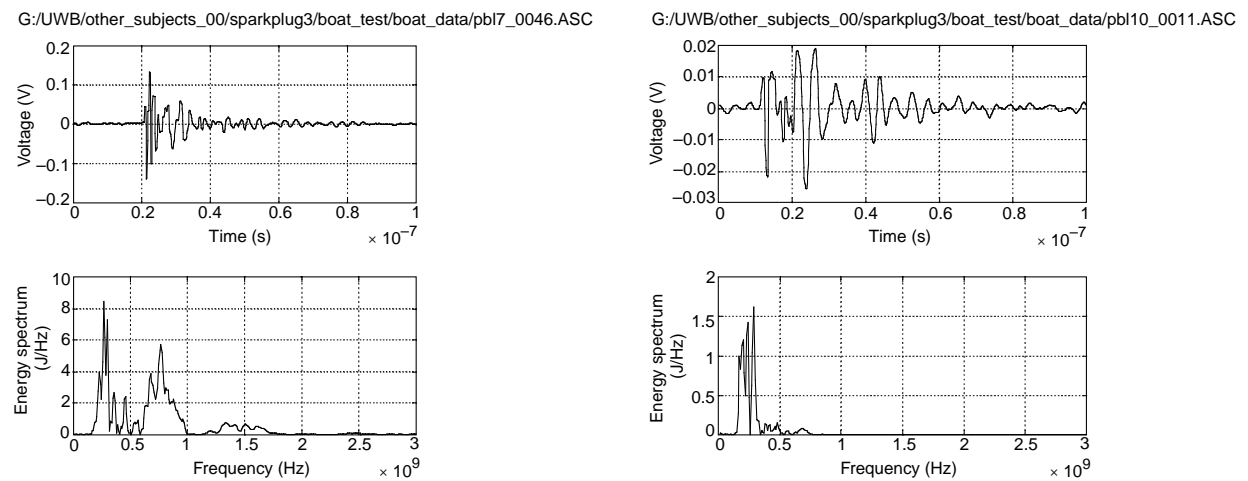


Figure 14. The EM emissions of the OMC engine (a) without foil and (b) with foil.

The upper right-hand plot in each slide is a semi-log scatter plot of amplitudes. The horizontal axis represents frequency in MHz, and the vertical axis represents amplitude in joules/Hz. The Fast Fourier Transform (FFT) of each of the waveforms in the waterfall is computed. From this FFT, the three highest amplitude peaks are selected. Each of these peaks is represented by one point on the scatter plot.

To make better sense of the data presented in the scatter plot, a histogram of the same data is plotted directly below the scatter plot. The frequency range along the horizontal axis is divided into bins. Each bin represents a range of frequencies. Each bin is equal in width. The frequency width of the bin in MHz appears above the histogram plot along with the number of shots for that run. The height of the histogram bar in a given bin represents the number of shots that had a top-three frequency in the frequency range represented by that bin. In the upper right-hand corner of the histogram the three most common frequency peaks are listed in numerical order. To the right of each frequency is the percentage of times that it was one of the top three frequency peaks of a shot.

The frequency peak data is summarized in figure 15. The plot on the left summarizes data collected from the Yamaha. This plot is based on data from all runs—dockside, pull-away, sweep and speed circle. The various frequencies are marked according to how often they occurred in all of the Yamaha runs. A blue diamond indicates that a frequency was the most common frequency peak in a run; a maroon square indicates a frequency was the second most common; and a yellow triangle indicates the third most common. Ovals highlight the frequencies with the most peaks in all the runs put together. There was a total of seven Yamaha runs. In some of these runs there was no third frequency peak, which accounts for the fact that there are only four triangles on this Yamaha plot. The frequencies with the most peaks for the Yamaha are 265, 220, and 240 MHz.

We applied the same analysis to the OMC frequency data, as is shown in the right plot of figure 15. Here the frequencies with most peaks are 300, 360, and 580 MHz. The frequency peaks from eleven runs comprise this plot. Only the pre-trigger and low trigger level runs were omitted.

Appendix A contains a sample waveform from each of the data sets. The upper plot in each slide is a plot of the sample signal itself (chosen because it is typical of the 50 or so waveforms that make up the data set). The lower plot is the FFT of the upper plot. The FFT allows one to determine the frequency content of the waveform. We are most interested in determining the frequencies present in the waveform with maximum amplitude. The peak frequencies stand out clearly in the FFT plots.

Appendix B contains slides with three figures on each slide that reflect the method of analysis performed on each data set. The left-hand plot is a waterfall plot consisting of a collection of the all the waveforms for that data set. The upper right-hand plot is a scatter plot of the frequency peaks for each of the shots making up a data set. The number of shots for each data set ranges from 36 to 114. The lower right-hand plot is a histogram of the

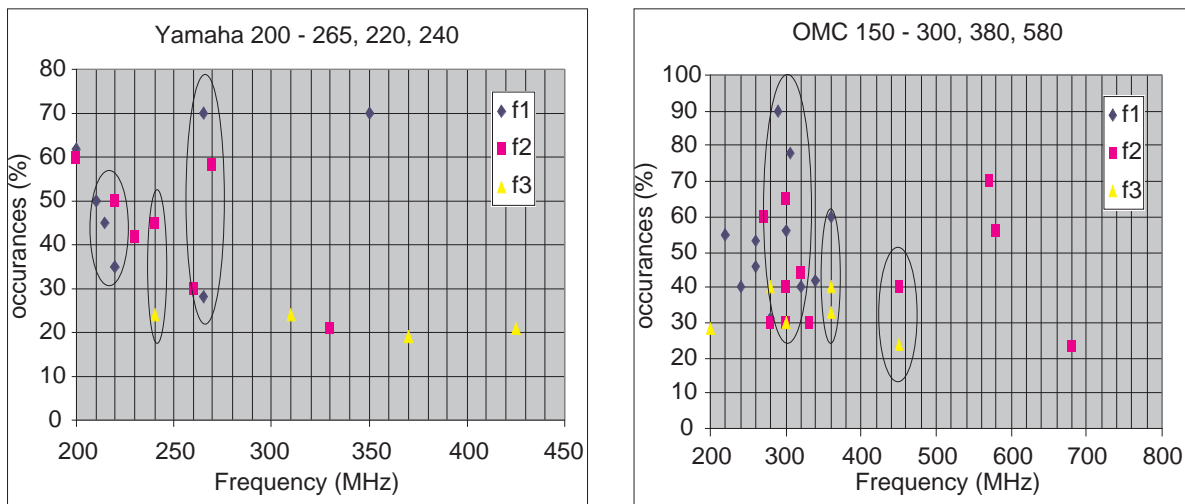


Figure 15. Frequency peak data for (a) Yamaha and (b) OMC.

frequency peaks. This enables one to determine the most common frequency peak and the number of times it appears in the complete data set. Analyses performed in appendix A and B show the principal frequency content expected from these targets.

Appendix C presents the time-frequency analysis of a spectrogram of each of the files in the sample library (appendix A). The value of this analysis is that it differentiates the waveforms in a manner more striking and clear-cut than the time or frequency components alone.

The Matlab program *jtfa_trunc*(filnam,tim1,tim2,maxfreq,width,overlap) generated the spectrograms in appendix C. Tim1 is 0 sec, tim2 is 0.1 μ sec, maxfreq is 1.5 GHz, the width of the window was 32 datapoints, and the overlap between windows was 6 datapoints. It was necessary to specify a maximum frequency of 1.5 GHz or the spectrogram routine would include spurious frequencies and aliasing up to 5 GHz because of the oversampled waveform. The peak frequencies appear with a reddish hue in a spectrogram. The frequencies with the lowest amplitude are blue. The plot on the bottom is the time plot of the voltage, and the upper left plot is a plot of the FFT. The signal in the spectrograms of pb datasets tend to be 10 ns wide, while the signal in the spectrograms of pbl datasets tend towards a width of 20 ns. The frequency content was analyzed in appendix B.

Conclusions

For both the OMC and Yamaha vehicles, the port and starboard engines had similar frequency peaks in their frequency-amplitude plots. Even though only two serial numbers were investigated, this leads us to believe that engine models can be identified through their frequency content for most of the serial numbers produced.

Amplification of a shot appeared to extend the dynamic range of frequency. An idling OMC engine has a voltage amplitude an order of magnitude larger than that of a high revolution engine at first and then settles down to an amplitude close to that of the high revolution engine. The engine at high revolution has a much narrower frequency spectrum than when at idle.

Time and frequency waveforms from different engines are unique and easy to distinguish. Time and frequency plots from different shots of the same engine look very similar (data is reproducible). This would indicate that perhaps time and frequency waveforms are appropriate and practical for engine identification.

Shielding an engine with aluminum foil proved to be inexpensive and effective, providing 14 dB of shielding. This would result in a factor of 25 decrease in power radiating out of the engine cavity. This means an observer would have to be at one-fifth the previous distance to observe a signal with the same amplitude.

This research project allowed us to compare the differences in transient emissions due to several parameters. These comparisons include finite range of transient, variations due to engine rpm differences, two-of-a-kind of the same engine model, amplification of received transient, and shielding effectiveness. Frequency components of each model type contain sets of frequencies that are unique and identifiable. These characteristics have several near-field applications.

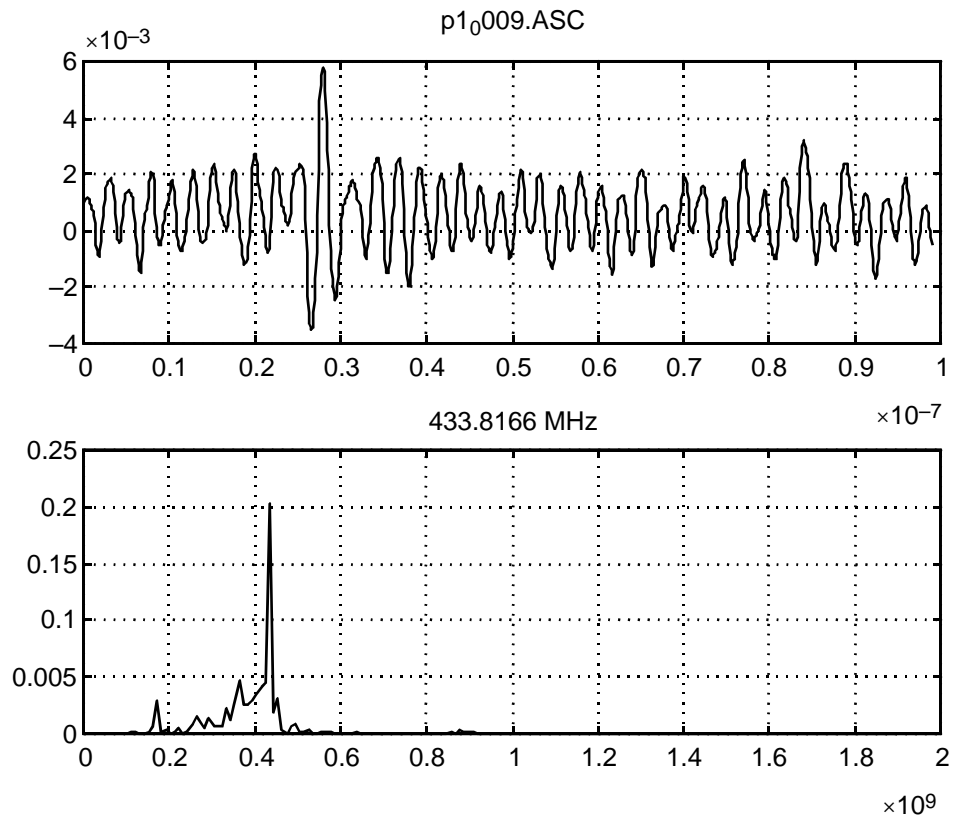
The range of measurements described in this report are all less than a mile, although the technique is not limited to these ranges. Solutions to the limited range of these measurements are varied. The primary difficulty in time-domain transient capture often lies in the triggering capability and trigger modes of the recording device. The triggering levels are often dependent on the background noise levels and the general noise clutter environment. This problem can be alleviated somewhat by a channelized filterbank. By splitting the wideband transient into many frequency bands, and time-correlating the results of the notched bands, a reliable presence detector could be fabricated that would enable signals close to the background noise floor to be identified and recorded for analysis purposes. This technique permits identification of the background noise, regardless of its level, and subsequent identification and detection of the new transient wideband signal in the presence of the background noise. Thus a low-level transient can be distinguished from background noise this way.

Appendix A. Sample Waveforms

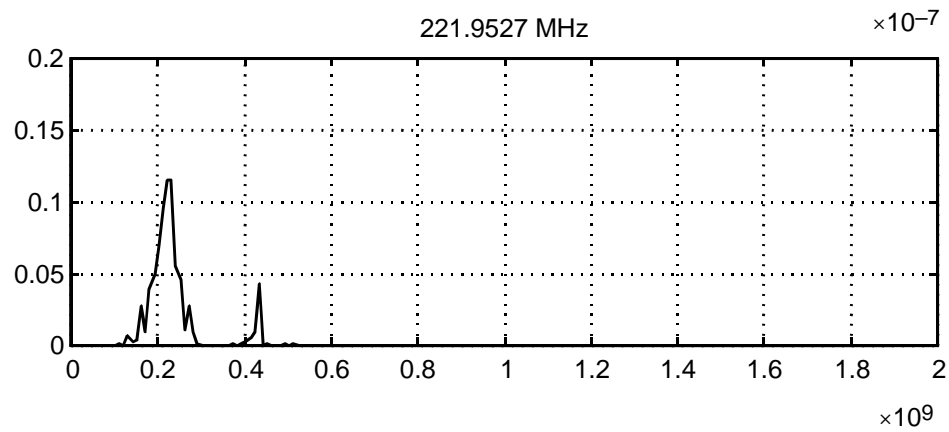
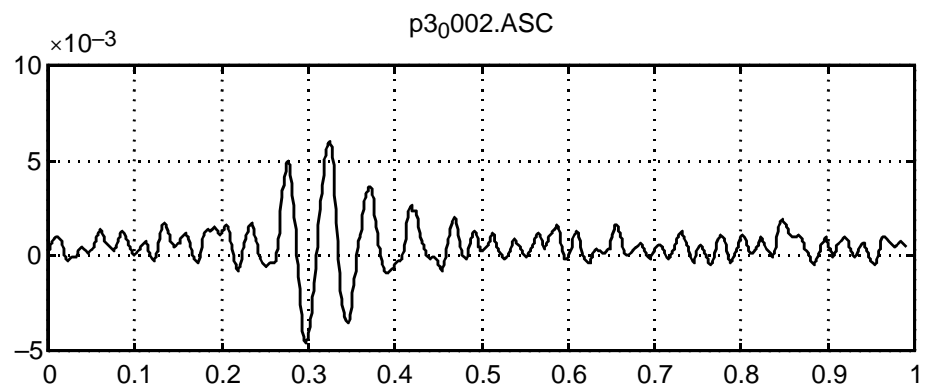
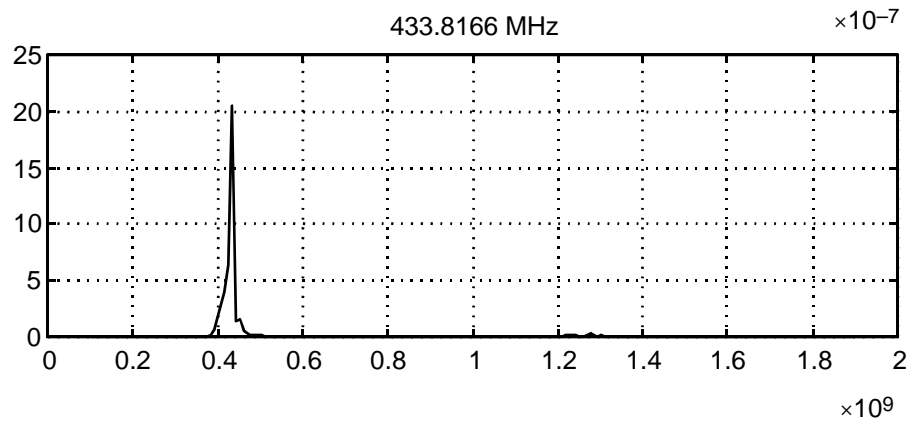
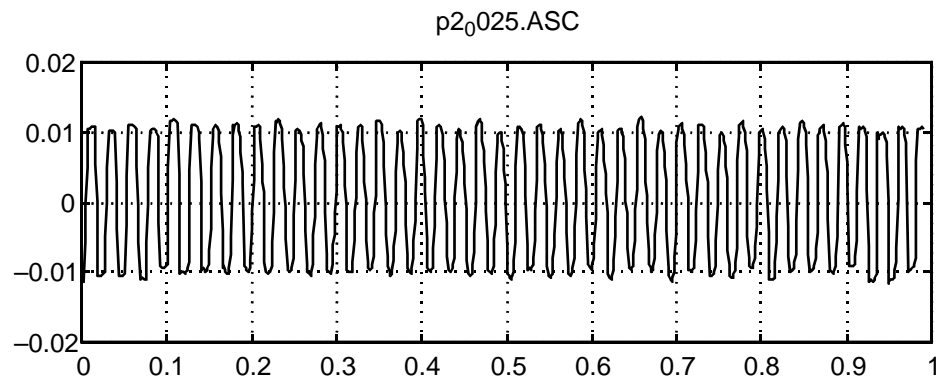
This appendix contains a sample waveform from each of the data sets. More than 1500 waveforms were acquired during the investigation. A typical waveform from each dataset was identified and displayed in this appendix.

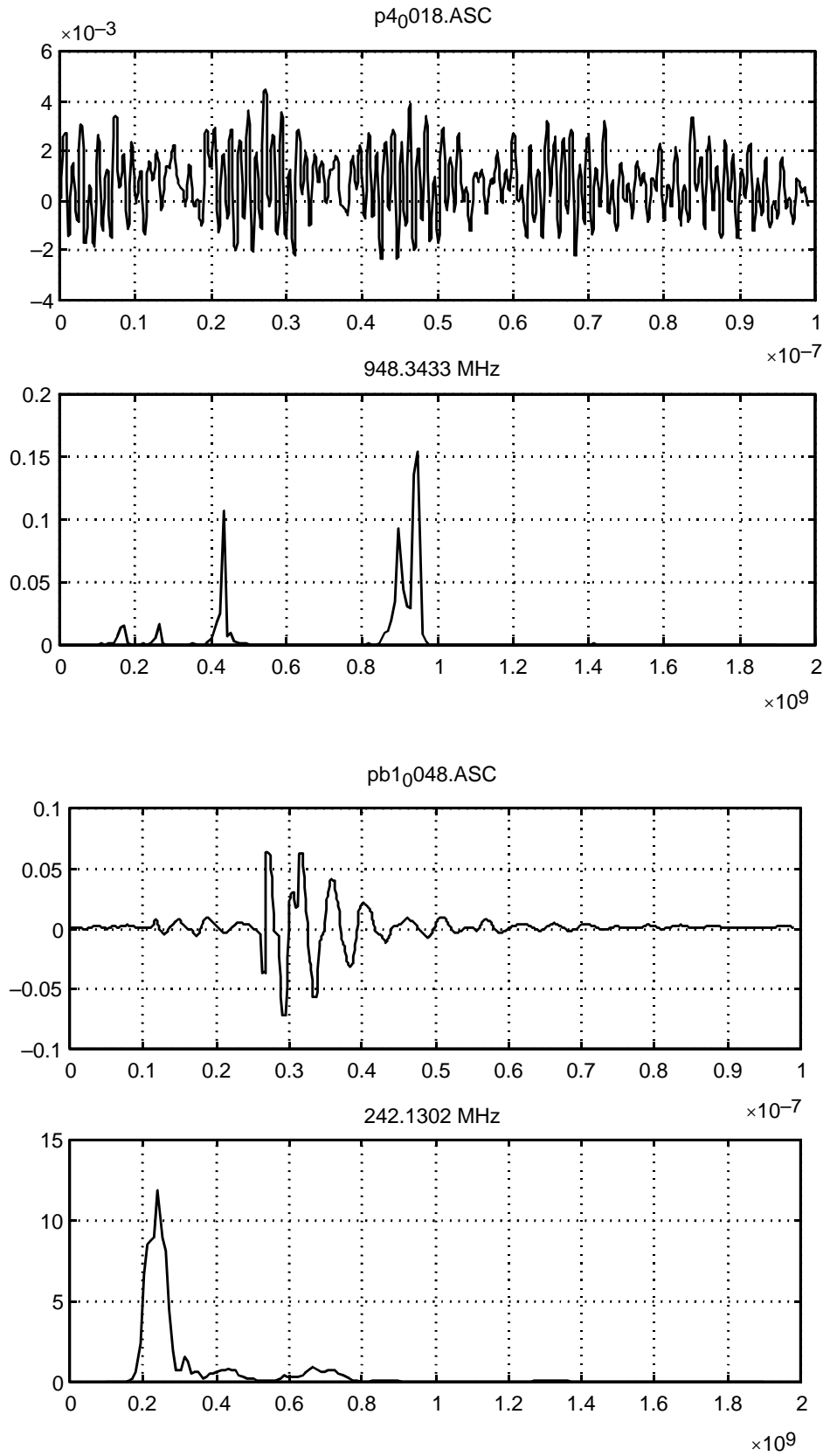
The upper plot in each slide is a plot of the sample signal itself (chosen because it is typical of the 50 or so waveforms that make up the data set). The lower plot is the Fast Fourier Transform (FFT) of the upper plot. The FFT allows one to determine the frequency content of the waveform. We are most interested in determining the frequencies present in the waveform with maximum amplitude. The peak frequencies stand out clearly in the FFT plots.

Filenames displayed for each waveform can be identified with particular vehicles using table 1 in the main text.

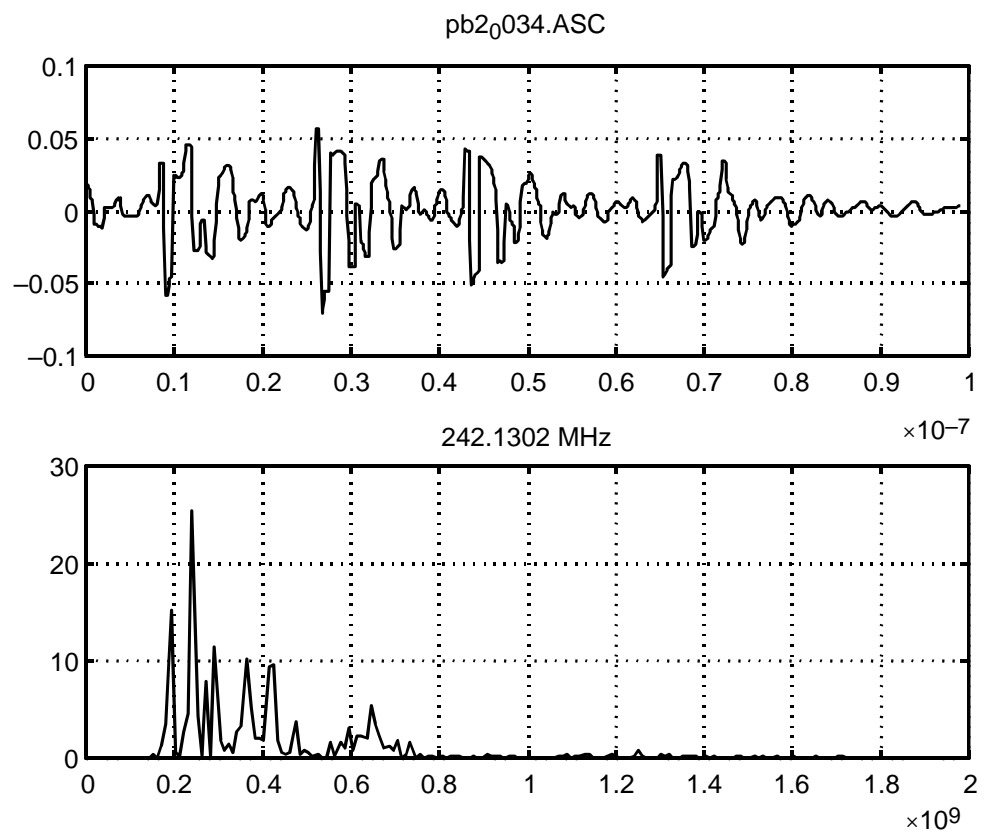
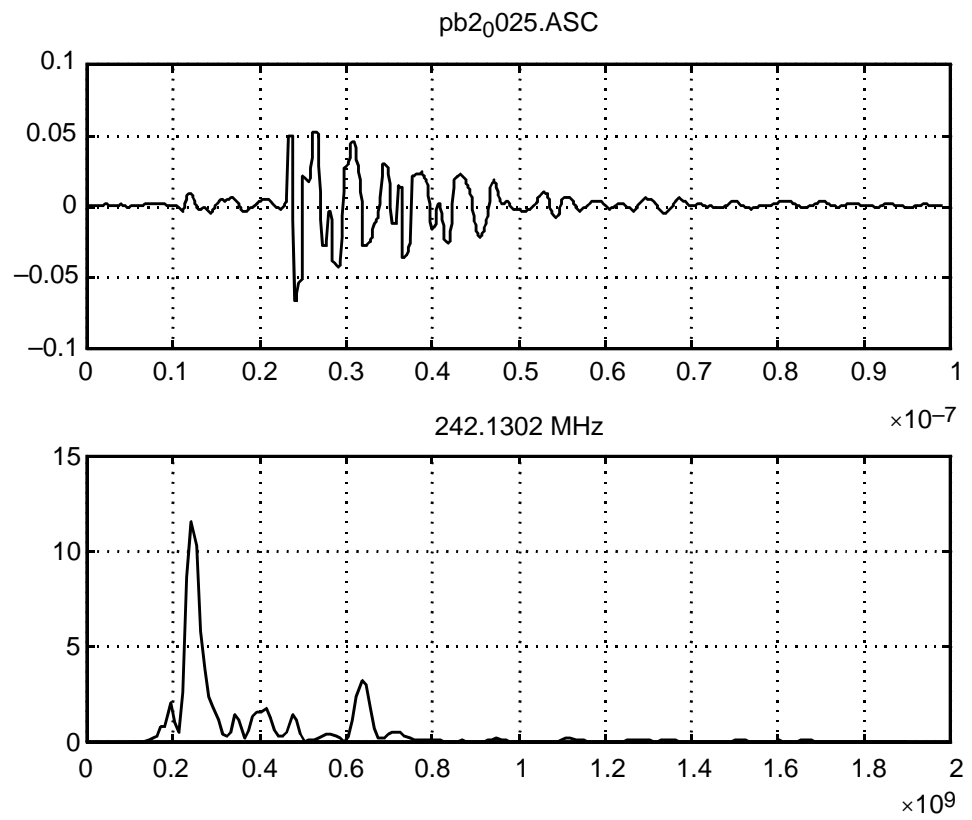


Appendix A

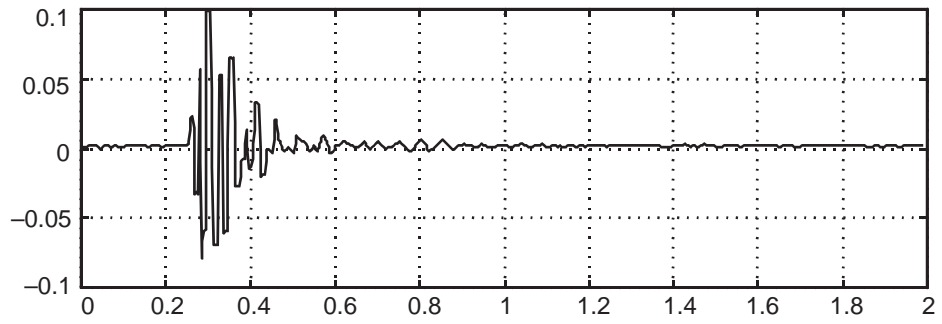




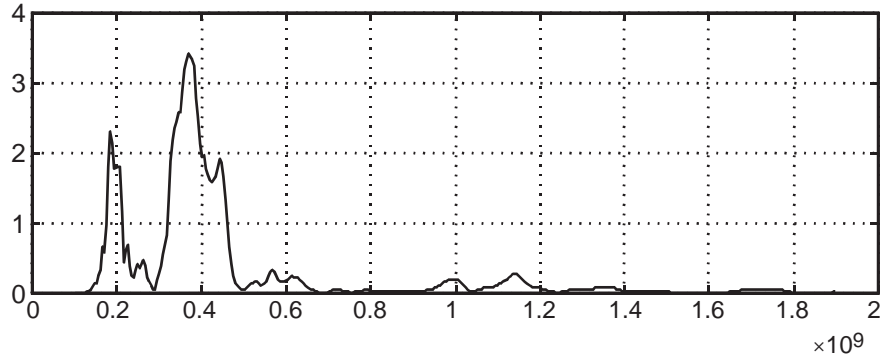
Appendix A



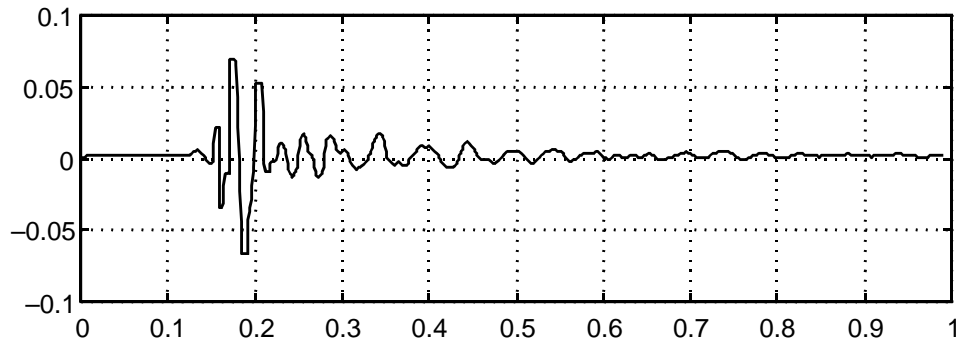
pb2a₀017.ASC



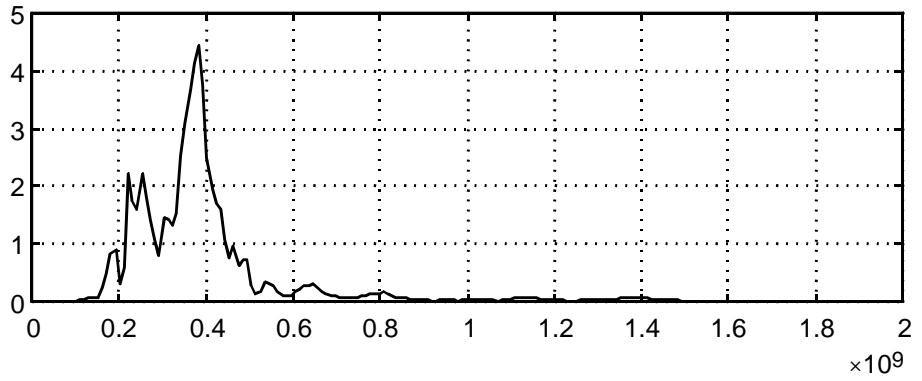
371.8181 MHz $\times 10^{-7}$



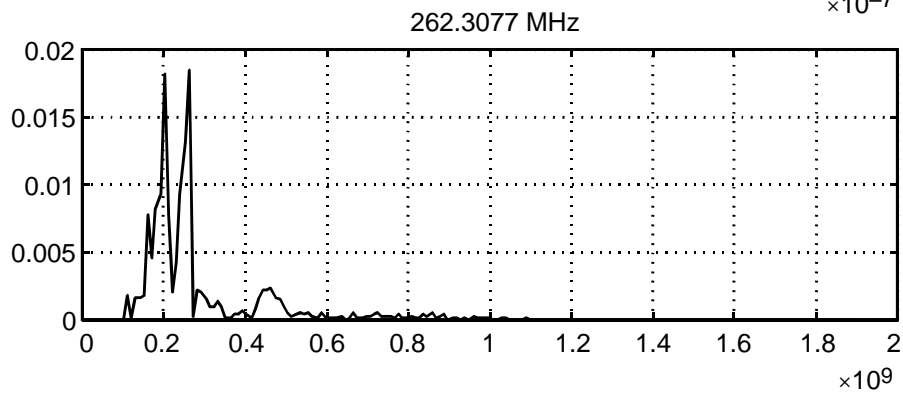
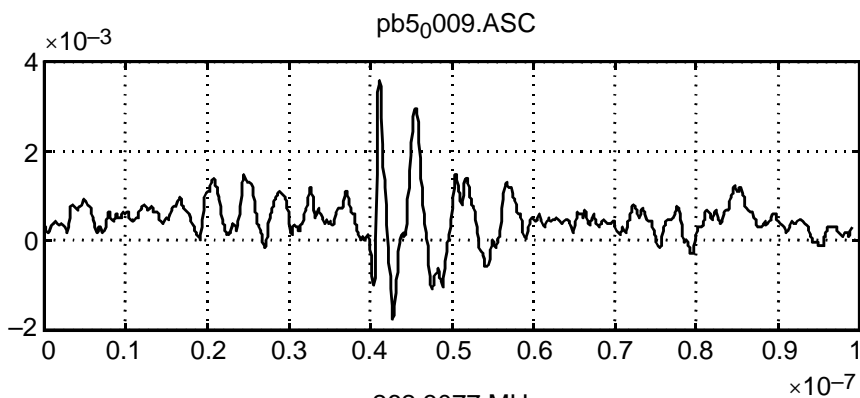
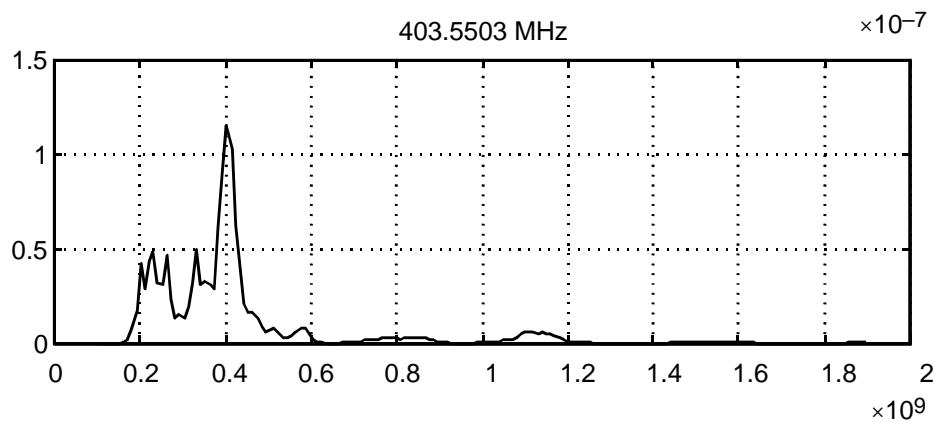
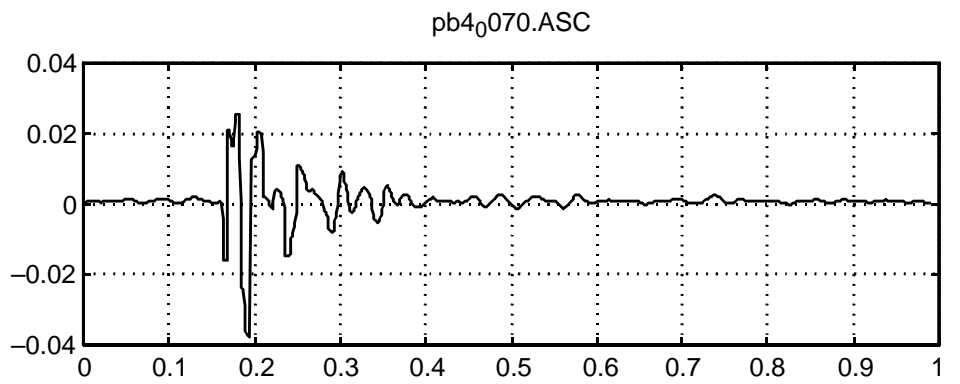
pb3₀004.ASC

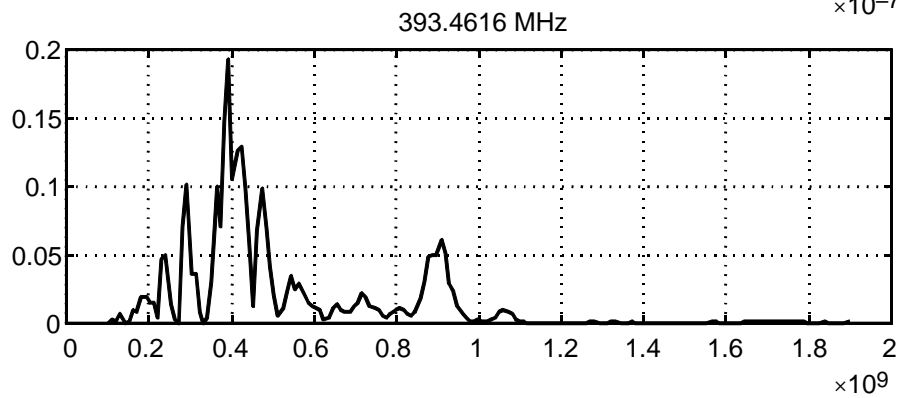
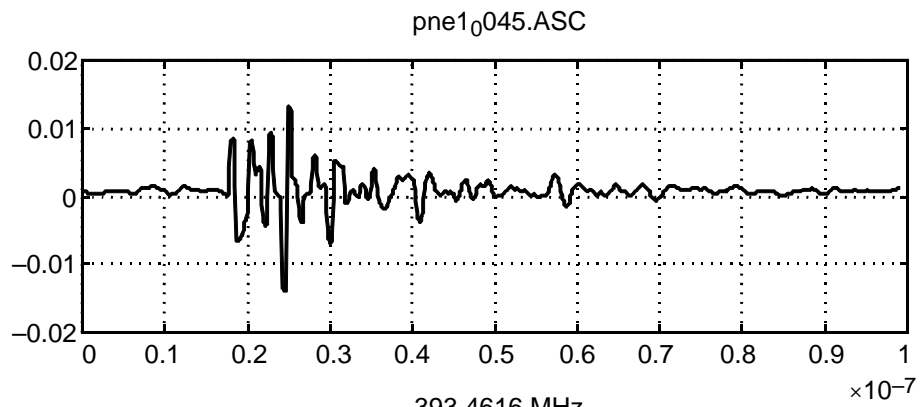
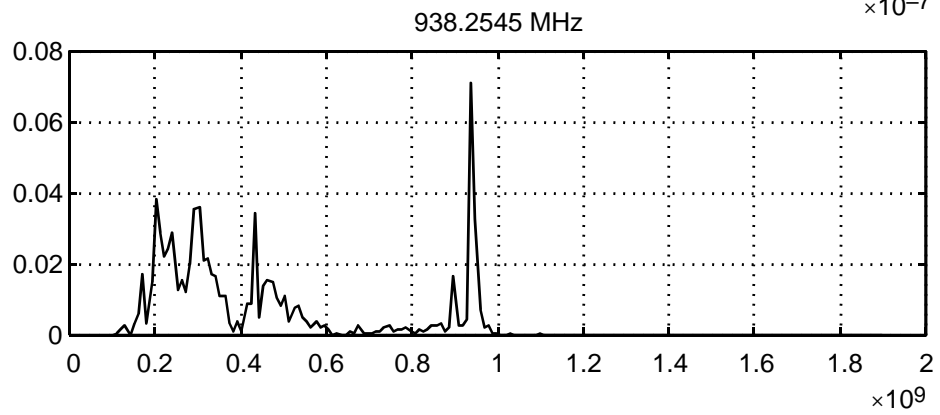
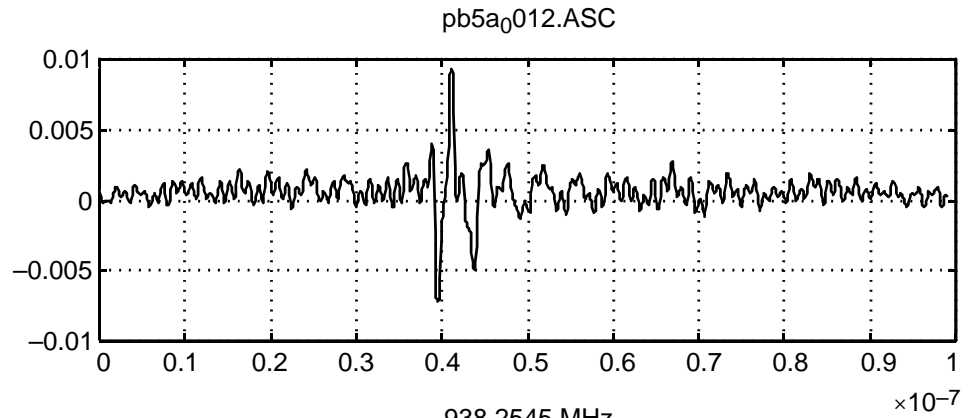


383.3728 MHz $\times 10^{-7}$

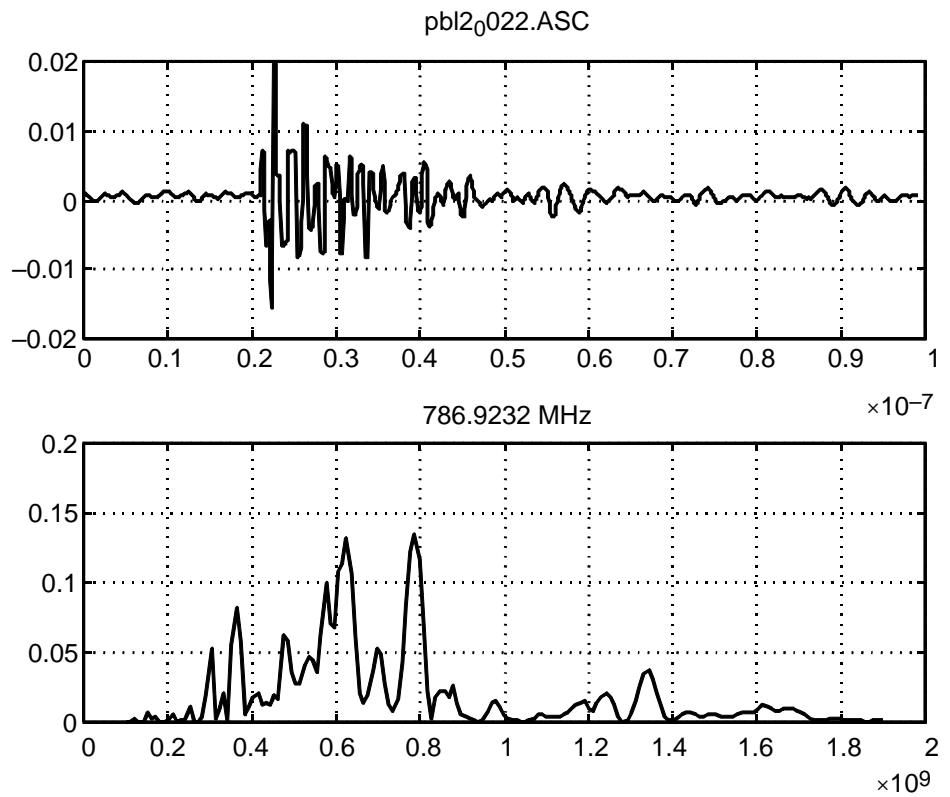
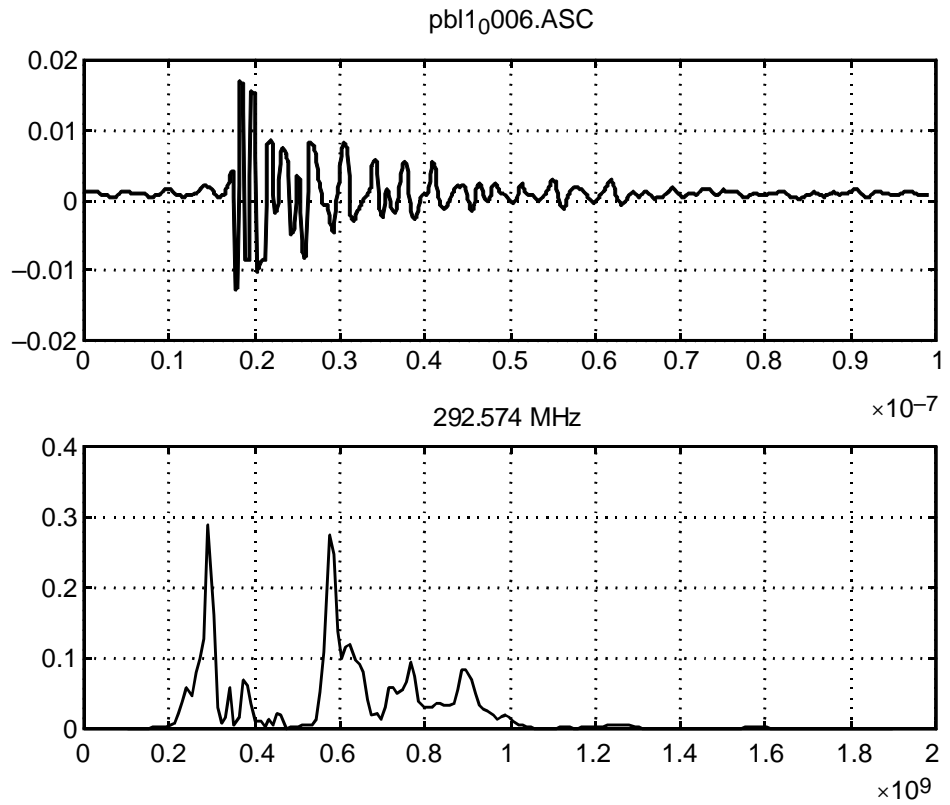


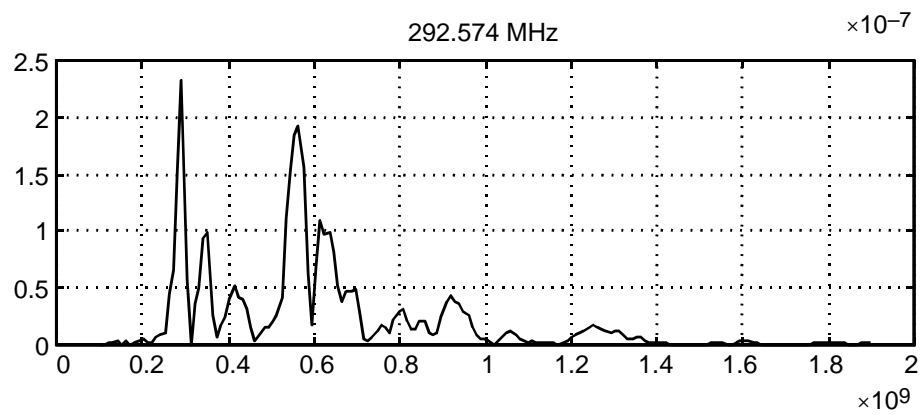
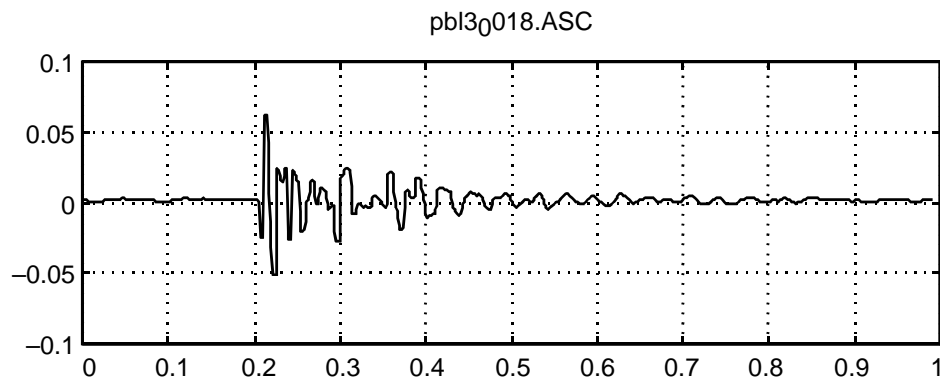
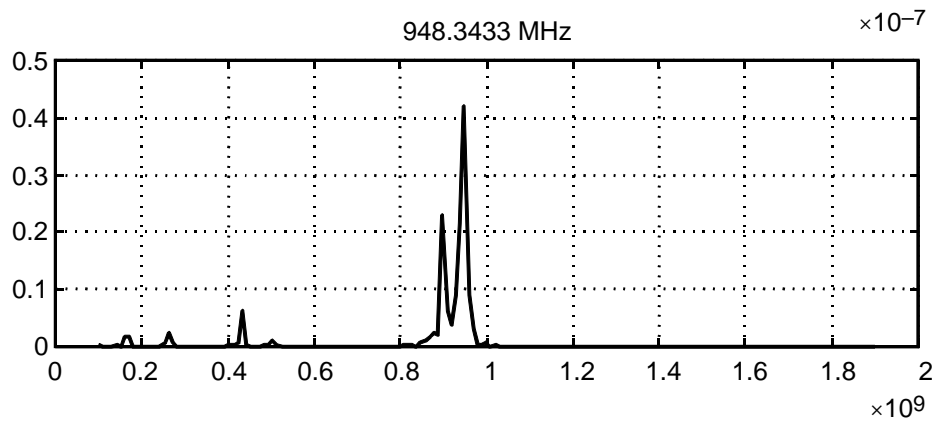
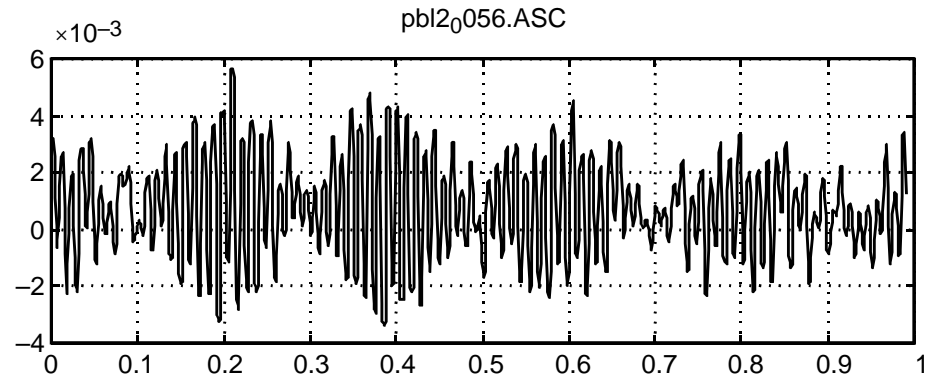
Appendix A



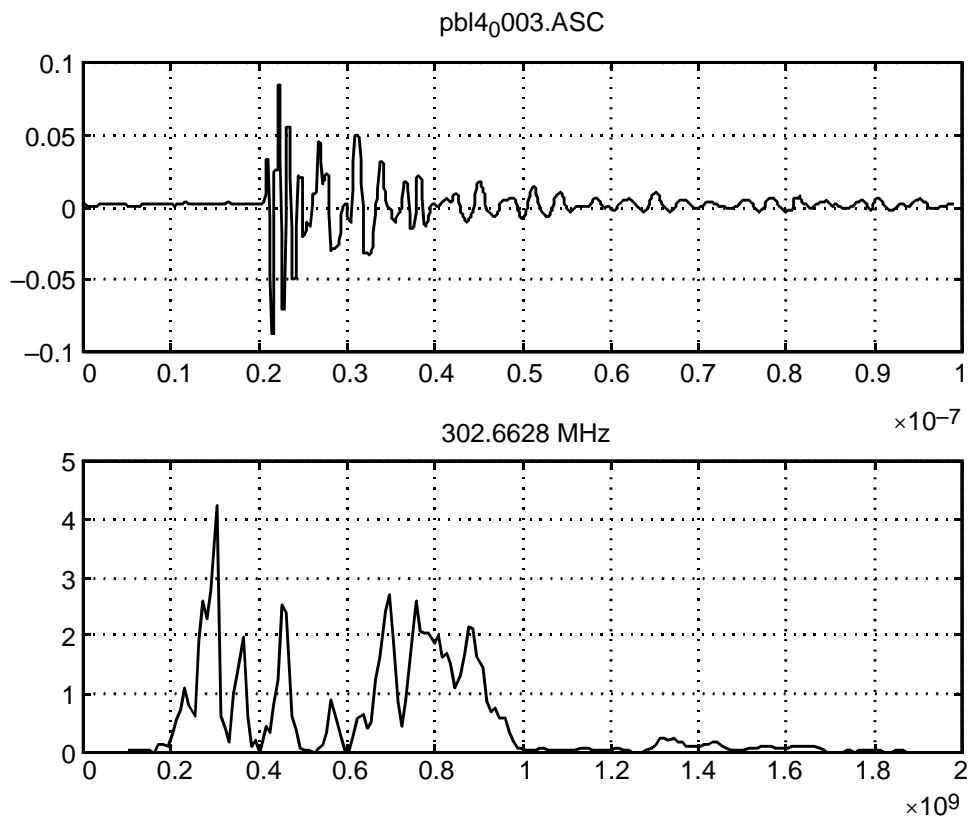
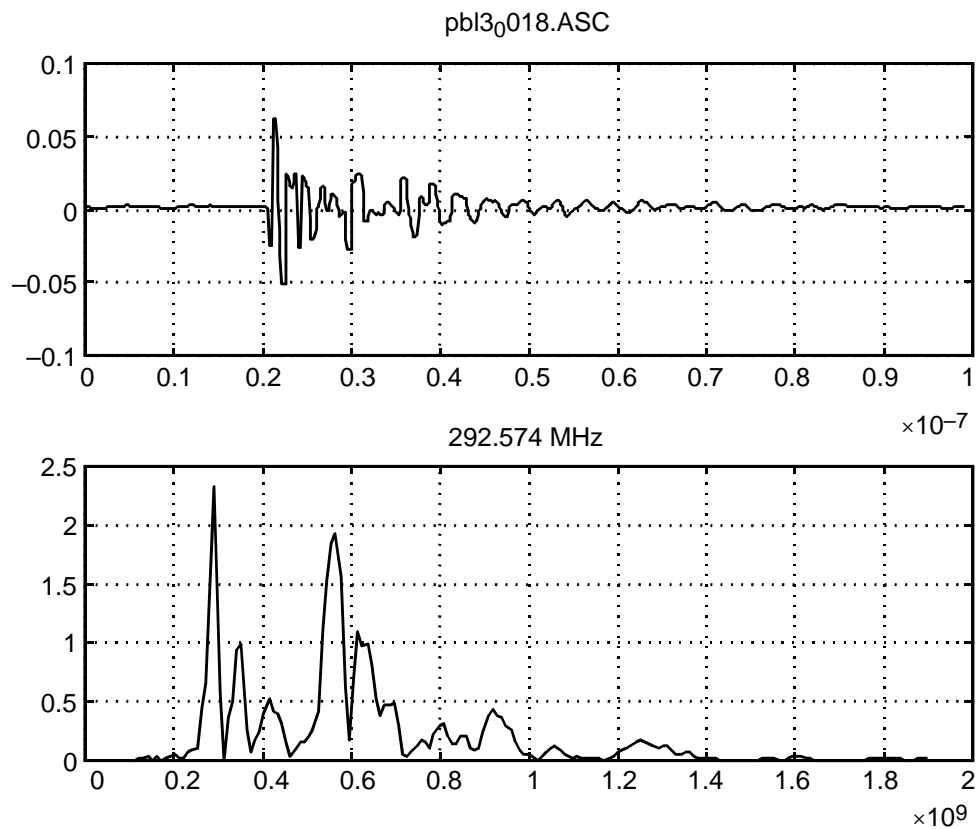


Appendix A

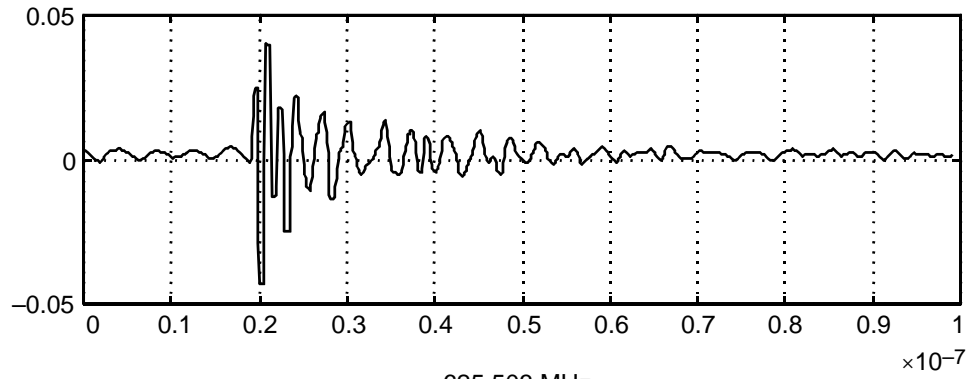




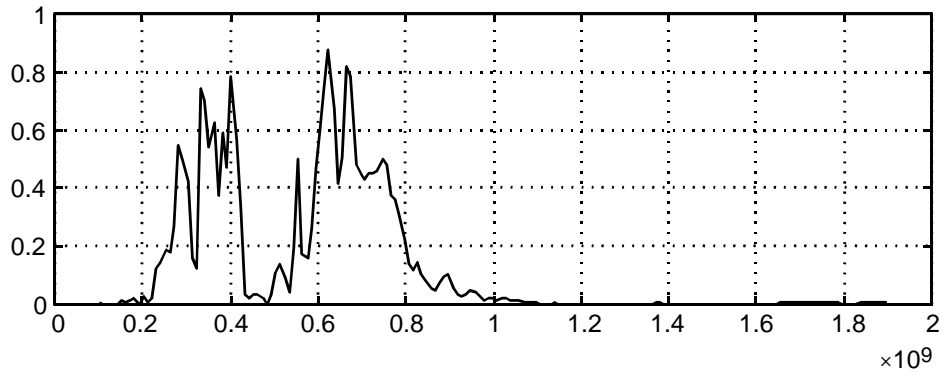
Appendix A



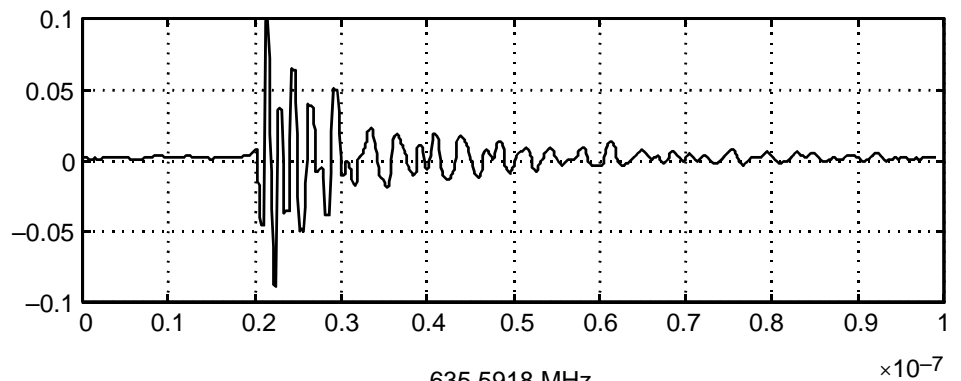
pbl5₀049.ASC



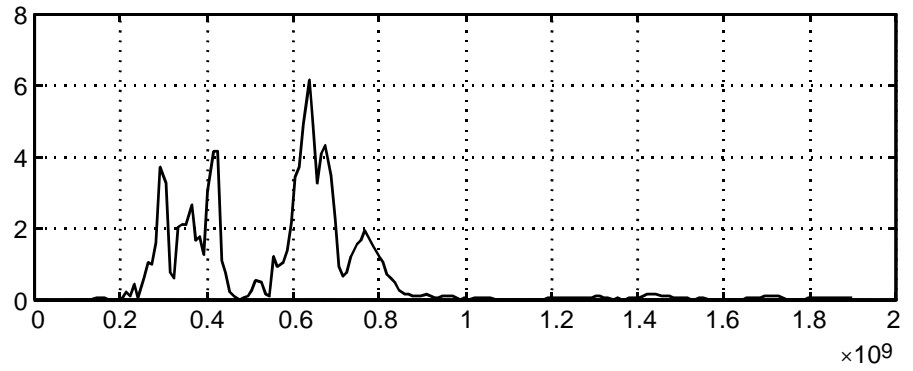
625.503 MHz



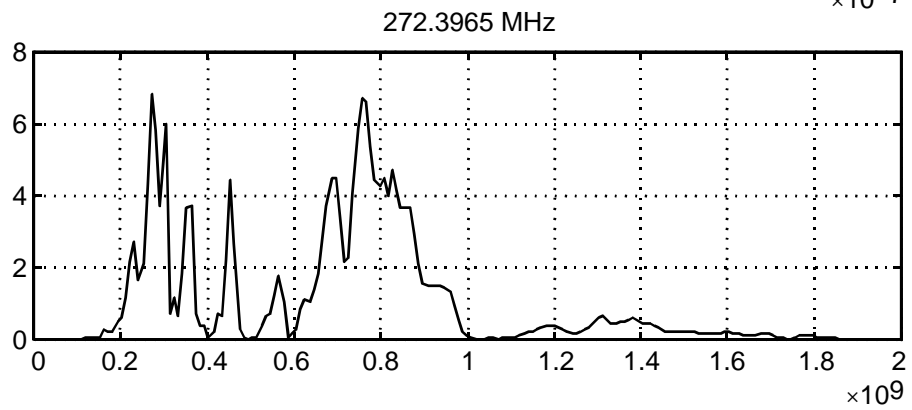
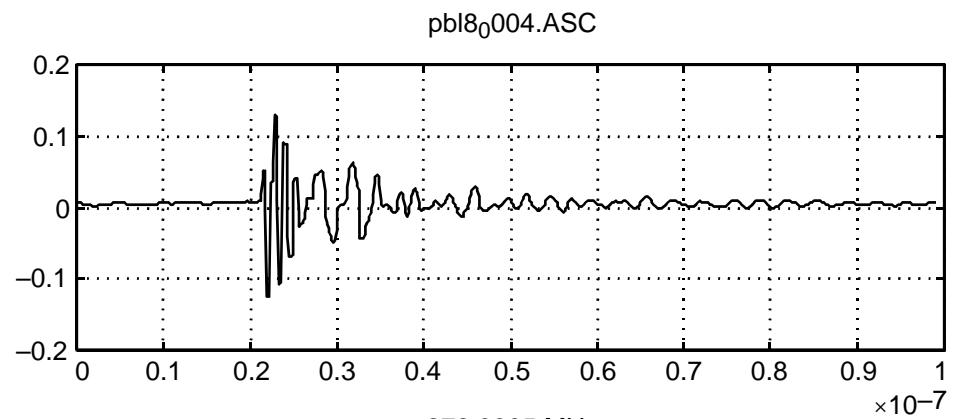
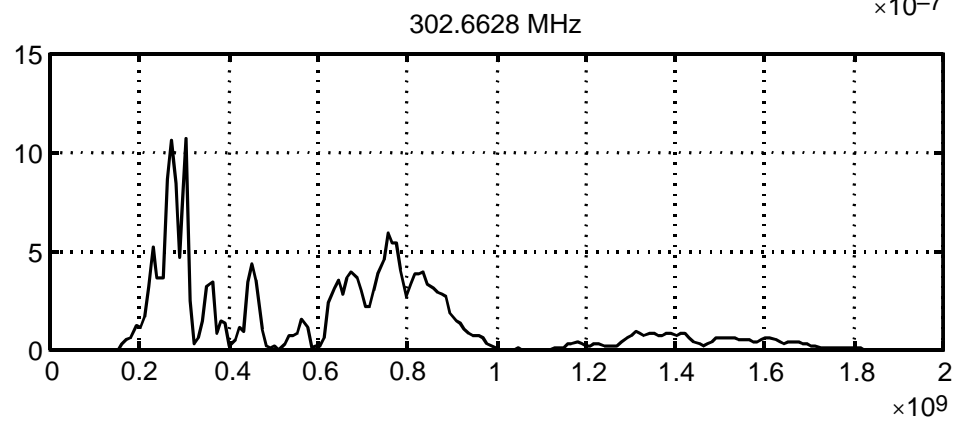
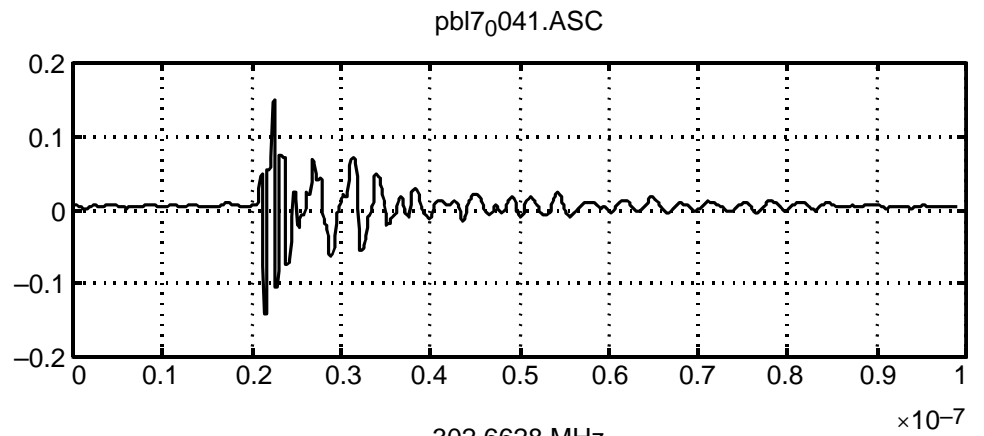
pbl6₀042.ASC



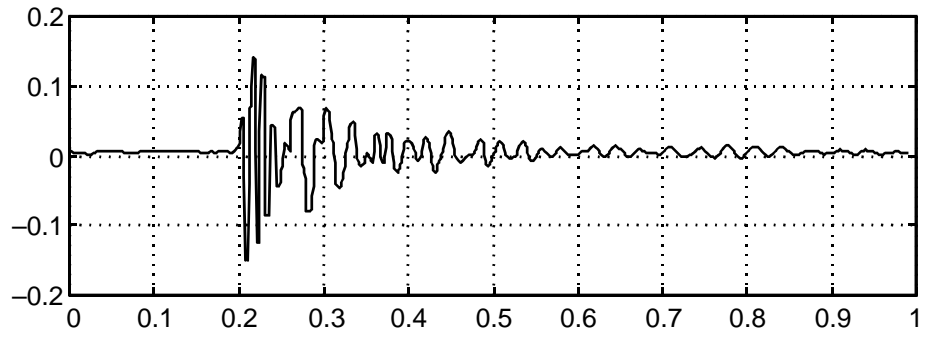
635.5918 MHz



Appendix A

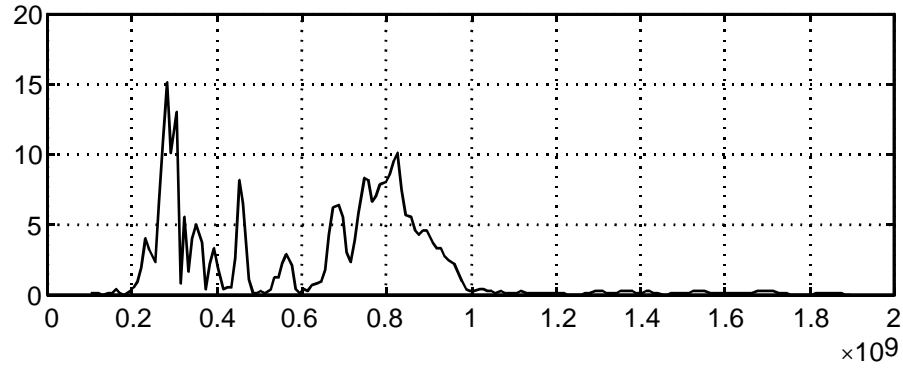


pbl9₀033.ASC

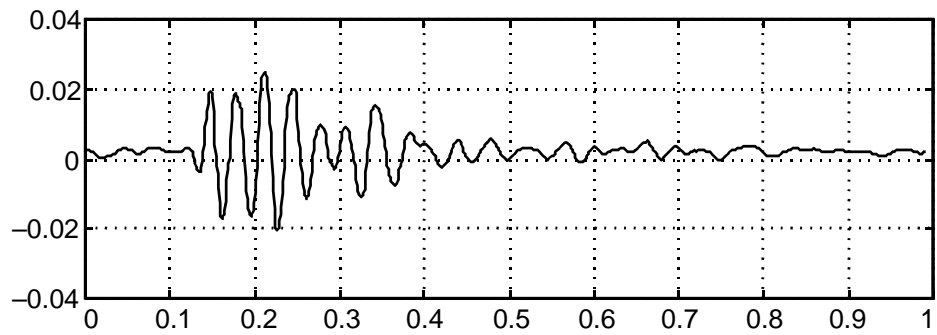


282.4852 MHz

$\times 10^{-7}$

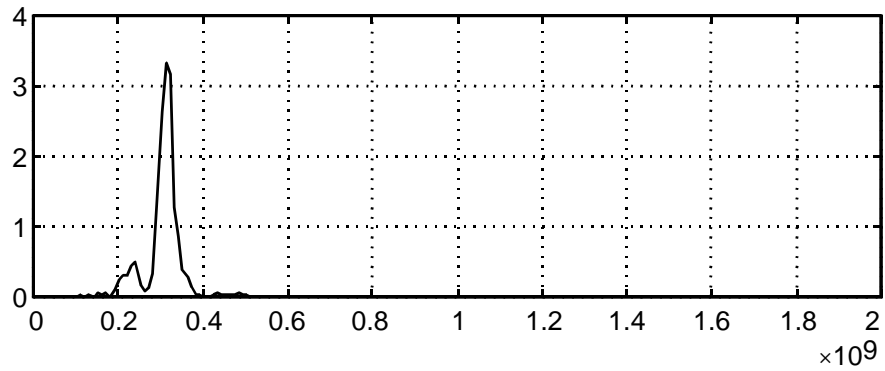


pbl10₀005.ASC

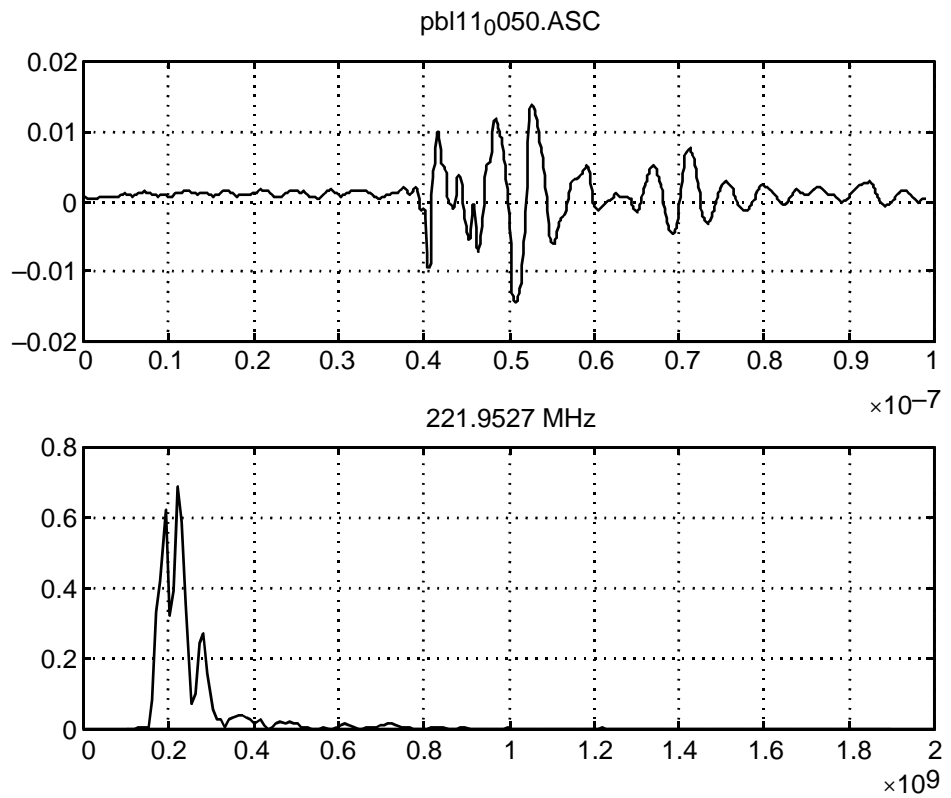
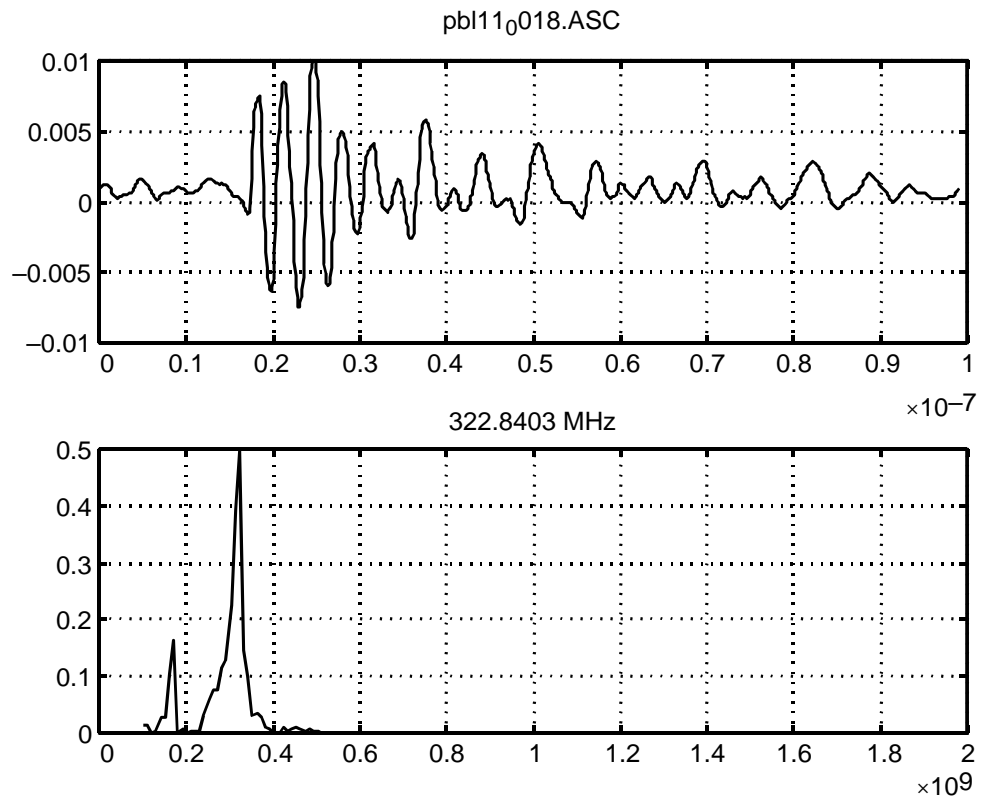


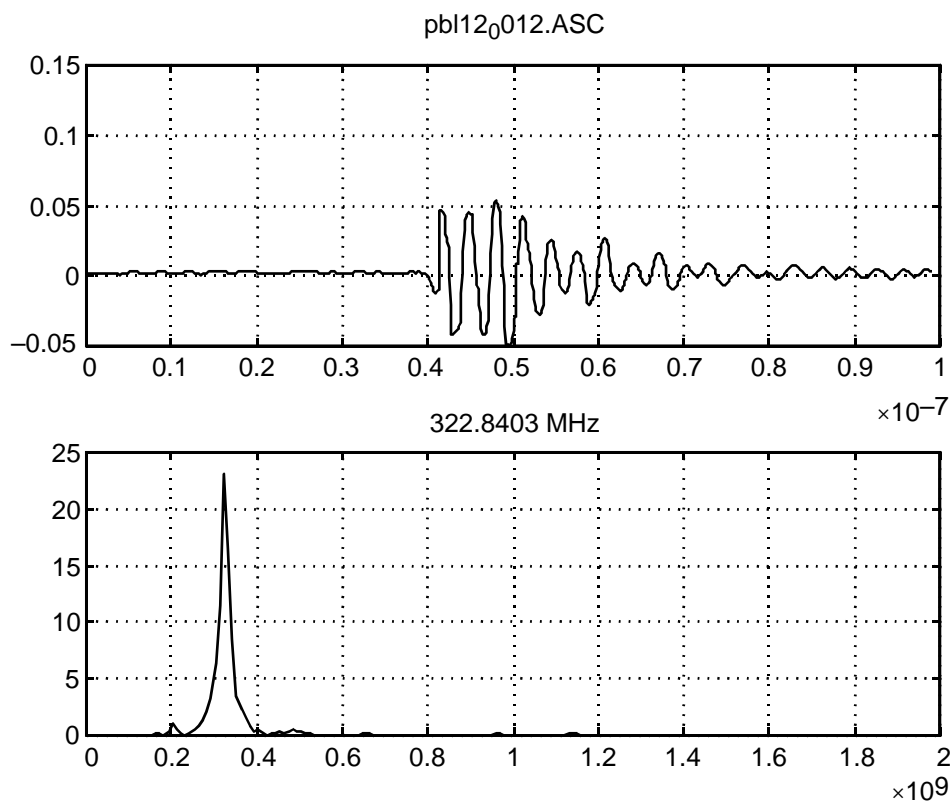
312.7515 MHz

$\times 10^{-7}$



Appendix A

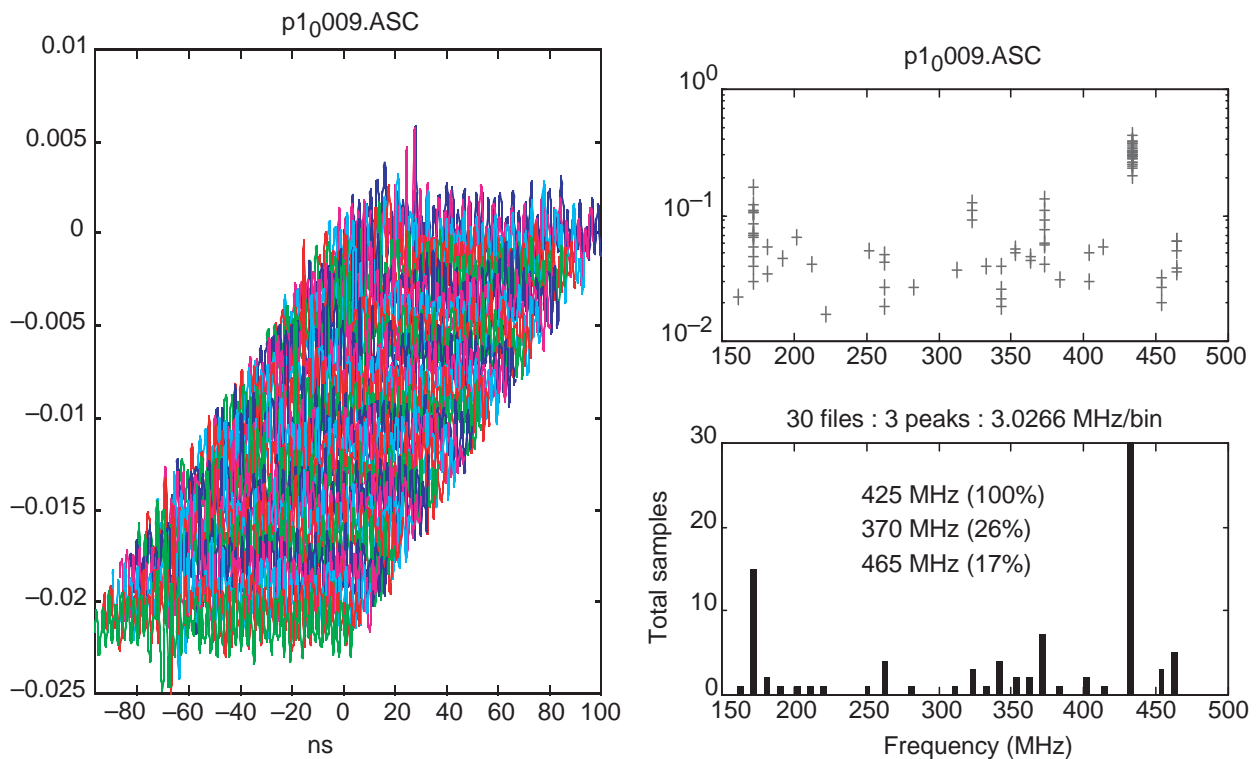




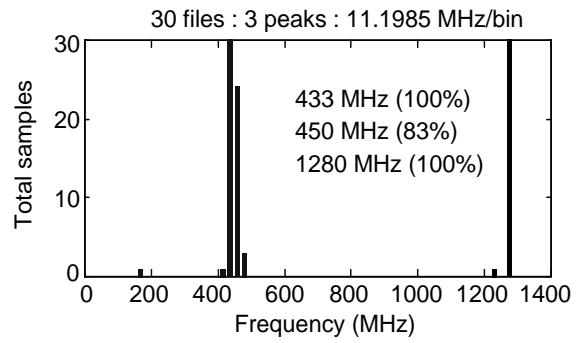
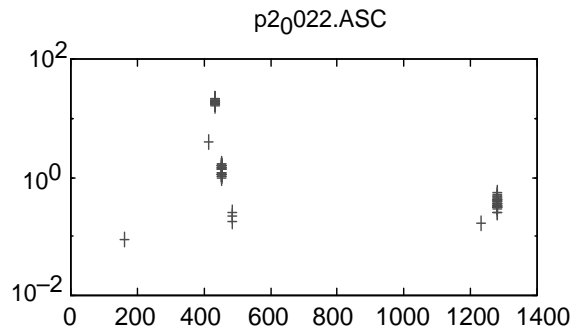
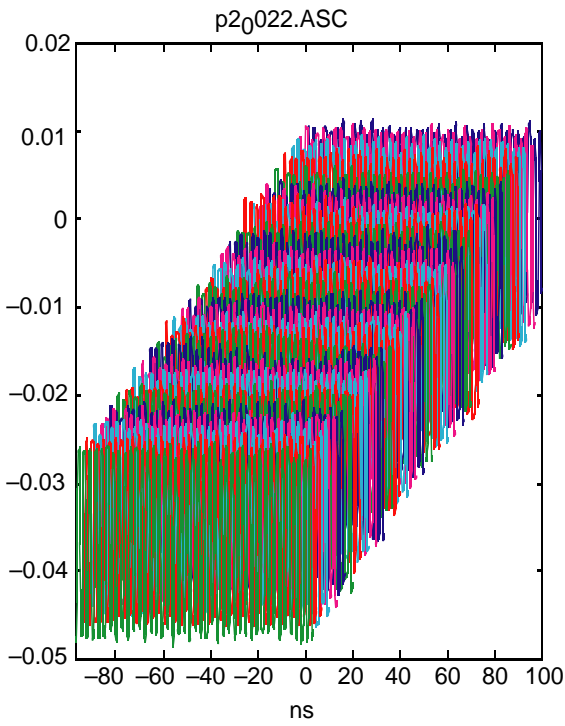
Appendix B. Method of Analysis

This appendix contains slides with three figures on each slide that reflect the method of analysis performed on each data set. The left-hand plot is a waterfall plot consisting of a collection of all the waveforms for that data set. The upper right-hand plot is a scatter plot of the frequency peaks for each of the shots making up a data set. The number of shots for each data set ranges from 36 to 114. The lower right-hand plot is a histogram of the frequency peaks. This enables one to determine the most common frequency peak and the number of times it appears in the complete data set.

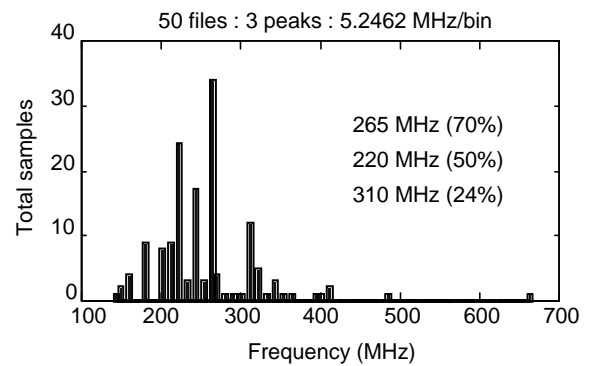
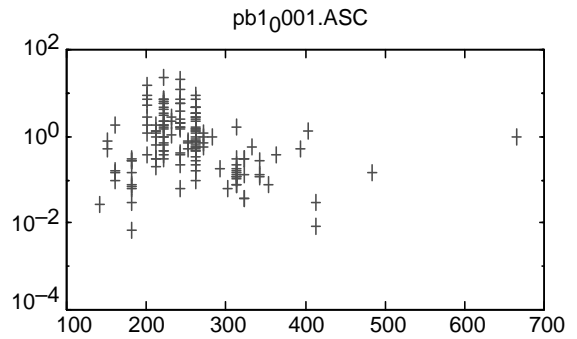
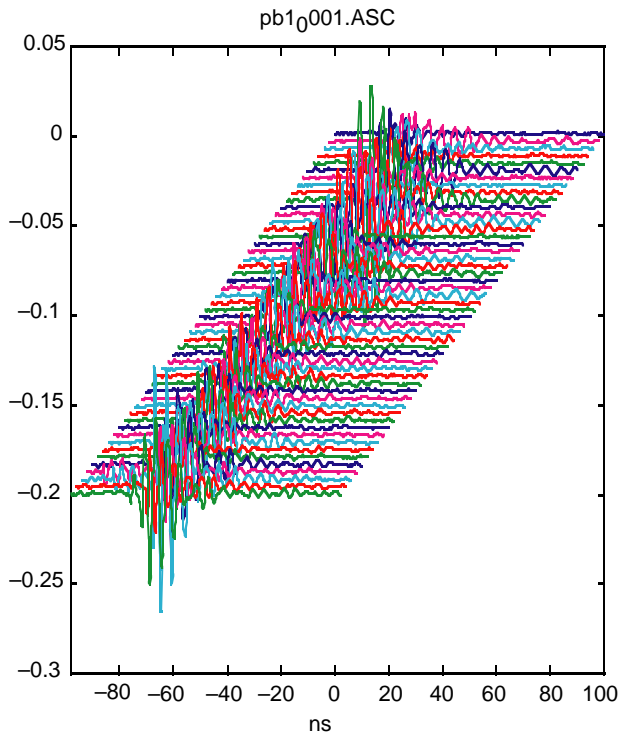
Background Environment (dockside measurements)



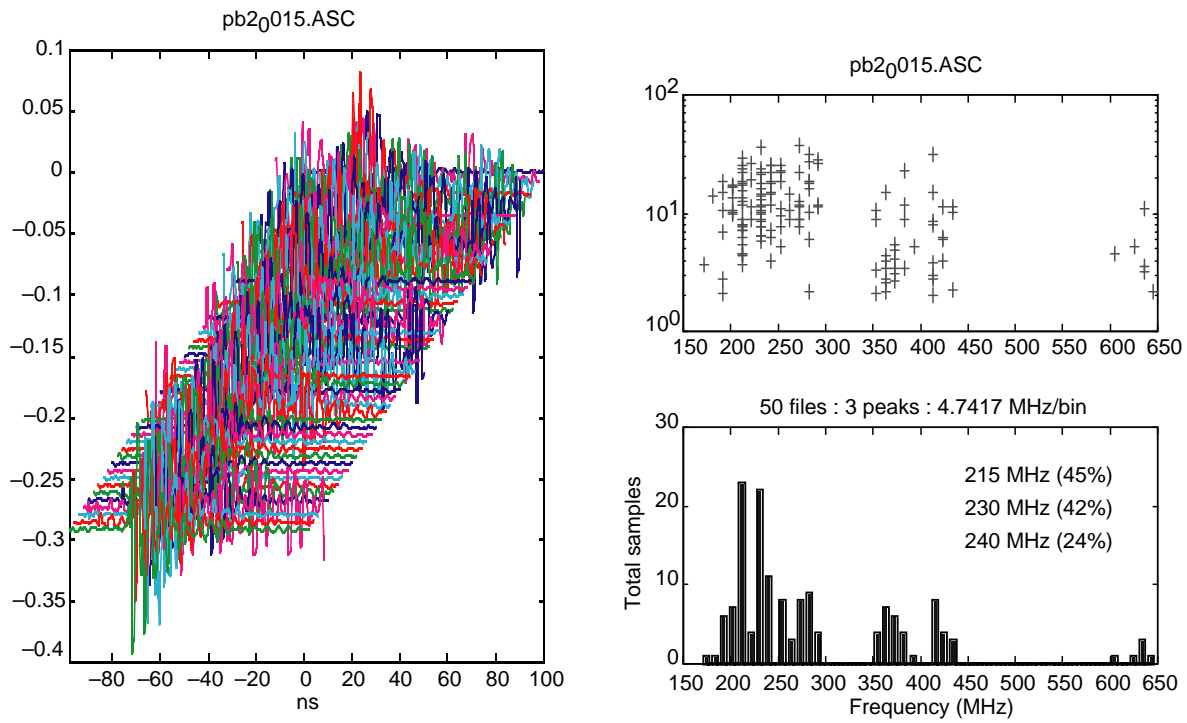
Background Environment



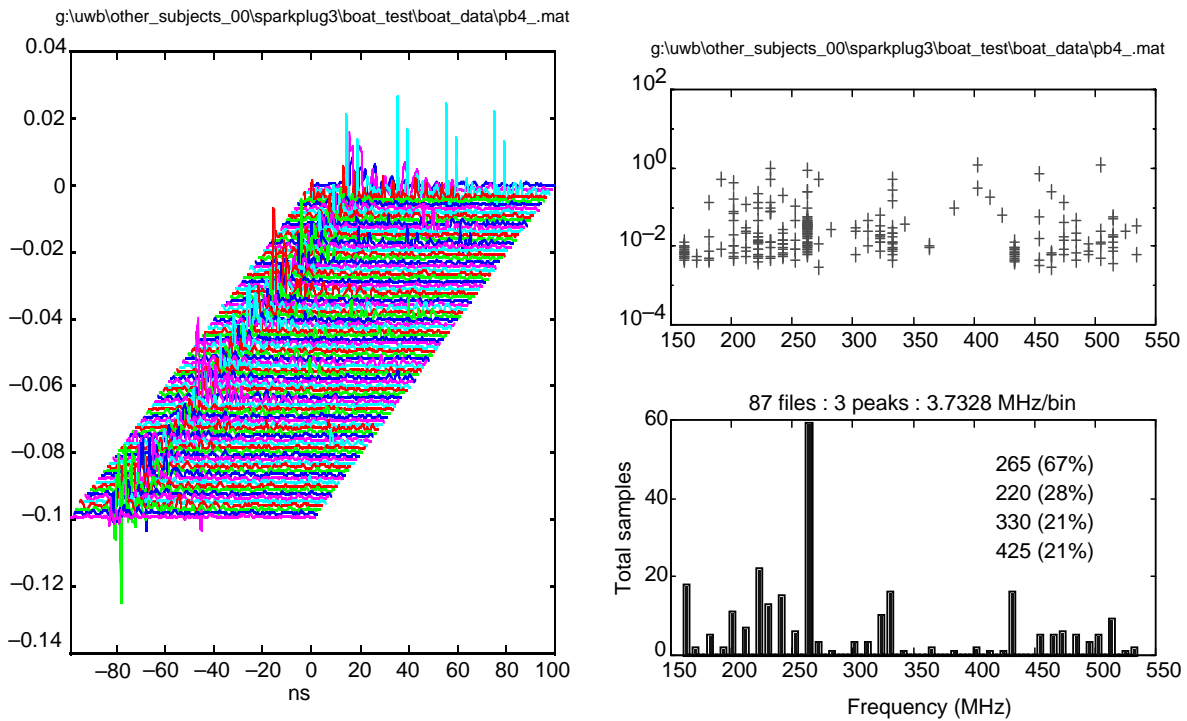
200 hp Yamaha - dockside



200 hp Yamaha - dockside



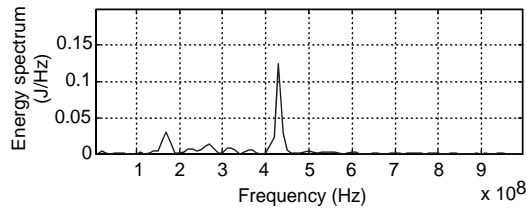
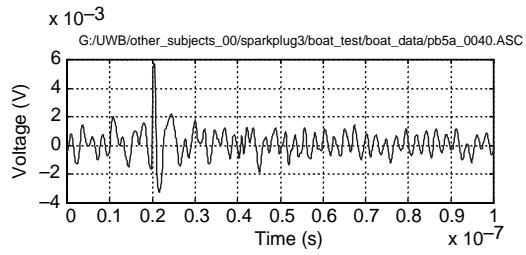
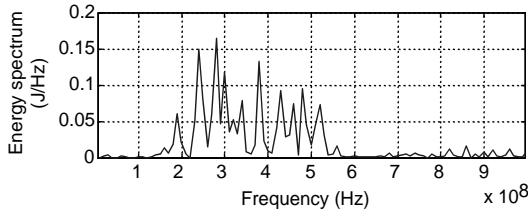
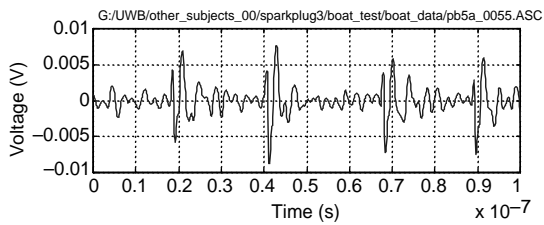
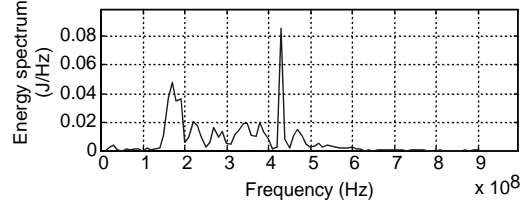
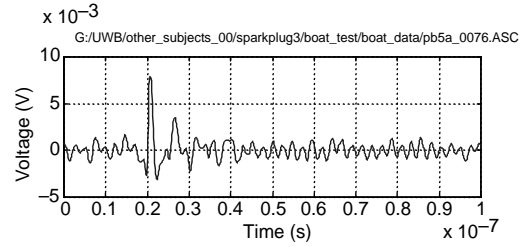
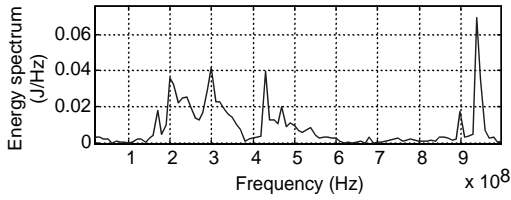
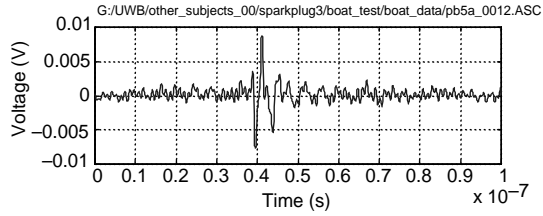
Yamaha - speed circles



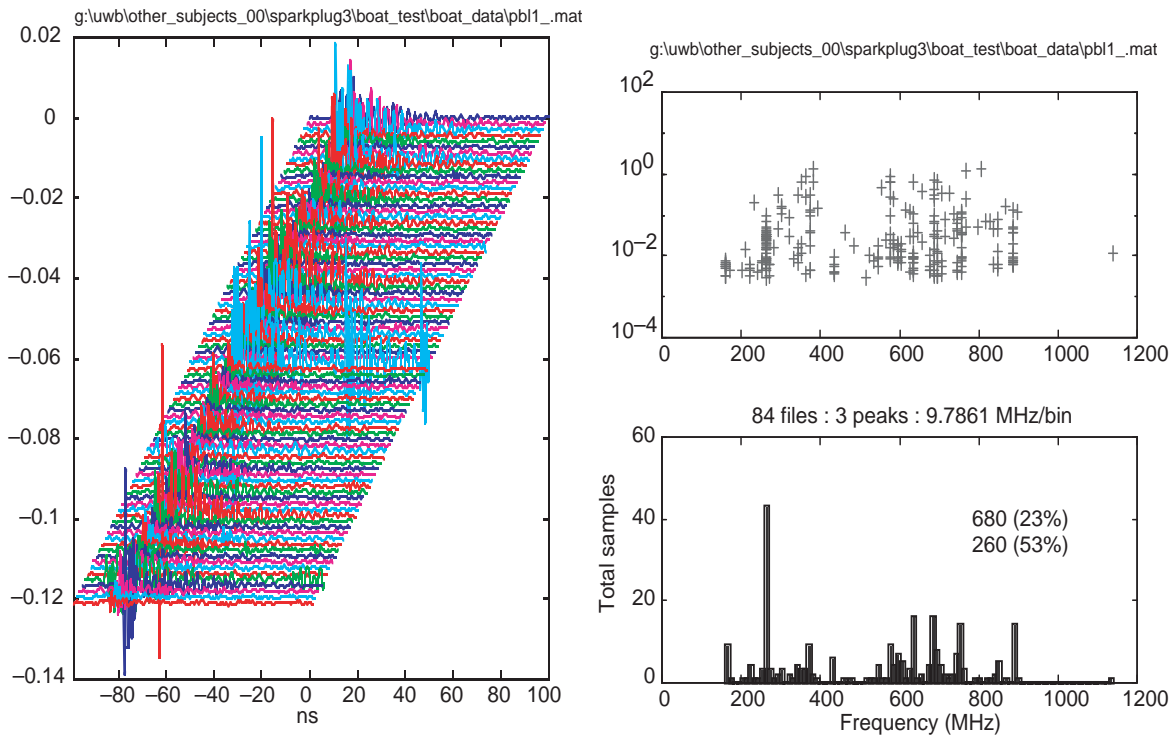
Yamaha - sweep -amp (much background noise) 2 types

220 (35%)

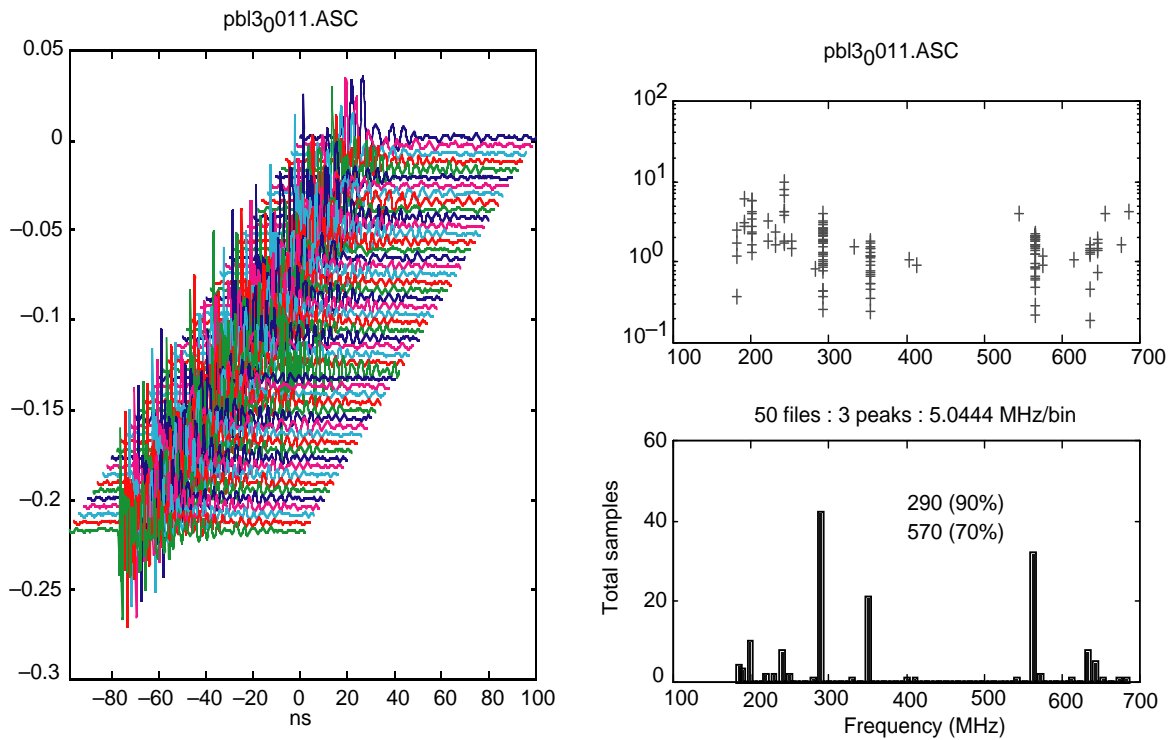
260 (30%)



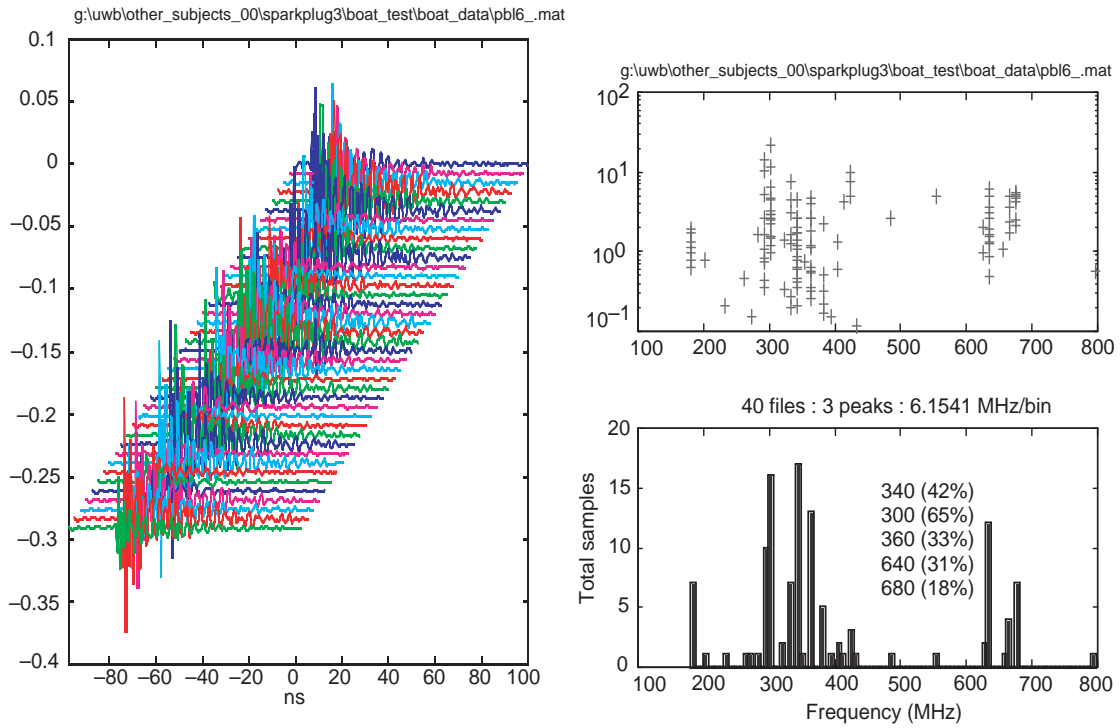
Whaler - speed circle(17)



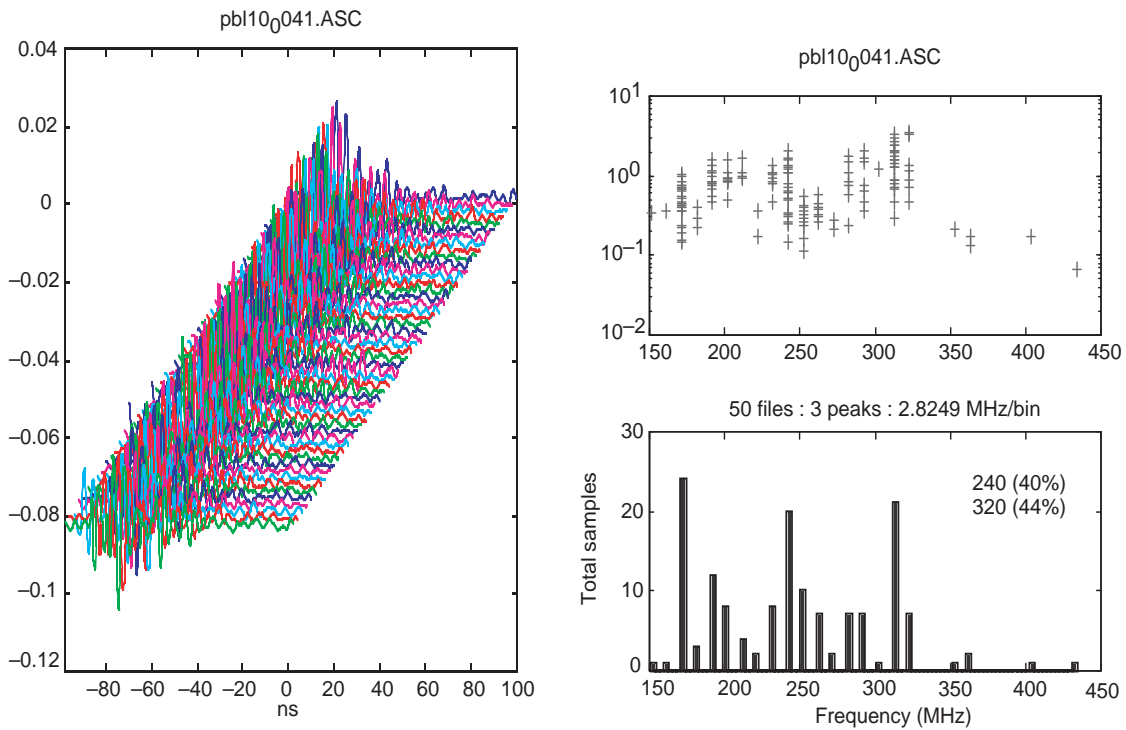
Whaler - dockside - starboard



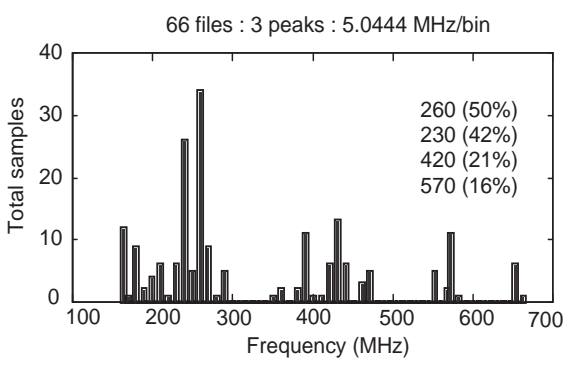
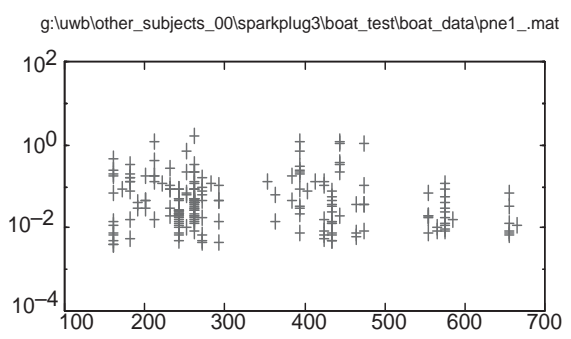
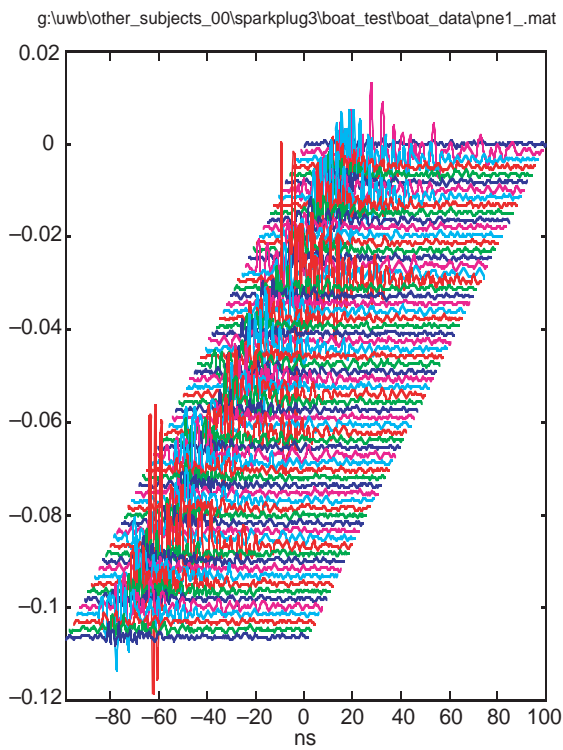
150 hp OMC - dockside - alt. hi/idle (port)



Al lined



NESEA



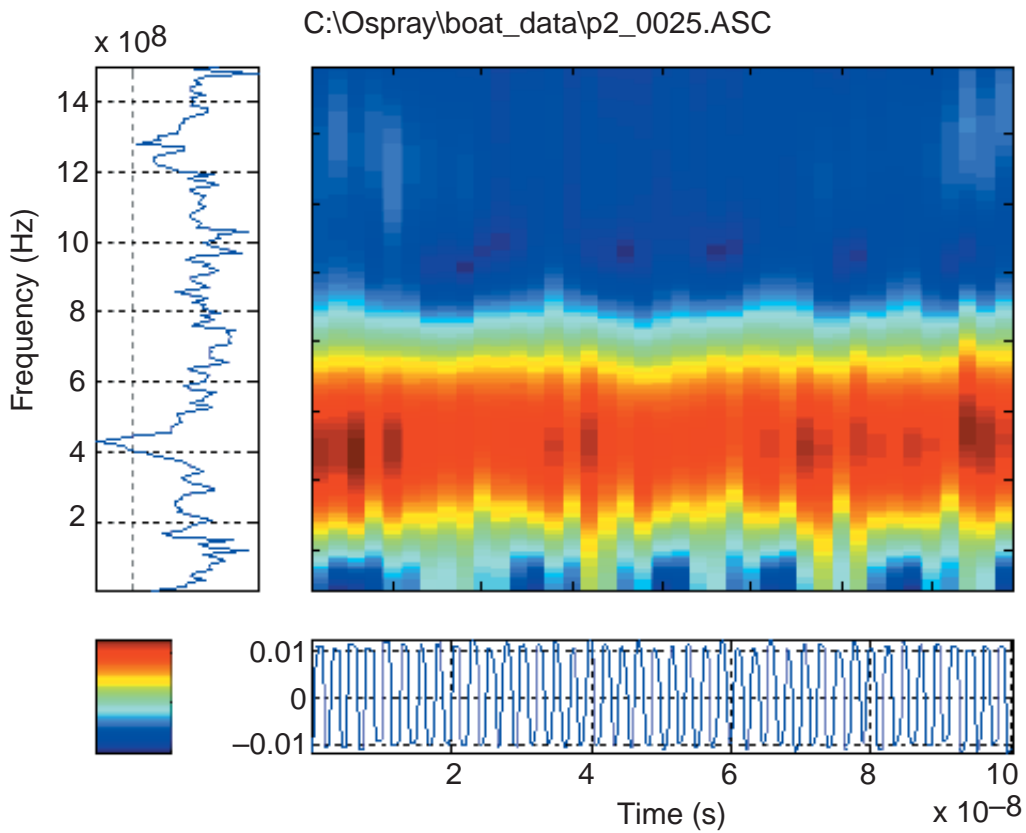
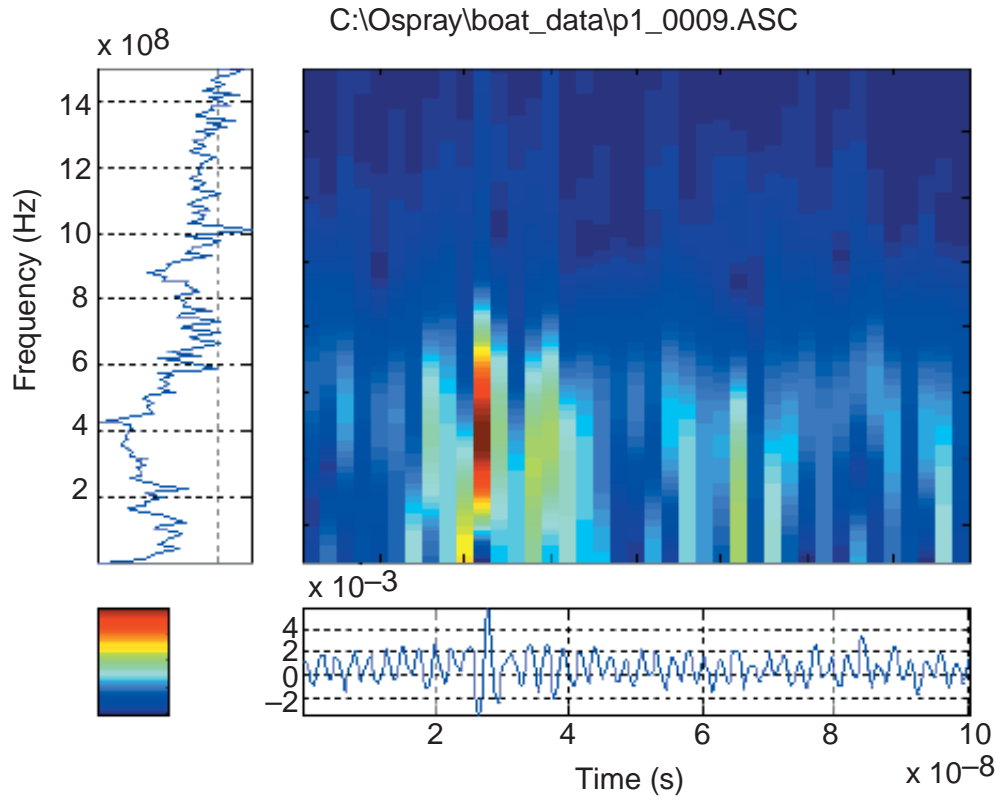
Appendix C. Time-Frequency Analysis

This appendix includes the time-frequency analysis of a spectrogram of each of the files in the sample library. The value of this analysis lies in that it differentiates the waveforms in a manner more striking and clear-cut than the time or frequency waveforms alone.

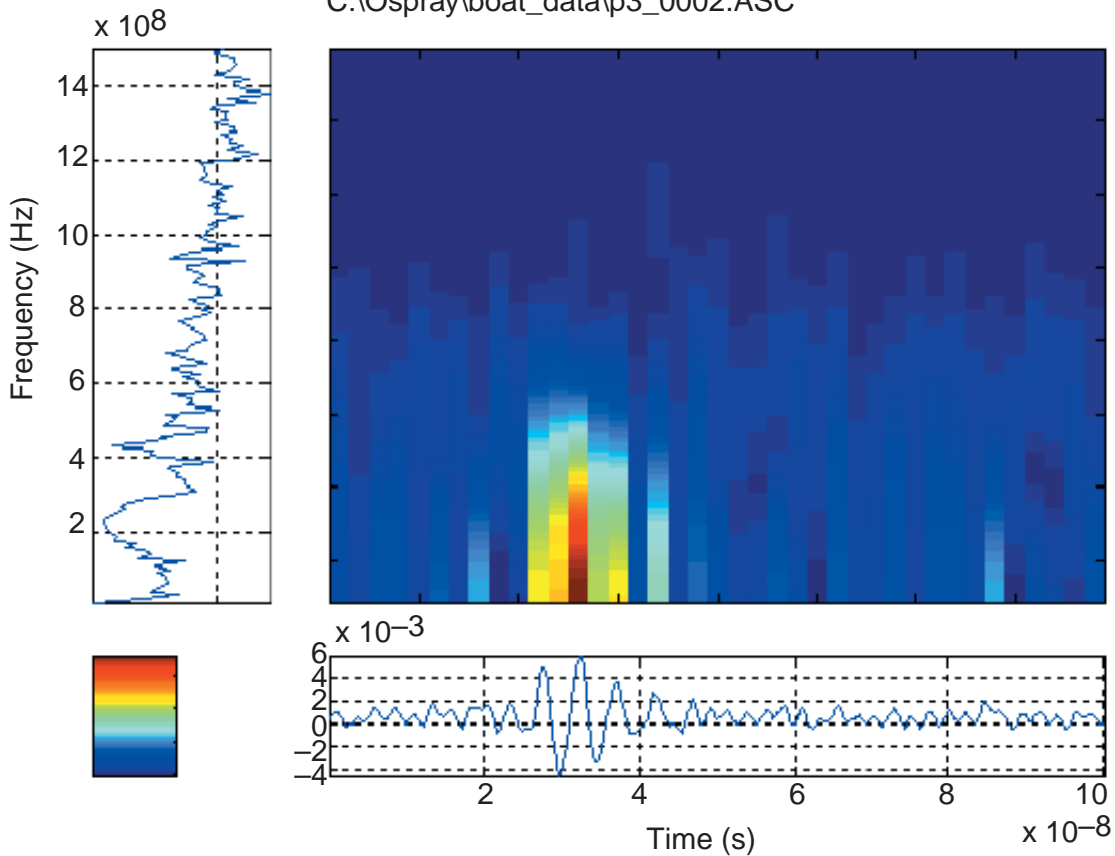
The Matlab program *jtfa_trunc* (*filnam,tim1, tim2,maxfreq, width,overlap*) generated the spectrograms in this appendix. *Tim1=0* (sec), *tim2=1e-1* (μ sec), *maxfreq=1.5e9* (Hz), the width of the window was 32 datapoints, and the overlap between windows was 6 datapoints. It was necessary to specify a maximum frequency of 1.5 GHz or the spectrogram routine would include spurious frequencies and aliasing up to 5 GHz because of the oversampled waveform. The program *jtfa_trunc.m* appears in appendix D.

The peak frequencies appear with a reddish hue in the spectrogram. The frequencies with the lowest amplitude are blue. The plot on the bottom is the time plot of the voltage, and the upper left plot is a plot of Fast Fourier Transform.

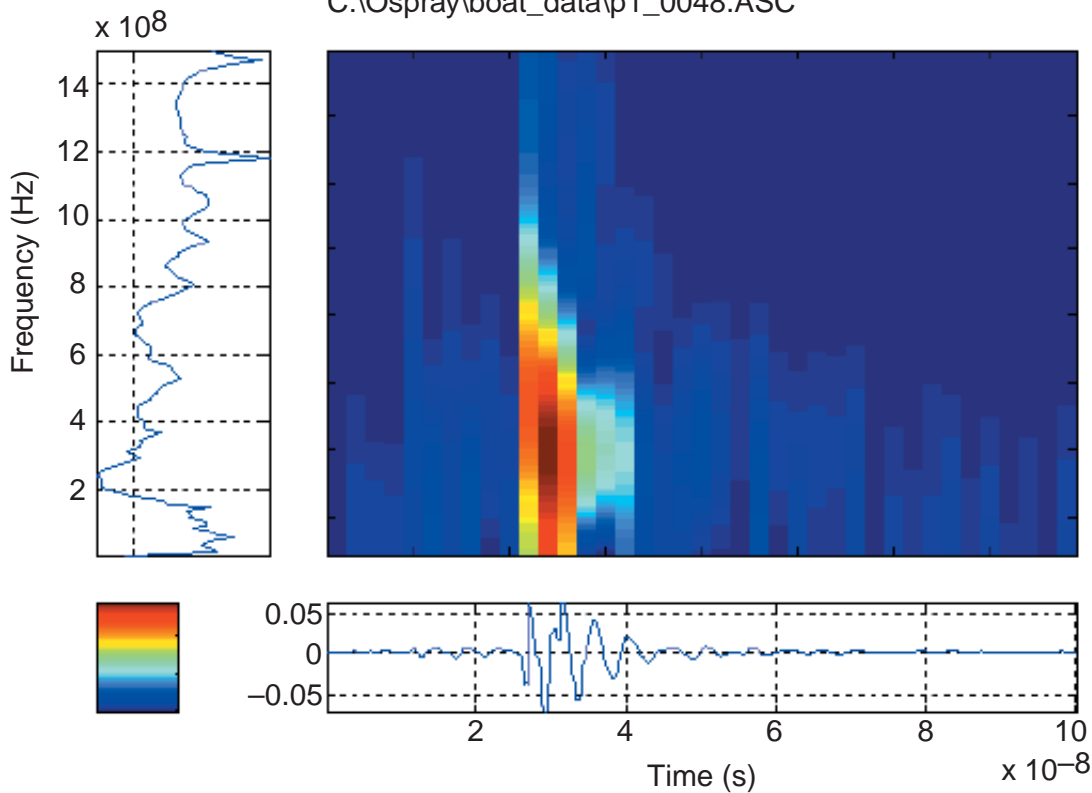
The pb datasets tend to be 10 ns wide while the pbl datasets tend towards 20 ns in width. The frequency content is statistically analysed in appendix B.

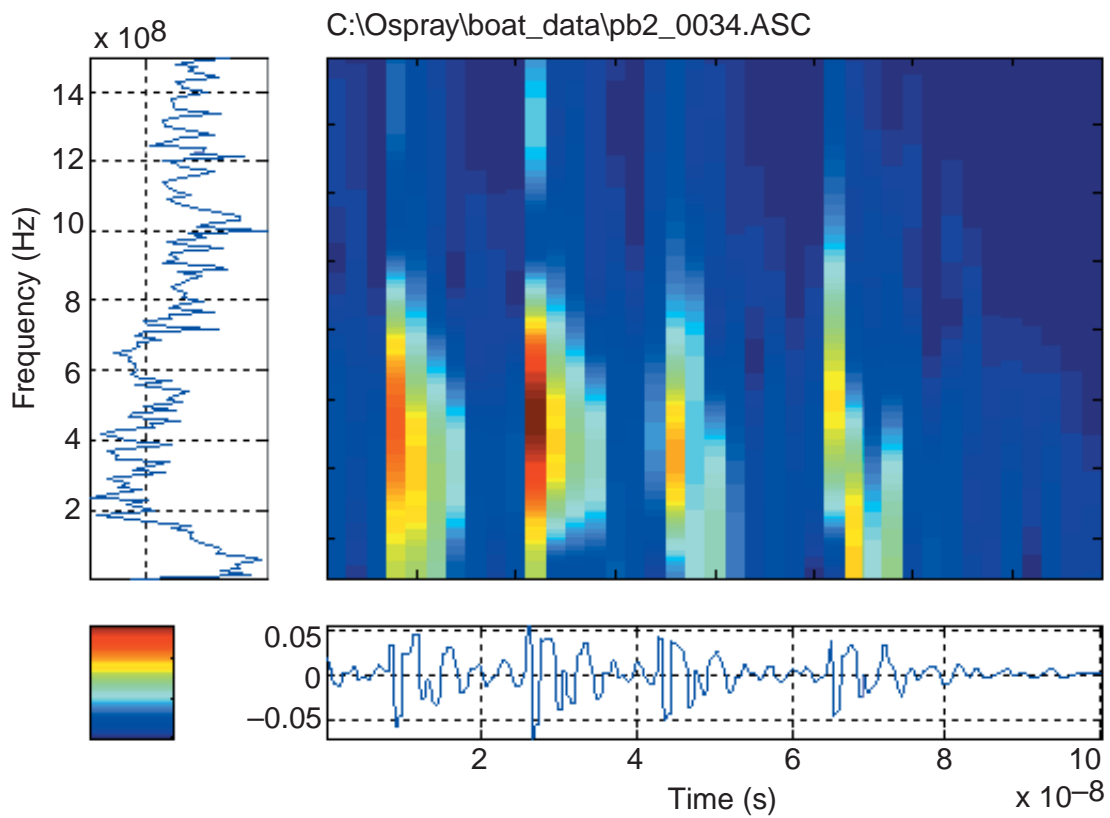
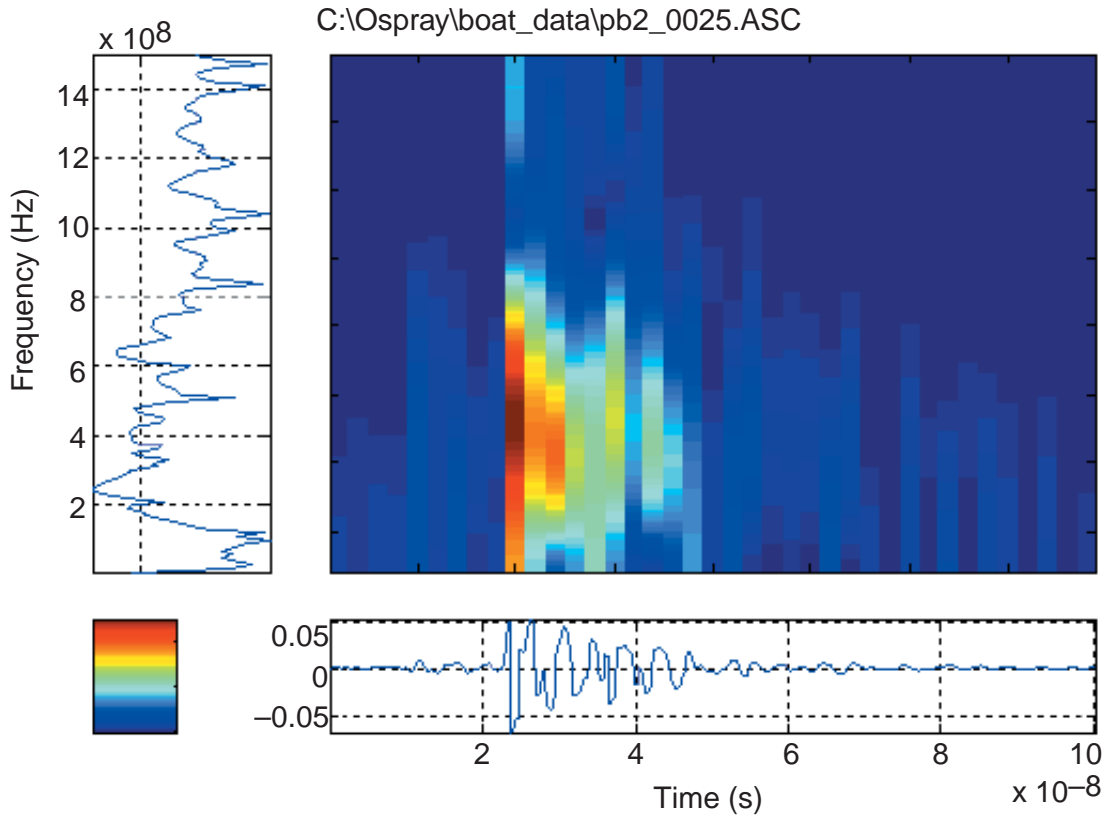


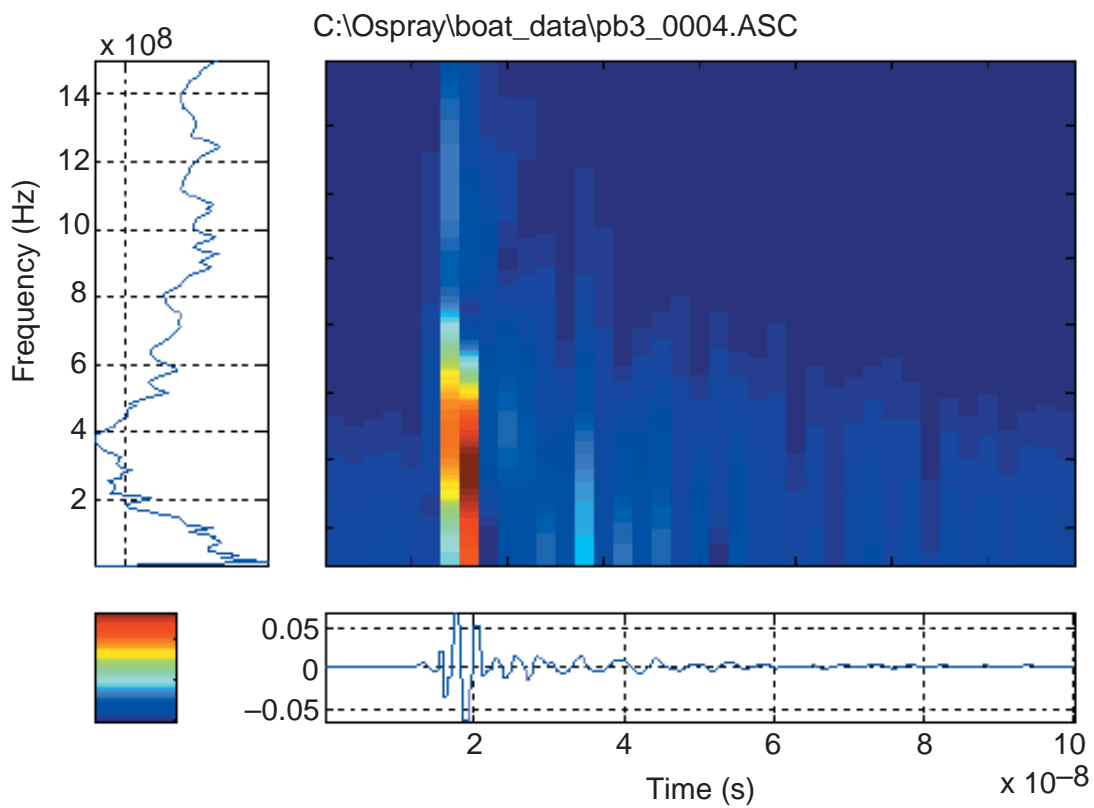
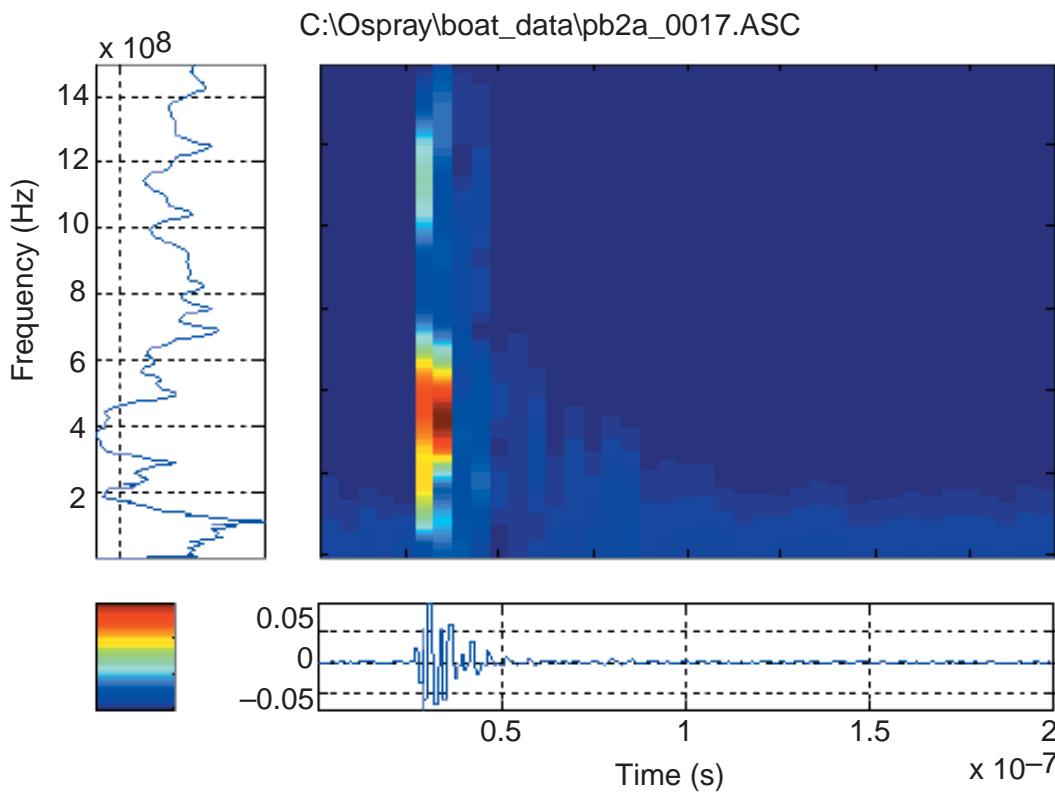
C:\Ospray\boat_data\p3_0002.ASC



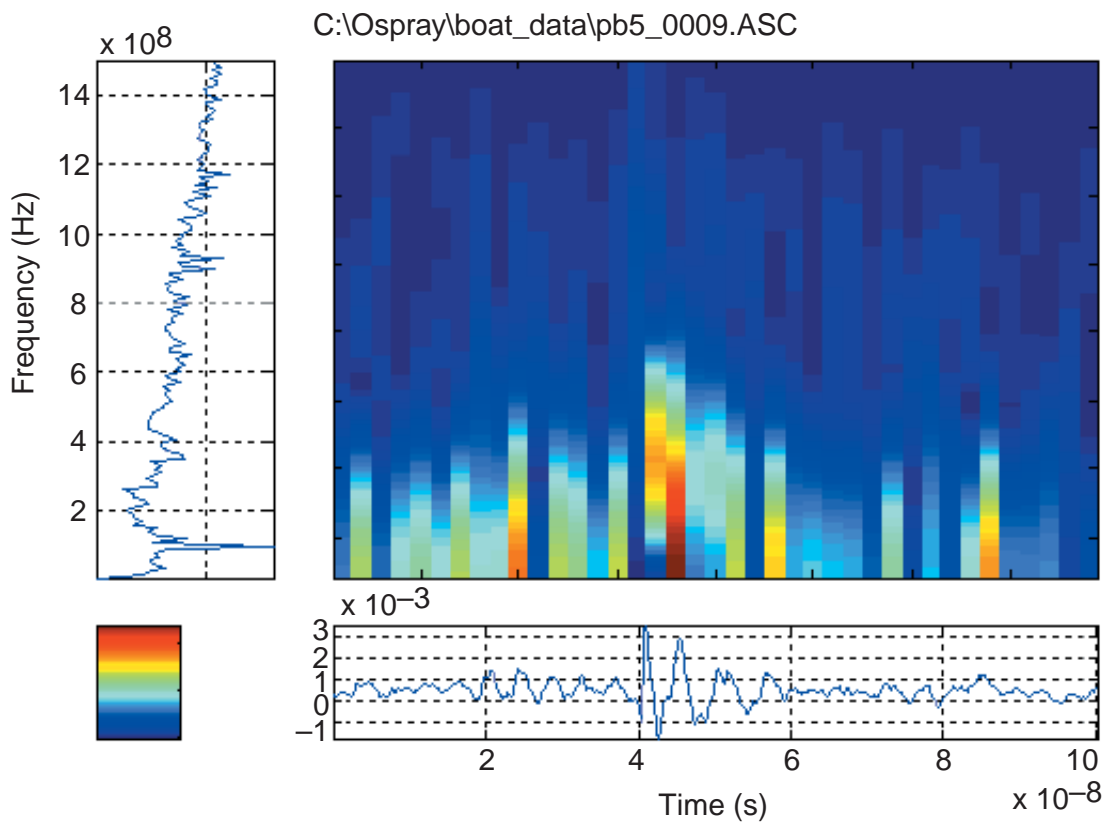
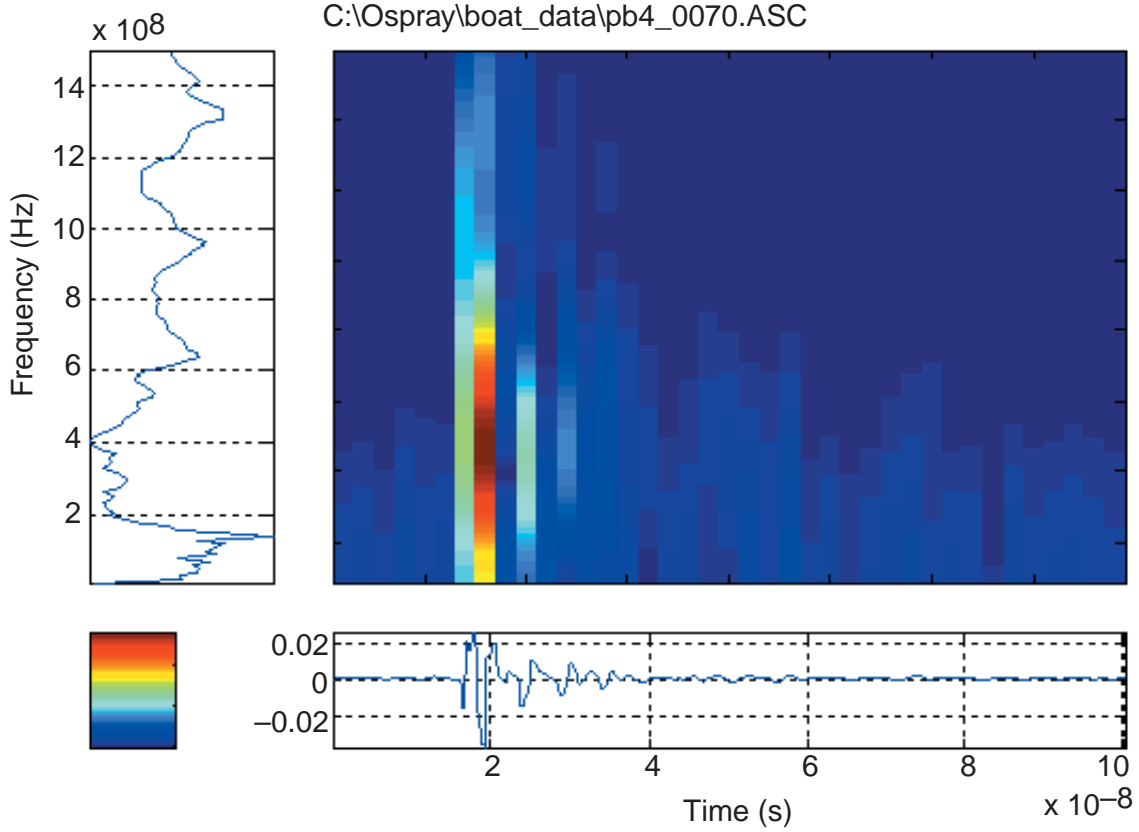
C:\Ospray\boat_data\p1_0048.ASC



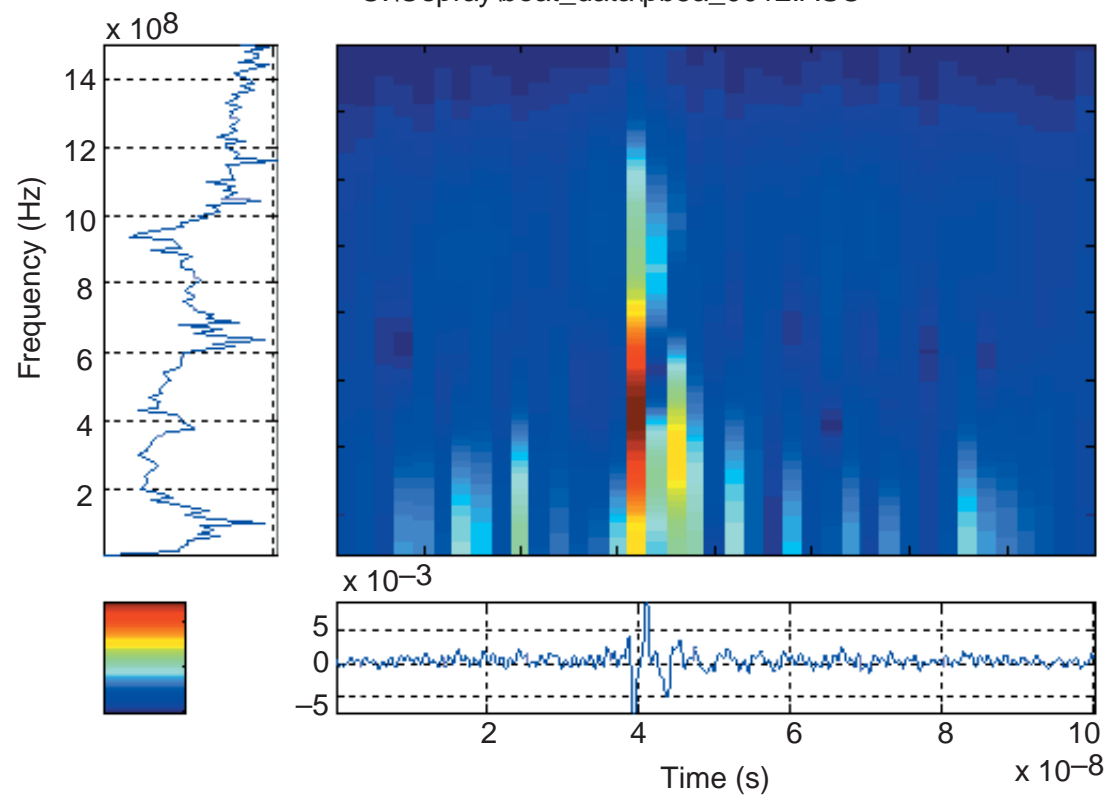




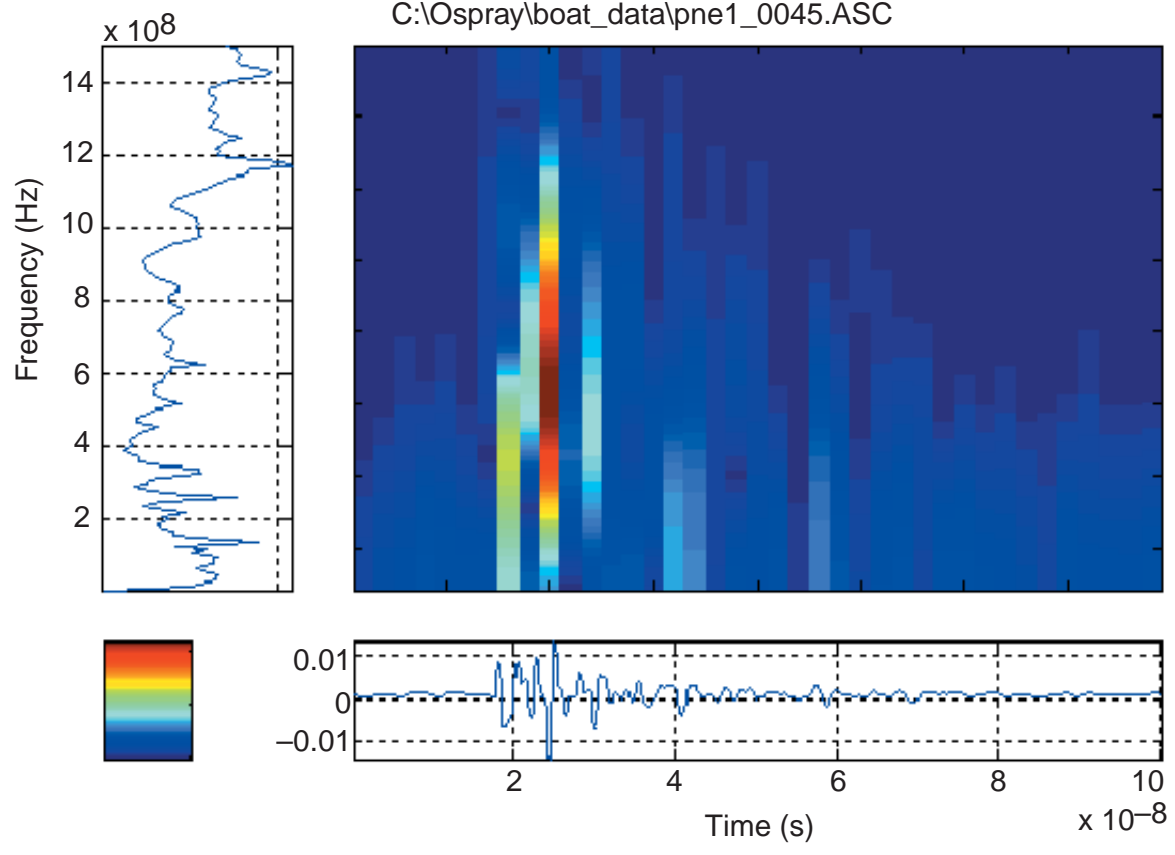
Appendix C

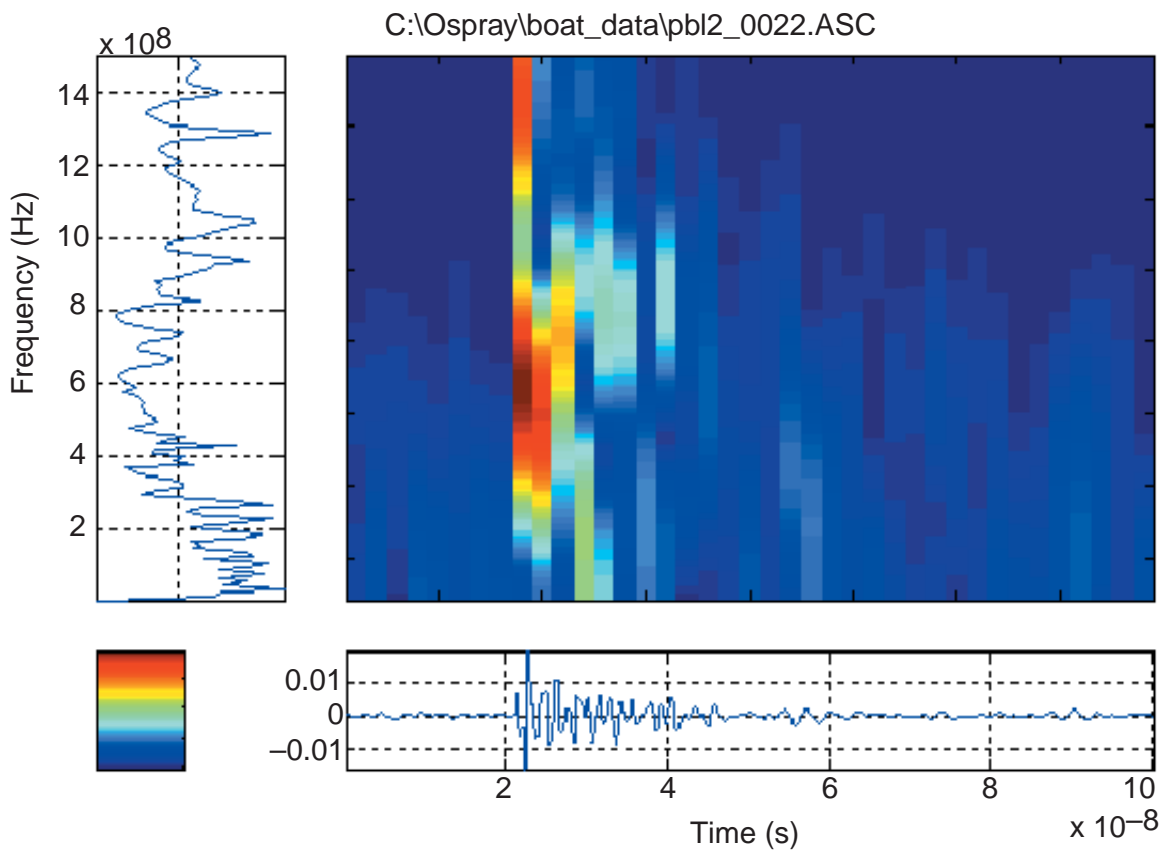
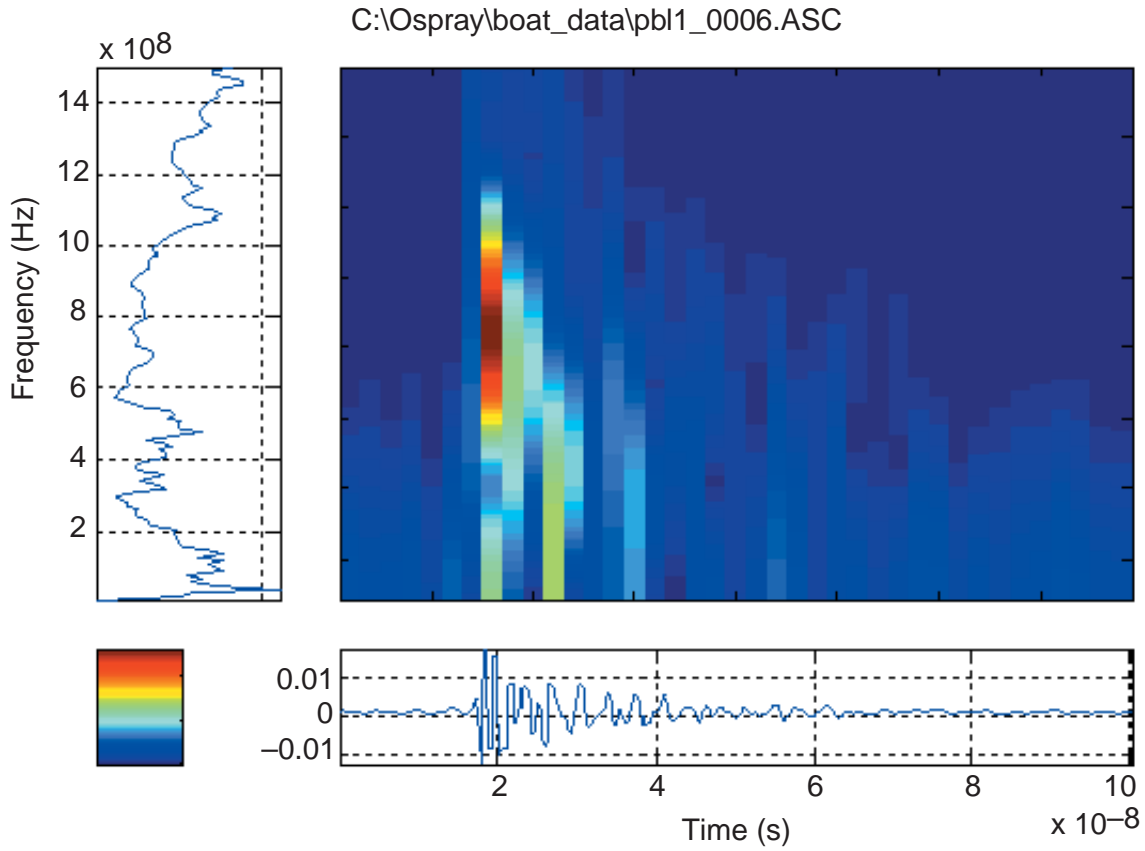


C:\Ospray\boat_data\pb5a_0012.ASC

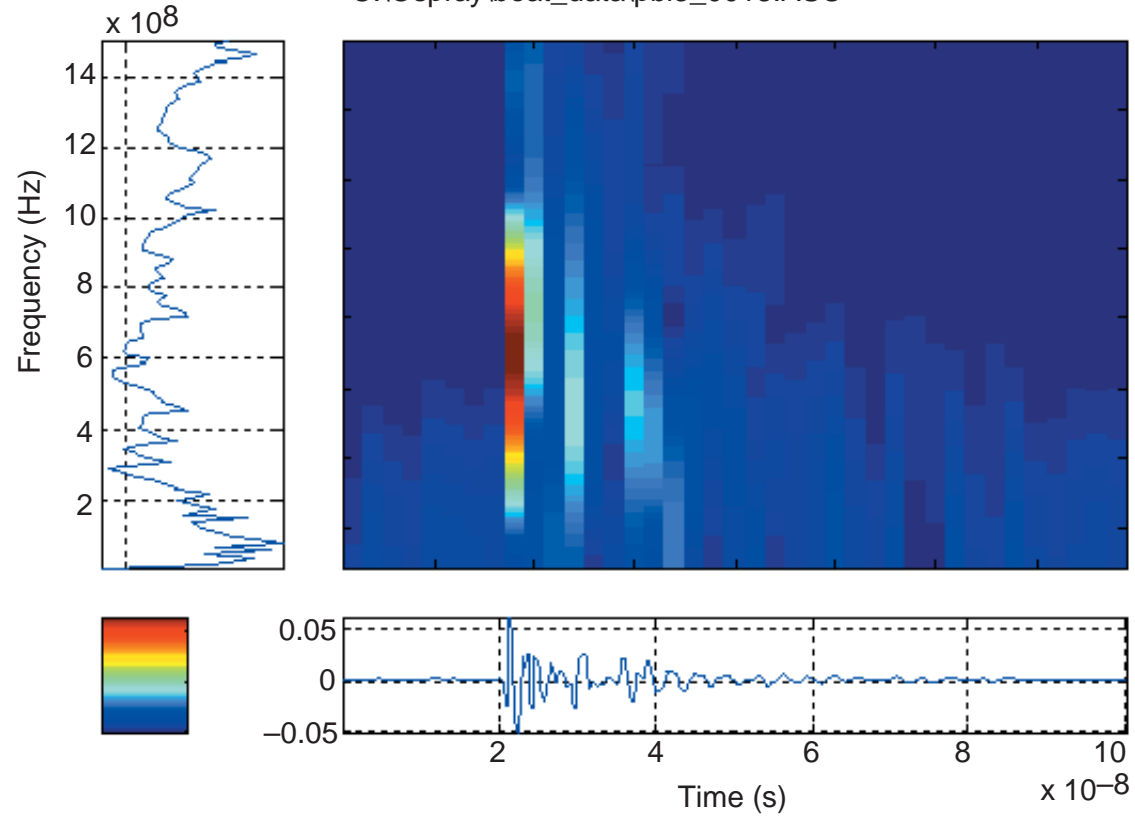


C:\Ospray\boat_data\pne1_0045.ASC

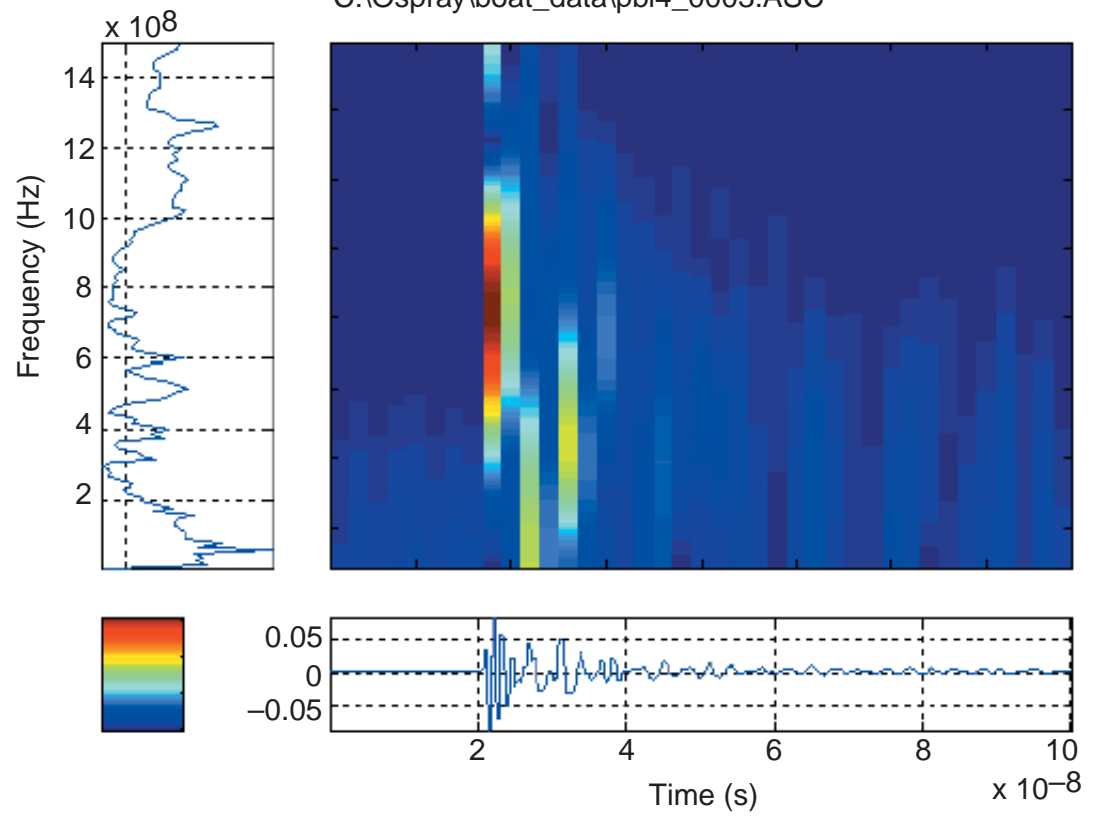




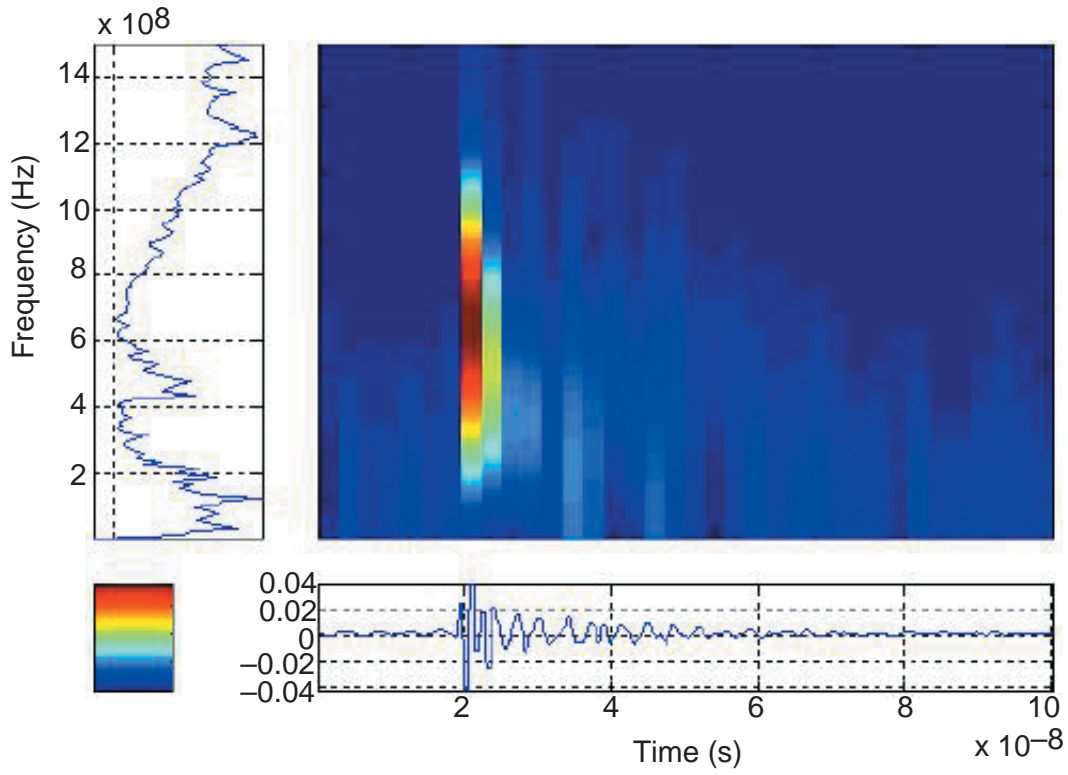
C:\Ospray\boat_data\pbl3_0018.ASC



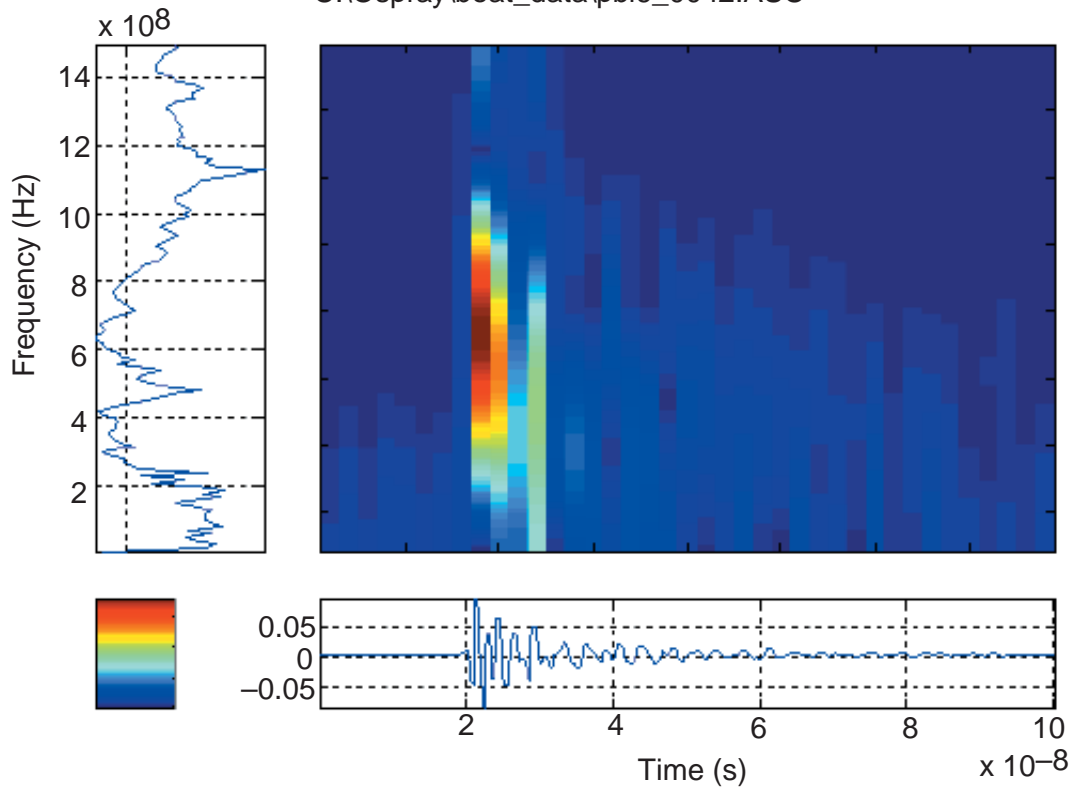
C:\Ospray\boat_data\pbl4_0003.ASC

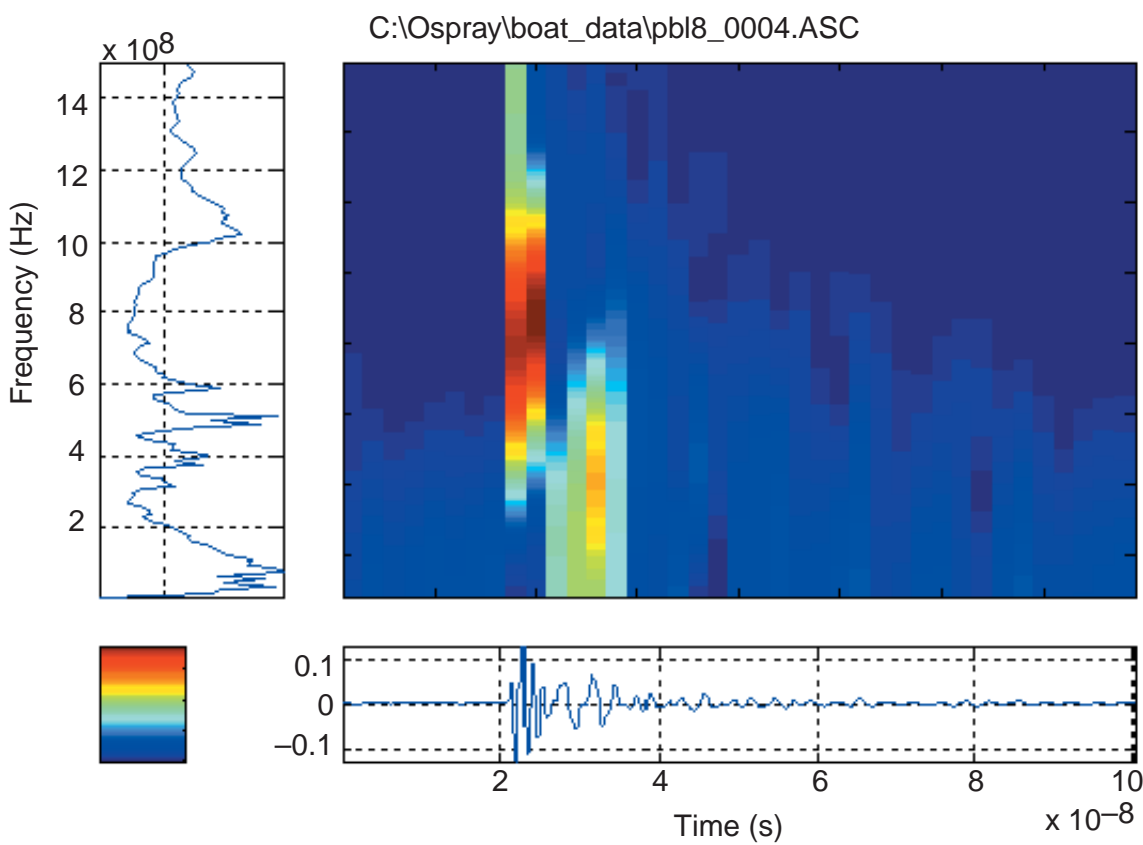
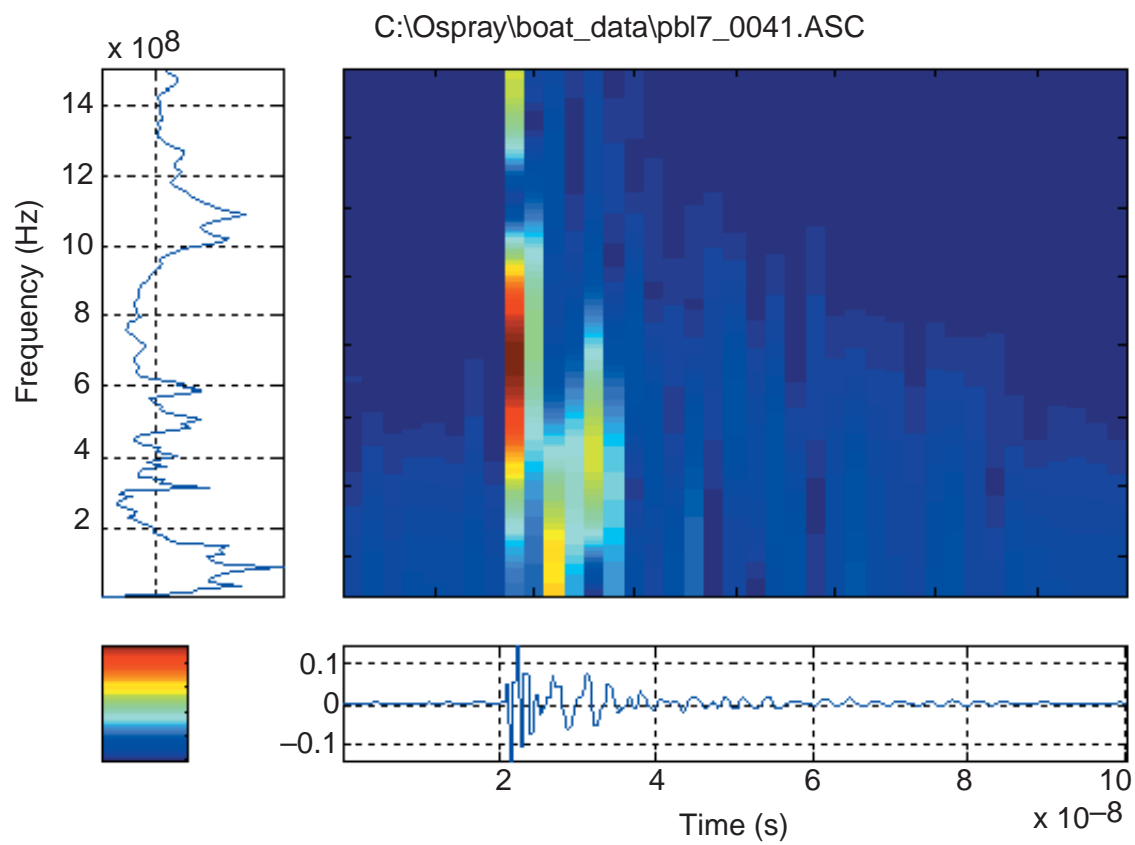


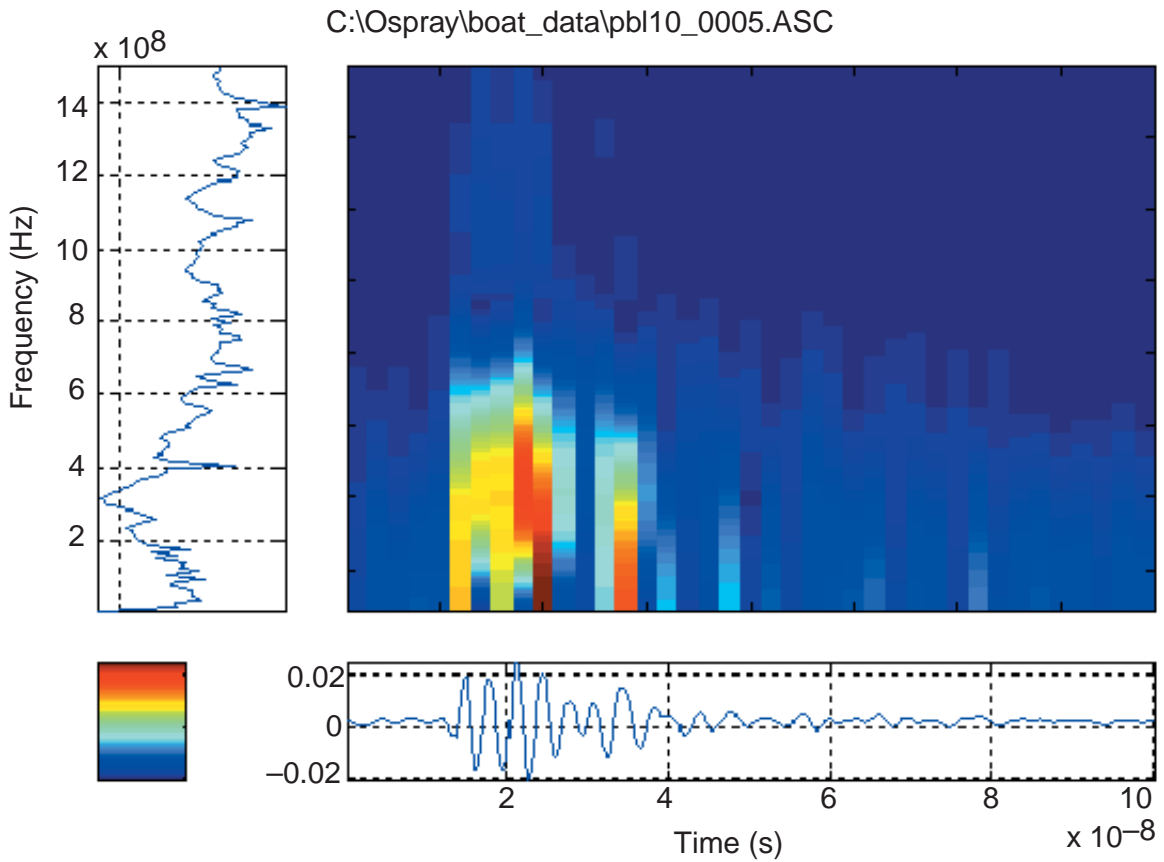
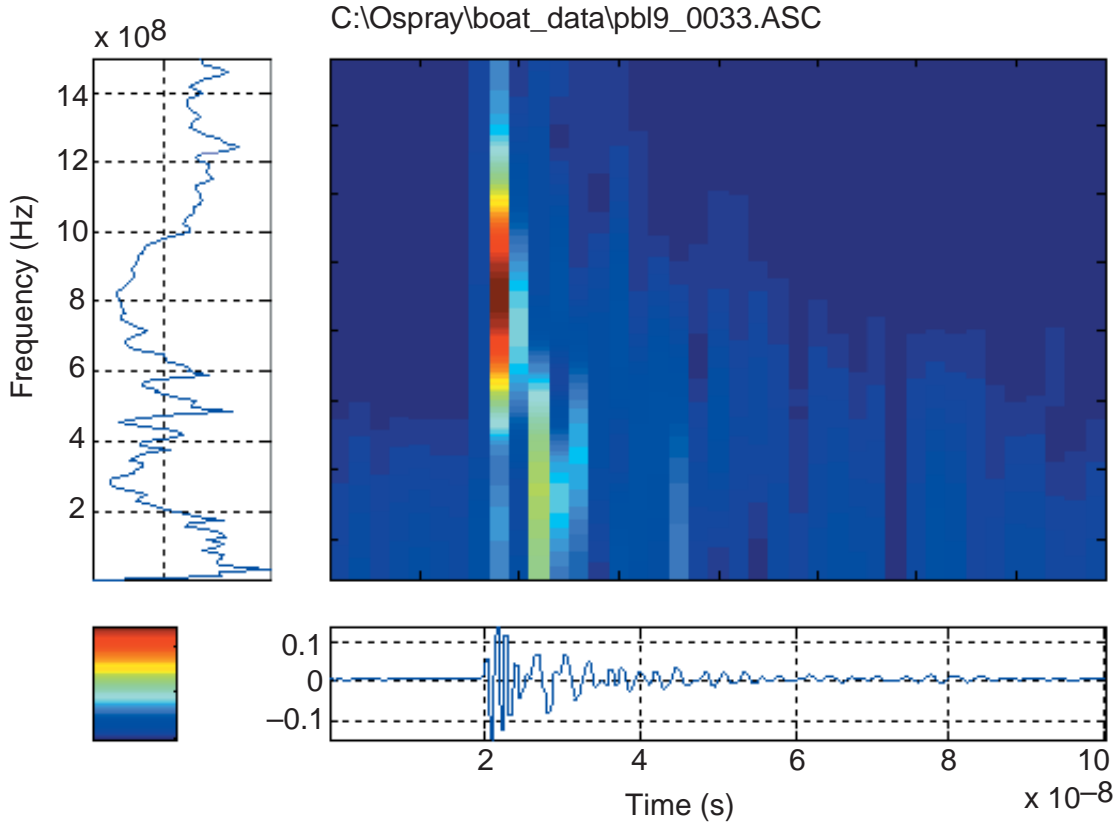
C:\Ospray\boat_data\pbl5_0049.ASC

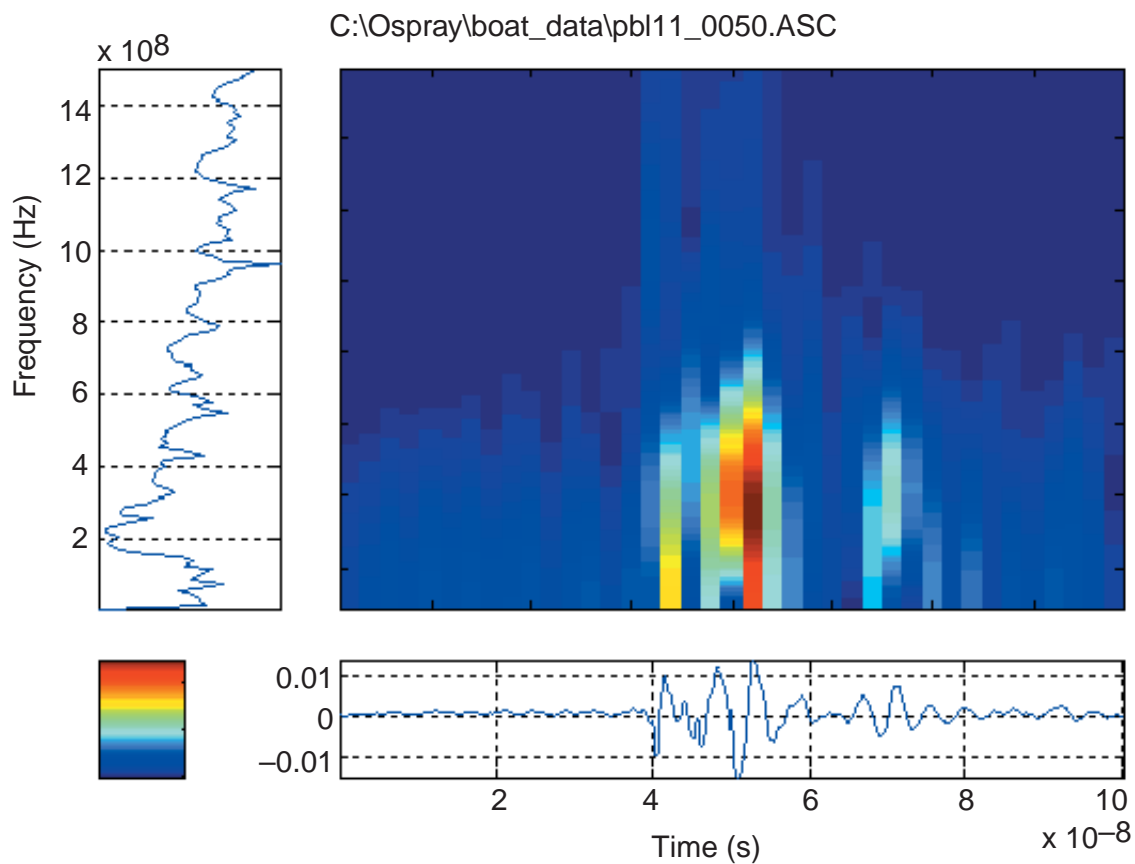
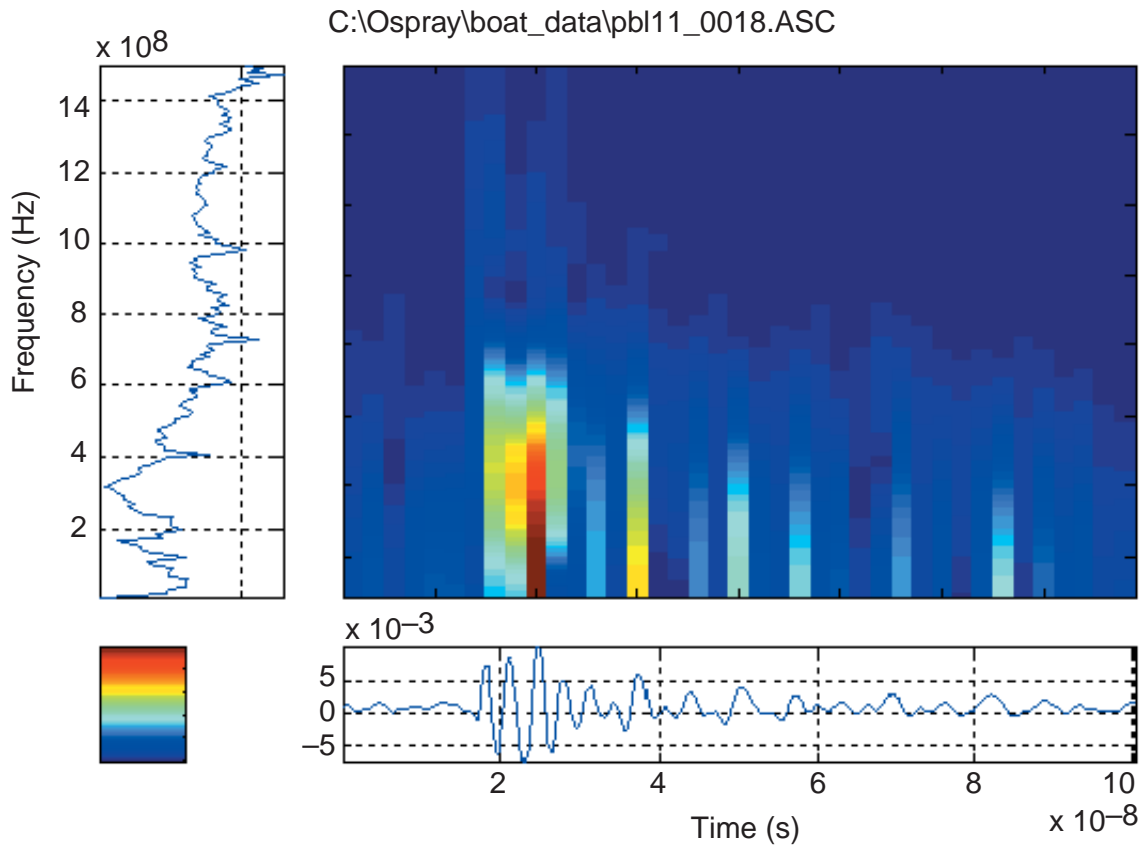


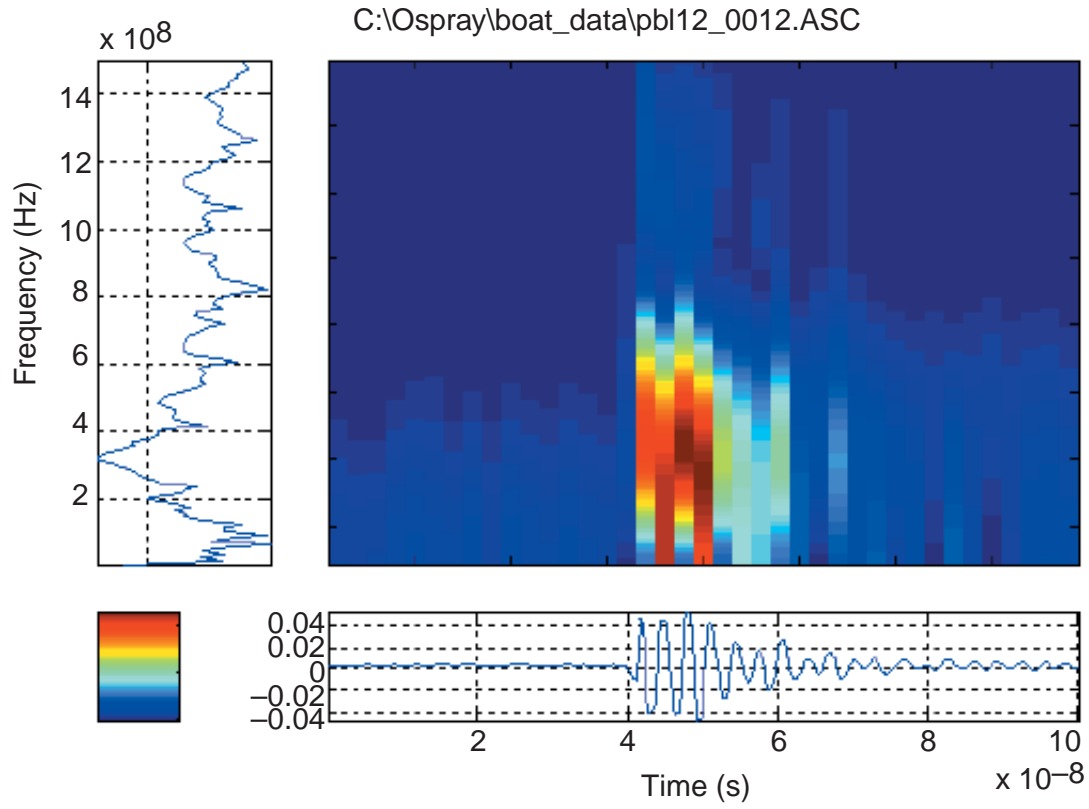
C:\Ospray\boat_data\pbl6_0042.ASC











Appendix D. Matlab Program

This is a listing of a Matlab program that generates spectrograms. It permits the user to specify a time range in microseconds over which a waveform is analyzed, and within that time range specify a window length with the amount of overlap between windows. The user specifies a maximum frequency to eliminate spurious frequencies and aliasing.

```
function jtfa_trunc(filnam,tim1,tim2,maxfreq,width,overlap)
%Truncates frequencies from spectrogram that do not exist.

[x,y,t1,t2,t3,t4]=ascread(filnam);
if (nargin>1) % check for timemark trimming of signal
    disp(['...jtfa tim1 tim2 ',num2str(tim1),' ',num2str(tim2)])
    if (tim1~=tim2)
        [x,y]=prepst(x,y,tim1,tim2);
    end
end

[f1,yf]=fft_ps(x,y);
nfft=arraylen(y);
fs=1.0/(x(10)-x(9));
[b]=specgram(y,nfft,fs,hanning(width),overlap);

if (nargin>1)
    sf1=size(f1);
    nelemorg=sf1(2)
    [f1,yf]=prepst(f1,yf,min(f1),maxfreq);
    sf1=size(f1)
    nelem=sf1(2)
    elemrat=nelem/nelemorg
    sb=size(b)
    c=ones(fix(sb(1)*elemrat)+1,sb(2));
    sc=size(c)
    numrows=sc(1)
    for i=1,numrows ; % vertical matrix cutoff
        c=b(1:numrows,:);
    end
    b=c;
end

[b]=flipud(b); % vertically reverse JTF matrix for plotting

figure % plot
colormap(jet)
bmag=sqrt((real(b).^2)+(imag(b).^2));
subplot(2,2,2),imagesc(bmag);shading('interp');colorbar;
%subplot(2,2,2), specgram(y,nfft,fs,hanning(96),32);colorbar
subplot(2,2,1),semilogy(f1,yf),xlabel('Frequency (Hz)'),grid on,axis([min(f1)
```

Appendix D

```
max(f1) min(yf) max(yf)])
subplot(2,2,4),plot(x,y),xlabel('Time (sec)'),grid on,axis([min(x) max(x) min(y)
max(y)])

fig=get(gcf,'child');
p1=[.3 .1 .65 .15];p2=[.1 .3 .15 .65];
p3=[.3 .3 .65 .65];p4=[.1 .1 .07 .15];
set(fig(1),'Position',p1) % transient
set(fig(2),'Position',p2) % full fft
set(fig(3),'Position',p4) %colorbar
set(fig(4),'Position',p3) %spectrogram
set(fig(2),'View',[-90,90])
set(fig,'FontSize',11)
set(fig(2),'yticklabels',[])
set(fig(3),'xticklabels',[])
set(fig(3),'yticklabels',[])
set(fig(4),'yticklabels',[])
set(fig(4),'xticklabels',[])
set(fig(4),'yticklabels',[])

suptitle([filnam]);
```

Distribution

Admnstr
Defns Techl Info Ctr
ATTN DTIC-OCF
8725 John J Kingman Rd Ste 0944
FT Belvoir VA 22060-6218

DARPA
ATTN S Welby
3701 N Fairfax Dr
Arlington VA 22203-1714

Ofc of the Secy of Defns
ATTN ODDRE (R&AT)
The Pentagon
Washington DC 20301-3080

AMCOM MRDEC
ATTN AMSMI-RD W C McCorkle
Redstone Arsenal AL 35898-5240

US Army TRADOC
Battle Lab Integration & Techl Dirctr
ATTN ATCD-B
FT Monroe VA 23651-5850

DIRNSA
ATTN D Henkin
9800 Savage Rd
FT Meade MD 20755-6514

US Military Acdmy
Mathematical Sci Ctr of Excellence
ATTN MADN-MATH MAJ M Johnson
Thayer Hall
West Point NY 10996-1786

Dir for MANPRINT
Ofc of the Deputy Chief of Staff for Prsnl
ATTN J Hiller
The Pentagon Rm 2C733
Washington DC 20301-0300

SMC/CZA
2435 Vela Way Ste 1613
El Segundo CA 90245-5500

TECOM
ATTN AMSTE-CL
Aberdeen Proving Ground MD 21005-5057

US Army ARDEC
ATTN AMSTA-AR-TD
Bldg 1
Picatinny Arsenal NJ 07806-5000

US Army Info Sys Engrg Cmnd
ATTN AMSEL-IE-TD F Jenia
FT Huachuca AZ 85613-5300

US Army Intlgn & Info Warfare Dirctr
ATTN AMSEL-RD-IW B Mak
ATTN AMSEL-RD-IW D Helm
ATTN AMSEL-RD-IW K Leshick
ATTN AMSEL-RD-IW MAJ R Martinsen
ATTN AMSEL-RD-IW T Provencher
Bldg 600
FT Monmouth NJ 07703-5211

US Army Natick RDEC Acting Techl Dir
ATTN SBCN-T P Brandler
Natick MA 01760-5002

US Army Simulation Train & Instrmntn
Cmnd
ATTN AMSTI-CG M Macedonia
ATTN J Stahl
12350 Research Parkway
Orlando FL 32826-3726

US Army Tank-Automtv Cmnd RDEC
ATTN AMSTA-TR J Chapin
Warren MI 48397-5000

Nav Surfc Warfare Ctr
ATTN Code B07 J Pennella
17320 Dahlgren Rd Bldg 1470 Rm 1101
Dahlgren VA 22448-5100

US Customs Ser
ATTN J Woolard-BAE
PO Box 18900
Corpus Christi TX 78480

Hicks & Assoc Inc
ATTN G Singley III
1710 Goodrich Dr Ste 1300
McLean VA 22102

Distribution (cont'd)

Palisades Inst for Rsrch Svc Inc
ATTN E Carr
1745 Jefferson Davis Hwy Ste 500
Arlington VA 22202-3402

Director
US Army Rsrch Lab
ATTN AMSRL-RO-D JCI Chang
ATTN AMSRL-RO-EN W D Bach
PO Box 12211
Research Triangle Park NC 27709

US Army Rsrch Lab
ATTN AMSRL-D D R Smith
ATTN AMSRL-DD J M Miller
ATTN AMSRL-CI-IS-R Mail & Records Mgmt
ATTN AMSRL-CI-IS-T Techl Pub (2 copies)
ATTN AMSRL-CI-OK-TL Techl Lib (2 copies)

US Army Rsrch Lab (cont'd)
ATTN AMSRL-CI-CN B Sadler
ATTN AMSRL-SE-D E Scannell
ATTN AMSRL-SE-DP C Lazard
ATTN AMSRL-SE-DP D Judy
ATTN AMSRL-SE-DP L Cheskis
ATTN AMSRL-SE-DP L Dilks
ATTN AMSRL-SE-DP M Litz (10 copies)
ATTN AMSRL-SE-DP N Tesny (10 copies)
ATTN AMSRL-SE-DP R A Kehs
ATTN AMSRL-SE-R B Wallace
ATTN AMSRL-SE-RE R del Rosario
ATTN AMSRL-SE-RU J Sichina
ATTN AMSRL-SE-RU M Ressler
Adelphi MD 20783-1197

REPORT DOCUMENTATION PAGE			<i>Form Approved OMB No. 0704-0188</i>	
Public reporting burden for this collection of information is estimated to average 1 hour per response, including the time for reviewing instructions, searching existing data sources, gathering and maintaining the data needed, and completing and reviewing the collection of information. Send comments regarding this burden estimate or any other aspect of this collection of information, including suggestions for reducing this burden, to Washington Headquarters Services, Directorate for Information Operations and Reports, 1215 Jefferson Davis Highway, Suite 1204, Arlington, VA 22202-4302, and to the Office of Management and Budget, Paperwork Reduction Project (0704-0188), Washington, DC 20503.				
1. AGENCY USE ONLY (Leave blank)		2. REPORT DATE April 2002		3. REPORT TYPE AND DATES COVERED Final, June 2000 to October 2000
4. TITLE AND SUBTITLE Transient Electromagnetic Signals from Internal Combustion Engines			5. FUNDING NUMBERS DA PR: AH94 PE: 62705A	
6. AUTHOR(S) Marc Litz, Neal Tesny, Lillian Dilks, and Leland M. Cheskis				
7. PERFORMING ORGANIZATION NAME(S) AND ADDRESS(ES) U.S. Army Research Laboratory Attn: AMSRL-SE-DP email: mlitz@arl.army.mil 2800 Powder Mill Road Adelphi, MD 20783-1197			8. PERFORMING ORGANIZATION REPORT NUMBER ARL-TR-1658	
9. SPONSORING/MONITORING AGENCY NAME(S) AND ADDRESS(ES) U.S. Army Research Laboratory 2800 Powder Mill Road Adelphi, MD 20783-1197			10. SPONSORING/MONITORING AGENCY REPORT NUMBER	
11. SUPPLEMENTARY NOTES ARL PR: 2NE6XX AMS code: 622705.H94				
12a. DISTRIBUTION/AVAILABILITY STATEMENT Approved for public release; distribution unlimited.			12b. DISTRIBUTION CODE	
13. ABSTRACT (Maximum 200 words) A series of tests focusing on the frequency content and transient characteristics of the electromagnetic emissions from three different boat engines was performed at the Patuxent Naval Air Station. The transient emissions were compared with respect to engine rpm, amplification, orientation, shielding and against emissions from an engine of the same model. It was found that engine models can be identified according to their frequency content.				
14. SUBJECT TERMS Emissions, amplification frequency spectrum, frequency peak			15. NUMBER OF PAGES 60	
			16. PRICE CODE	
17. SECURITY CLASSIFICATION OF REPORT Unclassified	18. SECURITY CLASSIFICATION OF THIS PAGE Unclassified	19. SECURITY CLASSIFICATION OF ABSTRACT Unclassified	20. LIMITATION OF ABSTRACT UL	